



ΕΘΝΙΚΟ ΜΕΤΣΟΒΙΟ ΠΟΛΥΤΕΧΝΕΙΟ

ΣΧΟΛΗ ΕΦΑΡΜΟΣΜΕΝΩΝ
ΜΑΘΗΜΑΤΙΚΩΝ
ΚΑΙ ΦΥΣΙΚΩΝ ΕΠΙΣΤΗΜΩΝ

ΣΧΟΛΗ ΜΗΧΑΝΟΛΟΓΩΝ
ΜΗΧΑΝΙΚΩΝ

ΕΚΕΦΕ «ΔΗΜΟΚΡΙΤΟΣ»

ΙΝΣΤΙΤΟΥΤΟ ΝΑΝΟΕΠΙΣΤΗΜΗΣ
ΚΑΙ ΝΑΝΟΤΕΧΝΟΛΟΓΙΑΣ

ΙΝΣΤΙΤΟΥΤΟ ΠΥΡΗΝΙΚΗΣ ΚΑΙ
ΣΩΜΑΤΙΔΙΑΚΗΣ ΦΥΣΙΚΗΣ



Διατμηματικό Πρόγραμμα Μεταπτυχιακών Σπουδών

«Φυσική και Τεχνολογικές Εφαρμογές»

**Ανάπτυξη προγράμματος Η/Υ για τον υπολογισμό
συντελεστών διόρθωσης λόγω αυτοαπορρόφησης σε
εφαρμογές γ-φασματοσκοπίας**

**Development of a computer code for the calculation
of self-absorption correction factors
in γ-spectrometry application**

ΜΕΤΑΠΤΥΧΙΑΚΗ ΔΙΠΛΩΜΑΤΙΚΗ ΕΡΓΑΣΙΑ

του Ιωάννη Αλαφογιάννη

Επιβλέπων: Μάριος Αναγνωστάκης

Αθήνα, Μάρτιος, 2021

ΠΡΟΛΟΓΟΣ

Η Διπλωματική Εργασία αυτή εκπονήθηκε στον Τομέα Πυρηνικής Τεχνολογίας του ΕΜΠ στα πλαίσια του ΔΠΜΣ “Φυσική και Τεχνολογικές Εφαρμογές” το χρονικό διάστημα Απρίλιος 2020 - Φεβρουάριος 2021. Οφείλω τις ευχαριστίες στον Δρ. Μ.Ι. Αναγνωστάκη, Αναπληρωτή Καθηγητή του Ε.Μ.Π. για την βοήθεια του στην έρευνα και την περάτωση της διπλωματικής καθώς και για την εμπιστοσύνη που μου έδειξε στις δύσκολες αυτές μέρες της πανδημίας Covid-19. Η διάθεση του να μοιραστεί τις γνώσεις του και την εμπειρία του ήταν το λιγότερο πολύτιμες και καθοριστικές για την περάτωση της συγκεκριμένης εργασίας αλλά και ολόκληρου του μεταπτυχιακού προγράμματος. Επίσης θα ήθελα να ευχαριστήσω τον υποψήφιο διδάκτορα Ιάσονα Μήτσιου, για την επίσης πολύτιμη βοήθεια του στις προσομοιώσεις M-C του προγράμματος PENELOPE και για τις γνώσεις του σε πολλά θέματα επιστήμης και ανάλυσης υλικών.

ΠΕΡΙΕΧΟΜΕΝΑ

ΠΕΡΙΛΗΨΗ.....	1
ABSTRACT	3
ΕΚΤΕΝΗΣ ΠΕΡΙΛΗΨΗ.....	1
CHAPTER 1	15
INTRODUCTION.....	15
CHAPTER 2	17
GAMMA SPECTROSCOPIC ANALYSIS OF ENVIRONMENTAL SAMPLES	17
2.1 Interactions of gamma rays with matter	18
2.1.1 Photoelectric Effect	18
2.1.2 Compton scattering	19
2.1.3 Rayleigh elastic scattering	20
2.1.4 Pair Production	20
2.1.5 Linear and mass attenuation coefficients.....	21
2.2 Basics of gamma ray spectrometry	23
2.2.1 Low Energy Germanium Detectors.....	26
2.2.2 Efficiency Correction Factor in Low energy gamma spectrometry.....	27
2.2.3 The Integral Method for the determination of ECF	28
2.2.4 The detector effective interaction depth	30
2.3 Naturally Occurring Radioactive Materials (NORM).....	31
2.3.1 Soil.....	33
2.3.2 Red Mud.....	34
2.3.3 Fly Ash.....	34
2.3.4 Phosphogypsum.....	35
2.3.5 Slags	36
CHAPTER 3	38
A MATLAB PROGRAM FOR THE CALCULATION OF THE EFFICIENCY CORRECTION FACTOR	38
3.1 MATLAB source code basics and execution.....	39
3.2 Efficiency Correction Factor results	42
3.3 Calculation of ECF using Monte Carlo simulation.....	44
3.3.1 The Monte Carlo simulation code PENELOPE.....	44
3.3.2 Results and comparisons	44
3.4 Calculation of ECF using program calceff.....	46

3.5 Conclusions	48
CHAPTER 4	50
MODIFICATIONS AND EXTENSION OF MATLAB CODE.....	50
4.1 Mass Attenuation Coefficient with PENELOPE	50
4.2 MATLAB program modifications	54
4.3 MATLAB and Graphical User Interface	56
CHAPTER 5	62
CALCULATION OF EFFICIENCY CORRECTION FACTORS WITH THE NEW MATLAB PROGRAM.....	62
5.1 ECF results obtained with the new MATLAB program	62
5.2 The effect of the detector effective interaction depth	70
CHAPTER 6	74
CONCLUSIONS.....	74
BIBLIOGRAPHY	76
Original MATLAB Code.....	80
ANNEX II	84
New MATLAB Code	84
ANNEX III	97
MATERIALS.....	97
ANNEX IV.....	105
MASS ATTENUATION COEFFICIENTS from PENELOPE	105
ANNEX V.....	114
Table of Densities	114
ANNEX VI.....	115
(I) Table of ECF – PENELOPE by F.Tugnoli	115
(II) Linear Attenuation Coefficient Vectors in MATLAB.....	116

ΠΕΡΙΛΗΨΗ

Η εργασία αυτή αφορά στην τροποποίηση και βελτίωση ενός προγράμματος σε MATLAB για τον υπολογισμό του συντελεστή διόρθωσης της απόδοσης, ο οποίος απαιτείται κατά τη γ-φασματοσκοπική ανάλυση περιβαλλοντικών υλικών όπως είναι τα υλικά NORM (Naturally Occurring Radioactive Materials), λόγω του φαινομένου της αυτοαπορρόφησης των ακτινών-γ χαμηλών κυρίως ενεργειών μέσα στο υλικό που αναλύεται. Τα NORM, τα οποία είναι συνήθως παραπροϊόντα βιομηχανικών διεργασιών, έχουν συχνά μεγάλη πυκνότητα και μπορεί να περιέχουν σε μεγάλο ποσοστό στοιχεία υψηλού Z και για το λόγο αυτό το φαινόμενο της αυτοαπορρόφησης είναι πολύ έντονο. Για τον υπολογισμό του συντελεστή διόρθωσης χρησιμοποιήθηκε η ολοκληρωτική μέθοδος που βασίζεται στον υπολογισμόν δύο ολοκληρωμάτων τα οποία είναι ανάλογα της απόδοσης της ανιχνευτικής διάταξης, ένα ολοκλήρωμα για το υλικό της πηγής βαθμονόμησης και ένα για το υλικό του δείγματος. Ο λόγος των δύο ολοκληρωμάτων αποτελεί το συντελεστή διόρθωσης λόγω της διαφορετικής αυτοαπορρόφησης (ECF, Efficiency Correction Factor), μεταξύ του υλικού της πηγής βαθμονόμησης και του υλικού του δείγματος που αναλύεται. Στα πλαίσια της Διπλωματικής Εργασίας (ΔΕ) βελτιώθηκε πρόγραμμα σε MATLAB που είχε αναπτυχθεί στα πλαίσια προηγούμενης ΔΕ. Η βελτίωση αφορά στην ακρίβεια των αποτελεσμάτων, την ευελιξία που παρέχει στο χρήστη μέσω της επιλογής διαφόρων παραμέτρων και στην ευκολία χρήσης. Όσον αφορά στη βελτίωση της ακρίβειας, αυτή επετεύχθη κυρίως μέσω της εισαγωγής στο πρόγραμμα βελτιωμένων συναρτήσεων αναδρομής που υπολογίζουν τον ολικό μαζικό συντελεστή εξασθένησης μ_m , μία παράμετρο εξαιρετικά κρίσιμη για τον υπολογισμό του ECF.

Τα αποτελέσματα του νέου προγράμματος συγκρίθηκαν με άλλες μεθόδους υπολογισμού του συντελεστή ECF, όπως είναι η προσομοίωση Monte-Carlo. Οι συγκρίσεις που έγιναν οδήγησαν σε βελτιώσεις που αφορούν στην ουσία της διαδικασίας υπολογισμού του συντελεστή διόρθωσης, και επέτρεψαν τη μελέτη της επίδρασης που έχουν στα αποτελέσματα παράμετροι, όπως είναι το ενεργό βάθος αλληλεπίδρασης των φωτονίων μέσα στον ανιχνευτή. Από τα αποτελέσματα του προγράμματος και τις συγκρίσεις που έγιναν διαπιστώθηκε ότι η ακρίβεια στον προσδιορισμό του ECF είναι επαρκής στις περισσότερες περιπτώσεις, με εξαίρεση μόνο τα υλικά υψηλής πυκνότητας και για φωτόνια σχετικά χαμηλής ενέργειας – κάτω των $\sim 100\text{keV}$. Επιπλέον, διαπιστώθηκε η σημαντική επίδραση παραμέτρων που δεν λαμβάνονταν υπόψη στην προηγούμενη εκδοχή του προγράμματος, όπως το ενεργό βάθος αλληλεπίδρασης των φωτονίων μέσα στον ανιχνευτή, το οποίο πρέπει να είναι συνάρτηση της ενέργειας και από το οποίο φαίνεται να εξαρτάται σημαντικά η τιμή του ECF. Επισημαίνεται ότι στο σημείο αυτό απαιτείται ενδελεχής και συστηματική μελέτη στο μέλλον.

Η ευκολία εκτέλεσης του προγράμματος επέτρεψε την παραμετρική μελέτη του συντελεστή ECF για παραμέτρους όπως η ενέργεια των φωτονίων και το είδος του υλικού. Η μελέτη αυτή έδειξε ότι για υλικά υψηλής πυκνότητας, υπάρχει ανάγκη χρήσης συντελεστή ECF ακόμα και για πολύ υψηλές ενέργειες φωτονίων, άνω των 1000 keV . Αυτό είναι πολύ σημαντικό, καθώς πολλά ισότοπα που παρουσιάζουν ενδιαφέρον σε αναλύσεις περιβαλλοντικών υλικών και ιδιαίτερα

υλικών NORM εκπέμπουν φωτόνια σε αρκετά υψηλές ενέργειες, που σε αρκετές περιπτώσεις υπερβαίνουν κατά πολύ τα 1000keV.

ABSTRACT

This thesis is focused on the upgrade of a MATLAB program for the calculation of the Efficiency Correction Factor (ECF) which is required for the gamma spectroscopic analysis of environmental materials such as NORM (Naturally Occurring Radioactive Materials), due to the self-absorption effect of low-energy gamma rays within the material being analyzed. NORMs, which are usually by-products of industrial processes, often have a high density and may contain a large percentage of high Z elements and therefore the self-absorption effect is very intense.

For the calculation of the correction factor the integral method was adopted. This method is based on the calculations of two integrals which are proportional to the detector efficiency, one integral for the material of the calibration standard and one for the material of the analyzed sample. The ratio of the two integrals is the correction factor ECF that is used to take into consideration the different self-absorption between the material of the calibration source and the material of the sample being analyzed. In this Thesis, a MATLAB program that had been previously developed was improved in terms of accuracy of results, flexibility and ease of use. The new program allows the user to select various parameters previously set by the program. The program accuracy was improved mainly through the introduction of better fittings to calculate the total mass attenuation coefficient μ_m , a parameter of vital importance for ECF calculation.

The results of the new program were compared with other methods of ECF calculation such as the Monte-Carlo simulation. The comparisons made led to improvements in the whole model of correction factor calculation and allowed the study of the effect of various parameters, such as the effective interaction depth (d) of the photons within the detector. The program results and the comparisons made during this work showed that the accuracy in ECF calculation is sufficient in most cases, with the exception of high density materials and relatively low energy photons - less than $\sim 100\text{keV}$.

In addition, the significant effect of parameters not taken into account in the previous version of the program, such as the effective interaction depth (d) was revealed. It appears that this depth is energy dependent and furthermore ECF seems to depend on depth (d). It should be noted that thorough and systematic study in this field is required.

The ease of program execution allowed for the parametric study of the ECF coefficient, with energy and material type. This study showed that for high density materials, there is a need to use ECF even for very high photon energies, above 1000 keV. This is very important, as many isotopes of interest in the analysis of environmental materials and especially NORM emit photons at fairly high energies, often exceeding 1000keV.

ΕΚΤΕΝΗΣ ΠΕΡΙΛΗΨΗ

Η Διπλωματική Εργασία (ΔΕ) αυτή εκπονήθηκε στον Εργαστήριο Πυρηνικής Τεχνολογίας του Εθνικού Μετσόβιου Πολυτεχνείου (ΕΠΤ-ΕΜΠ) και διερευνά το θέμα της αυτοαπορρόφησης των φωτονίων (ακτινών-γ) χαμηλής ενέργειας που εκπέμπονται από ένα δείγμα, κατά τη διάρκεια της γ-φασματοσκοπικής ανάλυσης του. Προς την κατεύθυνση αυτή αναβαθμίσθηκε και επεκτάθηκε ένας κώδικας σε MATLAB¹ ο οποίος είχε αρχικά αναπτυχθεί στο ΕΠΤ-ΕΜΠ. Τα υλικά που μελετήθηκαν κατά τη διάρκεια της εργασίας είναι φυσικά ραδιενεργά υλικά κυρίως NORM², συγκεκριμένα: χώμα με 3% υγρασία, ερυθρά λύς (παραπροϊόν της επεξεργασίας βωξίτη), ιπτάμενη τέφρα, φωσφογύψος, τρία διαφορετικά είδη σκωρίας (lead slag, granulated slag και shaft furnace slag) και νερό.

Όταν δείγμα ενός υλικού αναλύεται με γ-φασματοσκοπική ανάλυση, ένα ποσοστό των εκπεμπόμενων από το δείγμα φωτονίων απορροφάται ή σκεδάζεται μέσα στο δείγμα, με συνέπεια να μην φτάνει στον ανιχνευτή προκειμένου να ανιχνευθεί. Αυτή η εξασθένιση των φωτονίων μέσα στο ίδιο το δείγμα, «αυτοαπορρόφηση», εξαρτάται κυρίως από τα φυσικά χαρακτηριστικά του υλικού, όπως η σύσταση και η πυκνότητά του, από την ενέργεια των φωτονίων της ακτινοβολίας-γ και από τα γεωμετρικά χαρακτηριστικά του δοχείου μέσα στο οποίο βρίσκεται το δείγμα. Από τη στιγμή λοιπόν που τα φυσικά ραδιενεργά υλικά έχουν διάφορες συστάσεις και πυκνότητες, είναι πολύ σημαντικό να βρεθεί ένας συντελεστής διόρθωσης της απόδοσης ανίχνευσης των φωτονίων (efficiency correction factor, ECF) από τον ανιχνευτή, όποιος θα χρησιμοποιείται, σε συνδυασμό με την πειραματικά προσδιορισμένη απόδοση του ανιχνευτή, κατά τη γ-φασματοσκοπική ανάλυση. Τα υλικά τύπου “NORM” που μελετώνται στην παρούσα Διπλωματική Εργασία είναι υλικά μεγάλης πυκνότητας και συνήθως τα αντίστοιχα δείγματα που αναλύονται έχουν μεγάλο όγκο, συνεπώς ο συντελεστής διόρθωσης αποκτά μεγάλη σημασία. Επίσης, είναι σημαντικό να αναφερθεί πως αυτά τα υλικά μπορεί να υπόκεινται σε περιορισμούς, αναφορικά με την απελευθέρωση τους στο περιβάλλον, σύμφωνα με την ευρωπαϊκή [1], αλλά και την εθνική νομοθεσία, και για το λόγο αυτό έχει μεγάλη σημασία η ακριβής ανάλυσή τους, κάτι που συνδέεται άμεσα με τη χρήση συντελεστών ECF.

Η αναβάθμιση του κώδικα κινήθηκε στους εξής άξονες: βελτίωση της ακρίβειας προσδιορισμού του συντελεστή ECF, επέκταση σε ευρύτερη ενεργειακή περιοχή, ανάλυση περισσότερων υλικών και εισαγωγή στον κώδικά της δυνατότητας επιλογής σειράς γεωμετρικών χαρακτηριστικών που καθιστούν τον κώδικά πολύ πιο ευέλικτο και φιλικό στο χρήστη.

Στο ΕΠΤ-ΕΜΠ κατά την ανάλυση περιβαλλοντικών δειγμάτων χρησιμοποιούνται συντελεστές διόρθωσης λόγω αυτοαπορρόφησης οι οποίοι υπολογίζονται από κατάλληλο πρόγραμμα το οποίο έχει αναπτυχθεί σε γλώσσα FORTRAN [2], για τα ανιχνευτικά συστήματα και τις γεωμετρίες που χρησιμοποιούνται στο εργαστήριο και για περιορισμένο πλήθος υλικών. Η πρώτη προσπάθεια ανάπτυξης προγράμματος υπολογισμού του συντελεστή διόρθωσης της απόδοσης

¹ Έκδοση MATLABR2015a-64bit.

² NORM, Natural Occurring Radioactive Materials

σε γλώσσα MATLAB είχε γίνει σε προηγούμενη ΔΕ του Τομέα Πυρηνικής Τεχνολογίας [3]. Στη συγκεκριμένη εργασία είχαν μελετηθεί επτά υλικά NORM για φωτόνια ενέργειας έως 400 keV. Το πρόγραμμα αυτό μπορούσε υπολογίζει το συντελεστή ECF για συγκεκριμένο ανιχνευτή του ΕΠΤ-ΕΜΠ και για δύο συγκεκριμένες γεωμετρίες δείγματος. Τα αποτελέσματα υπολογισμού του συντελεστή ECF είχαν συγκριθεί με τα αποτελέσματα προσομοίωσης Monte-Carlo καθώς και του προγράμματος που ήδη χρησιμοποιείτο στο ΕΠΤ-ΕΜΠ. Η σύγκριση αυτή κατέληξε σε ουσιώδη συμπεράσματα, αλλά ανέδειξε και μία σειρά από αδυναμίες του προγράμματος, κυρίως λόγω των αποκλίσεων των αποτελεσμάτων του από τα αποτελέσματα της προσομοίωσης.

Ο βασικός σκοπός αυτής της ΔΕ είναι η επέκταση αυτού του προγράμματος MATLAB και η αναβάθμισή του όσον αναφορά στην ακρίβεια αλλά και τη λειτουργία του. Για την αξιολόγηση της αναβάθμισης αυτής έγιναν διάφορες συγκρίσεις κυρίως με αποτελέσματα προσομοίωσης M-C για την εύρεση του συντελεστή διόρθωσης ECF. Το ενδιαφέρον για τη βελτίωση της ακρίβειας εστιάστηκε κυρίως στις χαμηλές ενέργειες, όπου υπήρχαν και οι μεγαλύτερες αποκλίσεις μεταξύ των διαφόρων μεθόδων. Στη συνέχεια, έγινε η επέκταση του κώδικα για τον υπολογισμό του συντελεστή διόρθωσης σε υψηλότερες ενέργειες μέχρι τα 2000keV καθώς στην γ-φασματοσκοπική ανάλυση πολύ συχνά χρησιμοποιούνται φωτόνια σε αυτές τις υψηλές ενέργειες, όπως φωτόνια που εκπέμπονται από τα ^{212}Pb , ^{214}Pb , ^{228}Ac , ^{214}Pb και ^{40}K τα οποία είναι ιδιαίτερα σημαντικά σε αναλύσεις δειγμάτων φυσικής ραδιενέργειας.

Η ΔΕ αποτελείται από 6 κεφάλαια. Το πρώτο κεφάλαιο αποτελεί μια σύντομη εισαγωγή. Το δεύτερο κεφάλαιο ασχολείται βιβλιογραφικά με το πρόβλημα της αυτοαπορρόφησης κατά τη γ-φασματοσκοπική ανάλυση και την αναγκαιότητα εύρεσης κατάλληλου συντελεστή διόρθωσης. Στην συνέχεια, στο τρίτο κεφάλαιο γίνεται μια παρουσίαση του αρχικού προγράμματος που είχε αναπτυχθεί στην εργασία [3] σε γλώσσα MATLAB και των αποτελεσμάτων που δίνει, ενώ επίσης σχολιάζονται οι αδυναμίες που παρουσιάζει και προτείνονται διορθώσεις, βελτιώσεις και επεκτάσεις του προγράμματος που θα ήταν χρήσιμο να γίνουν. Στο τέταρτο κεφάλαιο παρουσιάζονται αναλυτικά οι διορθώσεις και οι αλλαγές που έγιναν στο πρόγραμμα, όσον αναφορά στην ακρίβεια των αποτελεσμάτων του αλλά και τη βελτίωση της λειτουργικότητας του. Στο πέμπτο κεφάλαιο παρουσιάζονται τα νέα αποτελέσματα από το αναβαθμισμένο πρόγραμμα καθώς και οι εκτενείς συγκρίσεις με τις άλλες μεθόδους εύρεσης του συντελεστή διόρθωσης που χρησιμοποιούνται στο ΕΠΤ-ΕΜΠ. Τέλος, στο έκτο κεφάλαιο παρουσιάζονται τα συμπεράσματα από τη χρήση του νέου προγράμματος, οι αδυναμίες που παρουσιάζει, καθώς και οι δυνατότητες επέκτασής του.

Σε όλα τα προγράμματα που έχουν κατά καιρούς αναπτυχθεί στο ΕΠΤ-ΕΜΠ, ο υπολογισμός του συντελεστή ECF βασίζεται στην ολοκληρωτική μέθοδο *"Integral Method"* [4], [5]. Πρόκειται για μια υπολογιστική μέθοδο που οδηγεί στην εκτίμηση κατάλληλου συντελεστή διόρθωσης της απόδοσης, μέσω του υπολογισμού δύο ολοκληρωμάτων, ένα για την πηγή βαθμονόμησης και ένα για το υπό ανάλυση δείγμα. Για τον υπολογισμό αυτών των δυο ολοκληρωμάτων απαιτείται η γνώση της γεωμετρίας πηγής-ανιχνευτή. Σύμφωνα με τη μέθοδο αυτή ο ανιχνευτής υποκαθίσταται από ένα φανταστικό σημειακό ανιχνευτή που βρίσκεται μέσα στον πραγματικό ανιχνευτή, σε βάθος που πρέπει να υπολογίζεται πειραματικά και χαρακτηρίζεται ως ενεργό βάθος αλληλεπίδρασης *"effective interaction depth (d)"*. Στην αρχική εκδοχή του προγράμματος

MATLAB γινόταν υπολογισμός του συντελεστή ECF για τον ανιχνευτή LEGe³ του ΕΠΤ-ΕΜΠ. Για τη συγκεκριμένη εφαρμογή το βάθος αυτό είχε θεωρηθεί σταθερό όπως . σταθερή (d=2cm) ήταν και η συνολική απόσταση του φανταστικού ανιχνευτή από το δείγμα.

Μία σημαντική παράμετρος για τον υπολογισμό του συντελεστή ECF είναι ο γραμμικός συντελεστής εξασθένησης φωτονίων μ (ή ο αντίστοιχος μαζικός μ_m) για το υλικό του δείγματος και της πηγής βαθμονόμησης. Η αρχική έκδοση του προγράμματος MATLAB, η οποία παρουσιάζεται στο παράρτημα (ANNEX I), απαιτεί από το χρήστη μόνο τρία δεδομένα εισόδου. Αρχικά, ζητείται η επιλογή της γεωμετρίας του δείγματος για το οποίο πρόκειται να υπολογισθεί ο συντελεστής διόρθωσης της απόδοσης. Υπήρχαν μόλις δυο από τις τυποποιημένες γεωμετρίες που χρησιμοποιούνται στο ΕΠΤ-ΕΜΠ, οι οποίες ουσιαστικά περιγράφουν ένα κυλινδρικό δοχείο. Οι δύο γεωμετρίες ορίζονται από δυο μεταβλητές: την ακτίνα του δείγματος “r” και το πάχος του δείγματος “t” μέσα στο δοχείο. Η πρώτη γεωμετρία ονομάζεται “Geometry 2” με διαστάσεις: r = 3,6cm και t = 6,9cm, και η δεύτερη γεωμετρία ονομάζεται “Geometry 8” με διαστάσεις: r = 3,6cm και t = 1,08cm. Μόλις ο χρήστης πληκτρολογήσει την εντολή για την γεωμετρία που επιθυμεί, το πρόγραμμα ζητάει από τον χρήστη να επιλέξει ένα από τα επτά διαθέσιμα υλικά τα οποία ήταν: χώμα (soil, 3% υγρασία), ερυθρά ιλύς (red mud), ιπτάμενη τέφρα (fly ash), φωσφογύψος (phosphogypsum) και τρία είδη σκωρίας (shaft furnace slag, granulated slag, lead slag). Τέλος, ο χρήστης θα πρέπει να πληκτρολογήσει την ενέργεια των φωτονίων για την οποία ενδιαφέρεται, ούτως ώστε το πρόγραμμα να υπολογίσει το συντελεστή ECF.

Ο μαζικός συντελεστής εξασθένησης ο οποίος απαιτείται για τον υπολογισμό του ECF υπολογίζεται από το πρόγραμμα, μέσω κατάλληλων συναρτήσεων αναδρομής της μορφής $\mu=f(E)$ οι οποίες έχουν παραχθεί προηγουμένως για όλα τα υλικά ενδιαφέροντος και εισαχθεί στο πρόγραμμα. Για το σκοπό αυτό είχαν χρησιμοποιηθεί κατάλληλα δεδομένα που είχαν υπολογισθεί μέσω του προγράμματος MuPlot⁴ το οποίο, έχει αναπτυχθεί στο University of Bologna και υπολογίζει συντελεστές εξασθένησης χρησιμοποιώντας δεδομένα από τη δημοσίευση [6]. Για τις ανάγκες του προγράμματος είχαν χρησιμοποιηθεί δεδομένα για την ενεργειακή περιοχή 30-400keV. Στο σχήμα 1 παρατίθεται ενδεικτικά η καμπύλη της συνάρτησης $\mu=f(E)$ για το υλικό της πηγής βαθμονόμησης 4M HCl, όπως είχε χρησιμοποιηθεί στην αρχική μορφή του προγράμματος.

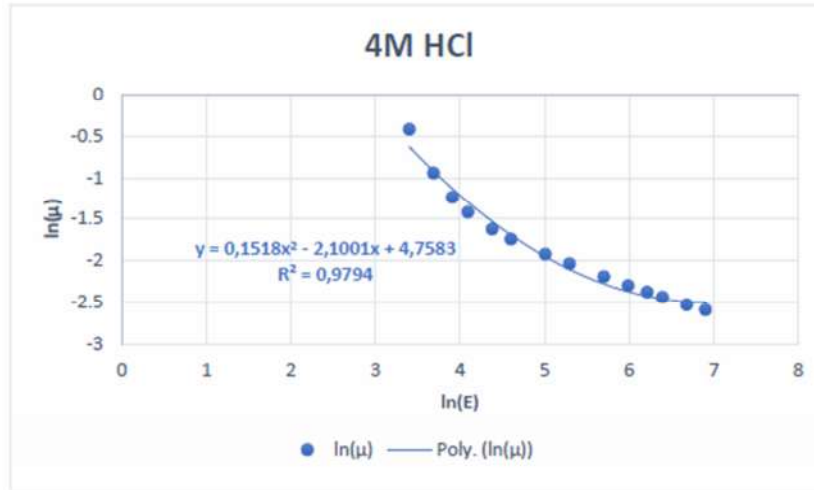
Όπως φαίνεται στο σχήμα 1 η προσαρμογή της συνάρτησης αναδρομής στα πειραματικά σημεία δεν είναι ιδιαίτερα επιτυχής, κυρίως στην περιοχή χαμηλών ενεργειών, με συνέπεια ο υπολογισμός του συντελεστή μ_m από μία σχέση της μορφής:

$$\ln(\mu_m) = A \cdot (\ln E)^2 + B \cdot \ln(E) + C$$

να μην είναι ικανοποιητικά ακριβής. Αντίστοιχες συναρτήσεις αναδρομής είχαν παραχθεί για όλα τα υλικά ενδιαφέροντος και είχαν εισαχθεί στο πρόγραμμα υπολογισμού του ECF. Στο παράρτημα (ANNEX II) παρατίθενται η σύσταση και οι τιμές των συντελεστών μ και μ_m για όλα τα υλικά. Όταν ο χρήστης εισάγει την ενέργεια για την οποία θέλει να υπολογίσει το ECF το πρόγραμμα υπολογίζει μέσω της αντίστοιχης σχέσης τους συντελεστές μ_m , εν συνεχεία τα αντίστοιχα ολοκληρώματα και τελικά το συντελεστή ECF.

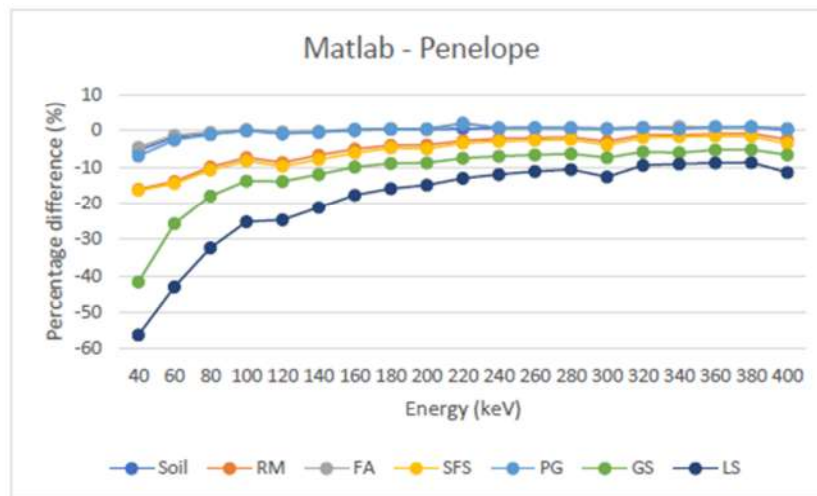
³ Low Energy Germanium Detector

⁴ Είναι διαθέσιμο στην ιστοσελίδα <http://shape.ing.unibo.it/html/muplot.htm>



Σχήμα 1: Διάγραμμα του φυσικού λογαρίθμου του μαζικού συντελεστή εξασθένησης μ_m συναρτήσει του φυσικού λογαρίθμου της ενέργειας E για το υλικό της πηγής βαθμονόμησης 4M HCl.

Στην εργασία [3] είχαν υπολογισθεί συγκεκριμένες τιμές για το συντελεστή ECF για όλα τα υλικά και για ενέργειες στην περιοχή 30-400 keV. Οι τιμές αυτές είχαν συγκριθεί με αντίστοιχες τιμές από υπολογισμούς προσομοίωσης Monte-Carlo⁵ και τα αποτελέσματα δεν ήταν ικανοποιητικά. Στο παρακάτω διάγραμμα (σχήμα 2) φαίνεται η ποσοστιαία διαφορά μεταξύ των τιμών της προσομοίωσης M-C και του προγράμματος MATLAB για τη γεωμετρία “8”. Εύκολα διαπιστώνεται ότι στις χαμηλές ενέργειες, ιδιαίτερα για τα υλικά υψηλής πυκνότητας, η διαφορά μεταξύ των δυο μεθόδων φτάνει έως και 60%.



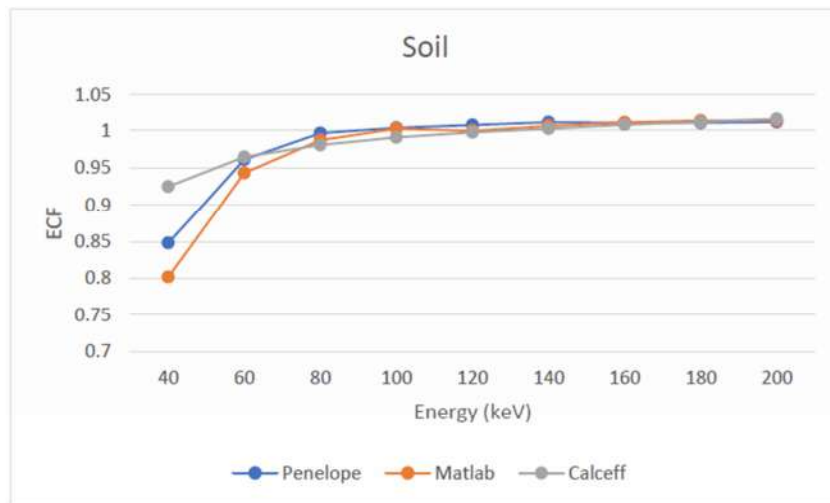
Σχήμα 2: Ποσοστιαία διαφορά μεταξύ των τιμών του συντελεστή ECF όπως υπολογιζόταν από το αρχικό πρόγραμμα MATLAB και μέσω προσομοίωσης M-C, [3].

Από τα παραπάνω γραφήματα προκύπτει ότι οι μεγάλες αποκλίσεις που παρατηρούνται στους συντελεστές ECF από τις δύο μεθόδους θα πρέπει σε κάποιο βαθμό να οφείλονται στην όχι πολύ επιτυχημένη προσαρμογή της καμπύλης $\mu_m=f(E)$ στα σημεία. Αυτό ήταν το πρώτο σημείο

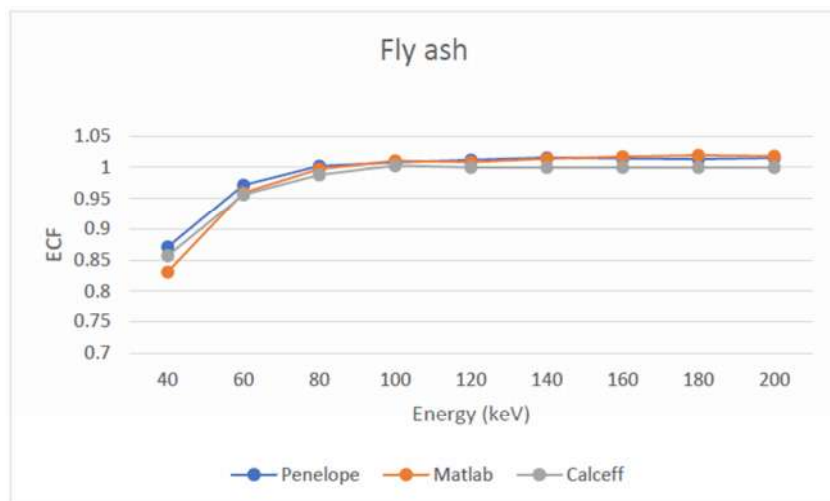
⁵ Οι υπολογισμοί προσομοίωσης έγιναν με χρήση του προγράμματος PENELOPE

βελτίωσης που εστίασε η ΔΕ αυτή. Επίσης, προκειμένου να υπάρχει καλύτερη σύγκριση των δύο μεθόδων υπολογισμού θα έπρεπε να εξασφαλισθεί ότι χρησιμοποιούνται τα ίδια πρωτογενή δεδομένα, σε όρους μ και μ_m .

Εκτός από τη σύγκριση των συντελεστών ECF που υπολογίσθηκαν από το πρόγραμμα MATLAB και μέσω προσομοίωσης M-C, έγινε σύγκριση και με τα αποτελέσματα του προγράμματος calceff, το οποίο έχει αναπτυχθεί και χρησιμοποιείται στο ΕΠΤ-ΕΜΠ και βασίζεται επίσης στην “integral method”. Η διαφορά του προγράμματος calceff από το πρόγραμμα MATLAB είναι πως το πρώτο παρέχει αποτελέσματα μόνο για τρία υλικά τα οποία είναι: χώμα, ιπτάμενη και υγρή τέφρα από θερμικό σταθμό, και μόνο για την περιοχή ενεργειών έως 200 keV. Επίσης, μια άλλη σημαντική διαφορά μεταξύ των δυο αυτών προγραμμάτων είναι πως το πρόγραμμα calceff χρησιμοποιεί πειραματικές τιμές του μαζικού συντελεστή μ_m εξασθένισης [7]. Η σύγκριση των τιμών του ECF και με τις τρεις μεθόδους υπολογισμού φαίνεται στα επόμενα δυο διαγράμματα (σχήμα 3 και σχήμα 4) από την εργασία [3].



Σχήμα 3: Σύγκριση τιμών ECF για χώμα, μεταξύ των τριών μεθόδων, MATLAB, calceff, προσομοίωση M-C, [3].



Σχήμα 4: Σύγκριση τιμών ECF για ιπτάμενη τέφρα μεταξύ των τριών μεθόδων, calceff, προσομοίωση M-C, [3].

Όπως παρατηρείται, υπήρχαν και πάλι αρκετά μεγάλες διαφορές στις χαμηλές ενέργειες, ειδικότερα για το χλώμα, όπου η διαφορά φτάνει στο 25%, με τα αποτελέσματα του προγράμματος MATLAB να είναι πιο κοντά στα αποτελέσματα της προσομοίωσης M-C η οποία θεωρείται και ως βάση σύγκρισης. Αυτό μπορεί να οφείλεται στο γεγονός ότι η χημική σύσταση των υλικών – και κατά συνέπεια ο συντελεστής εξασθένησης – που χρησιμοποιείται στο πρόγραμμα “calceff” είναι διαφορετικά με αυτά των δύο άλλων μεθόδων.

Η αναβάθμιση του κώδικα που έγινε στα πλαίσια αυτής της ΔΕ κινείται σε τρεις βασικούς άξονες:

- στην βελτίωση της ακρίβειας του κώδικα μέσω της αλλαγής του τρόπου με τον οποίο υπολογίζεται ο μαζικός συντελεστής εξασθένησης μέσα σε αυτόν,
- στην εισαγωγή περισσότερων επιλογών για τον χρήστη ώστε να γίνει ο κώδικας πιο ευέλικτος με περισσότερες δυνατότητες και
- στην δημιουργία εν τέλει ενός προγράμματος φιλικού στο χρήστη, ανεξάρτητου από το δύσχορηστο MATLAB σε μορφή .exe.

Προς την κατεύθυνση αυτή, όλες οι τιμές του γραμμικού και του μαζικού συντελεστή εξασθένησης υπολογίστηκαν εκ νέου με την βοήθεια του προγράμματος προσομοίωσης PENELOPE. Πρέπει να τονισθεί ότι οι συντελεστές υπολογίστηκαν έως και τα 2000 keV, καθώς στη δημοσίευση [33] υπάρχουν περιπτώσεις όπου ο συντελεστής ECF είναι σημαντικά διαφορετικός από τη μονάδα, κάτι που δείχνει ότι υπάρχει ανάγκη διόρθωσης της απόδοσης ακόμα και για υψηλές ενέργειες. Τα σχετικά αποτελέσματα παρατίθενται στο παράρτημα (ANNEX IV).

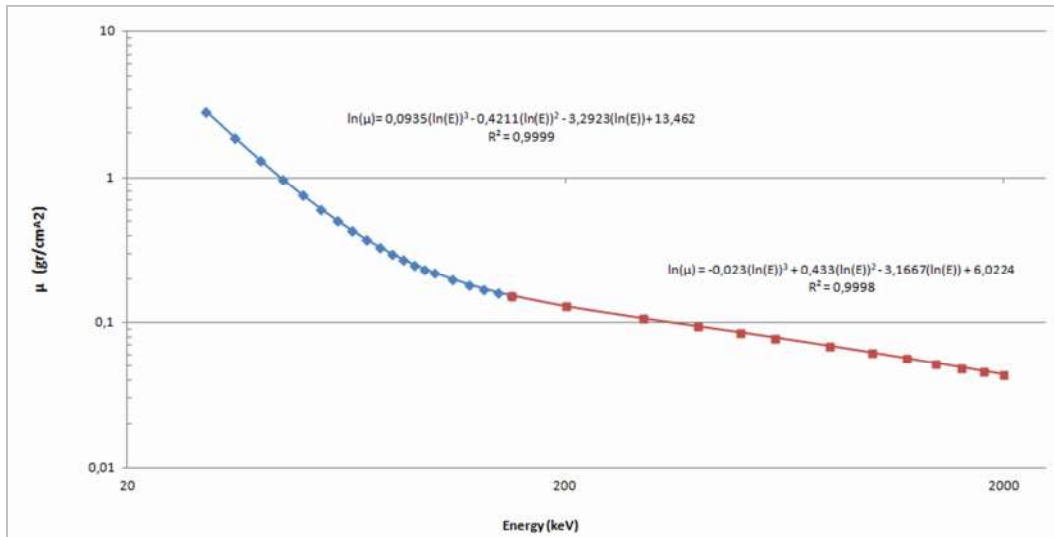
Για την προσαρμογή κατάλληλων συναρτήσεων της μορφής $\mu_m = f(E)$ στην περιοχή 30-2000 keV πλέον, χρησιμοποιήθηκαν 14 επίπεδα ενέργειας για κάθε υλικό, με εξαίρεση το υλικό lead slag, όπου χρησιμοποιήθηκαν 27 επίπεδα ενέργειας. Μετά από αρκετές δοκιμές συναρτήσεων αναδρομής επιλέχθηκε τελικά η λύση να διαιρεθεί η ενεργειακή περιοχή 30-2000keV σε δύο υπό-περιοχές με όριο τα 150keV και να χρησιμοποιηθούν δύο συναρτήσεις αναδρομής της μορφής:

$$\ln(\mu_m) = A \cdot (\ln E)^3 + B \cdot (\ln E)^2 + C \cdot \ln(E) + D$$

Στο σχήμα 5 παρατίθενται ενδεικτικά οι σχετικές συναρτήσεις για το υλικό lead slag.

Στην συνέχεια, οι αλλαγές επικεντρώθηκαν κυρίως στην λειτουργικότητα του προγράμματος και στην ευελιξία που μπορεί να παρέχει στο χρήστη. Μέχρι το σημείο αυτό, όπως αναφέρθηκε και προηγουμένως, ο χρήστης είναι πολύ περιορισμένος στα δεδομένα εισόδου που μπορεί να δώσει, αφού οι γεωμετρικές, οι πυκνότητες των υλικών και το ενεργό βάθος αλληλεπίδρασης του ανιχνευτή είναι όλα προκαθορισμένα με σταθερές τιμές μέσα στο πρόγραμμα. Η πρώτη αλλαγή μέσα στο πρόγραμμα αφορούσε στη δυνατότητα επιλογής του ενεργού βάθους αλληλεπίδρασης. Στο νέο πρόγραμμα αυτό επιλέγεται από το χρήστη. Στην πραγματικότητα, ο χρήστης επιλέγει τη **συνολική απόσταση d** από τη βάση του δείγματος έως τον φανταστικό ανιχνευτή, η οποία συμπεριλαμβάνει και το ενεργό βάθος αλληλεπίδρασης. Αυτή η αλλαγή στο πρόγραμμα επέτρεψε τη μελέτη της επίδρασης που έχει η επιλογή του d πάνω στον υπολογισμό του ECF. Οι υπόλοιπες αλλαγές που έγιναν αφορούσαν στην επιλογή των γεωμετρικών χαρακτηριστικών της πηγής και της πυκνότητας των υπό μελέτη υλικών. Ο χρήστης εξακολουθεί να μπορεί να επιλέξει

μεταξύ των δύο τυπικών γεωμετριών (“2” και “8”) ή να κατασκευάσει μία δική του κυλινδρική γεωμετρία, επιλέγοντας ύψος και διάμετρο του κυλινδρικού δείγματος, αλλά και την απόσταση από τον ανιχνευτή, μέσω του d.



Σχήμα 5: Διάγραμμα του λογαρίθμου του μ_m συναρτήσει του λογαρίθμου της ενέργειας για το υλικό lead slag

Οι υπόλοιπες αλλαγές στο πρόγραμμα έγιναν με την βοήθεια του MATLAB -⁶GUI το οποίο περιέχεται στην έκδοση του MATLAB και επιτρέπει τη δημιουργία εφαρμογής μέσω του προϋπάρχοντος κώδικα. Η εφαρμογή που δημιουργήθηκε με το GUI δίνει στο χρήστη τη δυνατότητα υπολογισμού του συντελεστή ECF χωρίς να έχει στην κατοχή του το MATLAB και χωρίς να έχει γνώσεις προγραμματισμού. Μέχρι το σημείο αυτό ο κώδικας ήταν αρκετά δύσχρηστος και λειτουργούσε εφόσον ήταν το MATLAB εγκατεστημένο στον Η/Υ. Πλέον, με τις αλλαγές που έγιναν το πρόγραμμα μπορεί να λειτουργεί σε κάθε υπολογιστή από οποιονδήποτε χρήστη ως “standalone” εφαρμογή. Στο σχήμα 6 που ακολουθεί παρατίθεται η εικόνα της εφαρμογής αυτής όπως τη βλέπει ο χρήστης. Ο χρήστης πλέον έχει τη δυνατότητα επιλογής:

- της γεωμετρίας δείγματος,
- απόστασης μεταξύ του φανταστικού ανιχνευτή και του δείγματος⁷,
- του υλικού,
- της πυκνότητας του υλικού,
- της ενέργειας των φωτονίων,

ενώ το πρόγραμμα υπολογίζει και εμφανίζει:

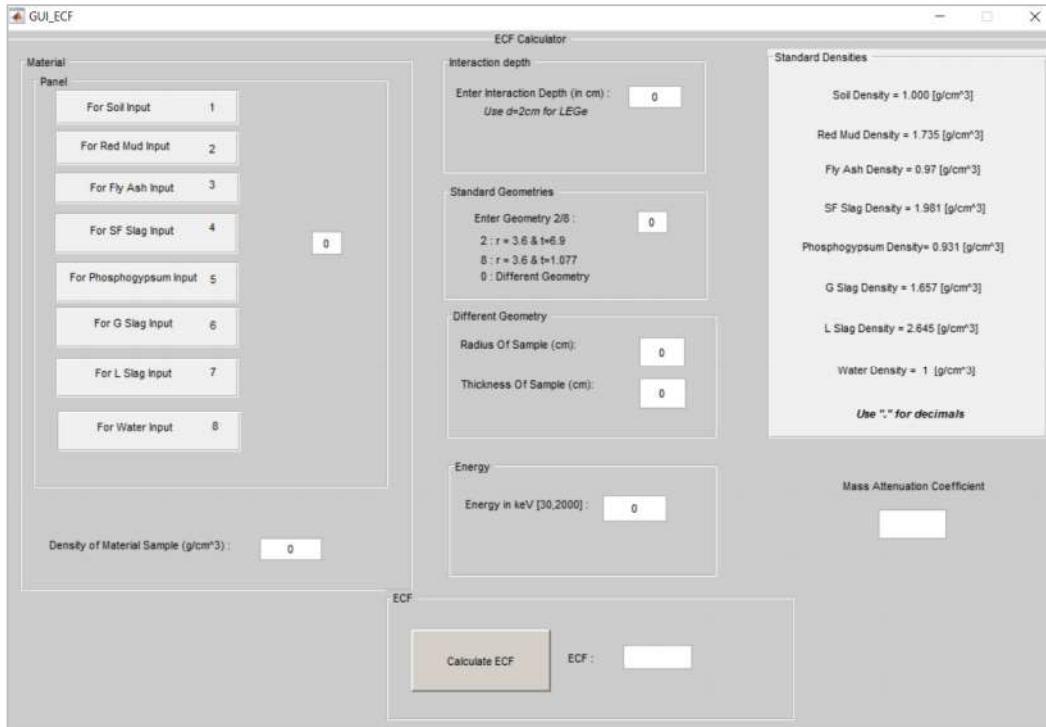
- το συντελεστή διόρθωσης αυτοαπορρόφησης ECF
- τον ολικό μαζικό συντελεστή εξασθένησης των φωτονίων μ_m για το υπό μελέτη υλικό.

Η ευκολία και ευελιξία του προγράμματος επέτρεψε τόσο τη σύγκριση με τις τιμές του ECF που υπολογίζονται με τις άλλες μεθόδους υπολογισμού οι οποίες αναφέρθηκαν προηγουμένως, όσο

⁶ Graphical User Interface

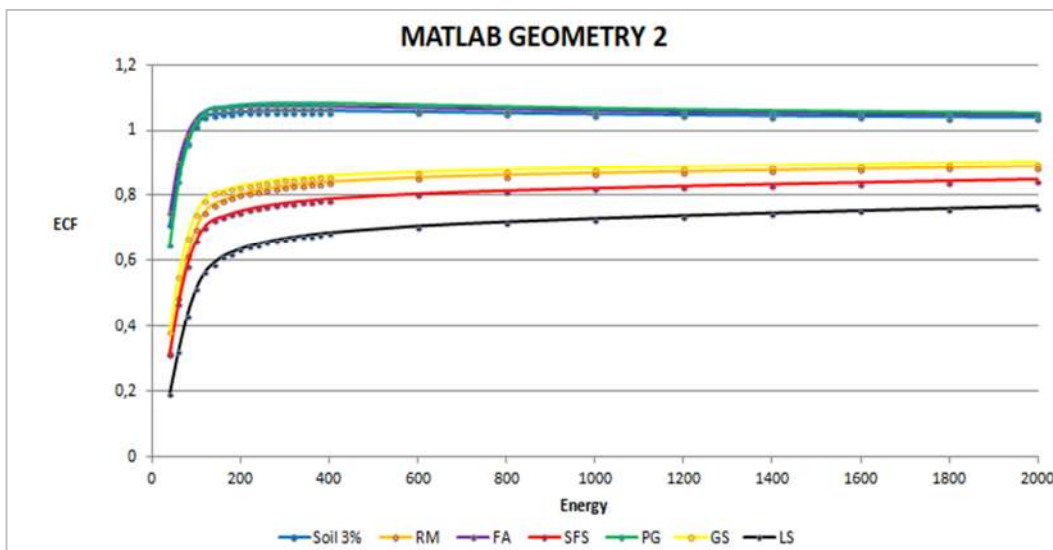
⁷ Πρέπει στο σημείο αυτό να επισημανθεί ότι, καθώς δίνεται συνολικά η απόσταση d, που περιλαμβάνει τόσο το ενεργό βάθος αλληλεπίδρασης όσο και την απόσταση της βάσης της πηγής από την επιφάνεια του ανιχνευτή, επιτρέπεται στο χρήστη να μελετήσει την επίδραση και των δύο αυτών παραμέτρων.

και τη μελέτη της επίδρασης που έχουν στο συντελεστή ECF μία σειρά παραμέτρων, όπως η ενέργεια των φωτονίων, η πυκνότητα του υλικού και το βάθος d.

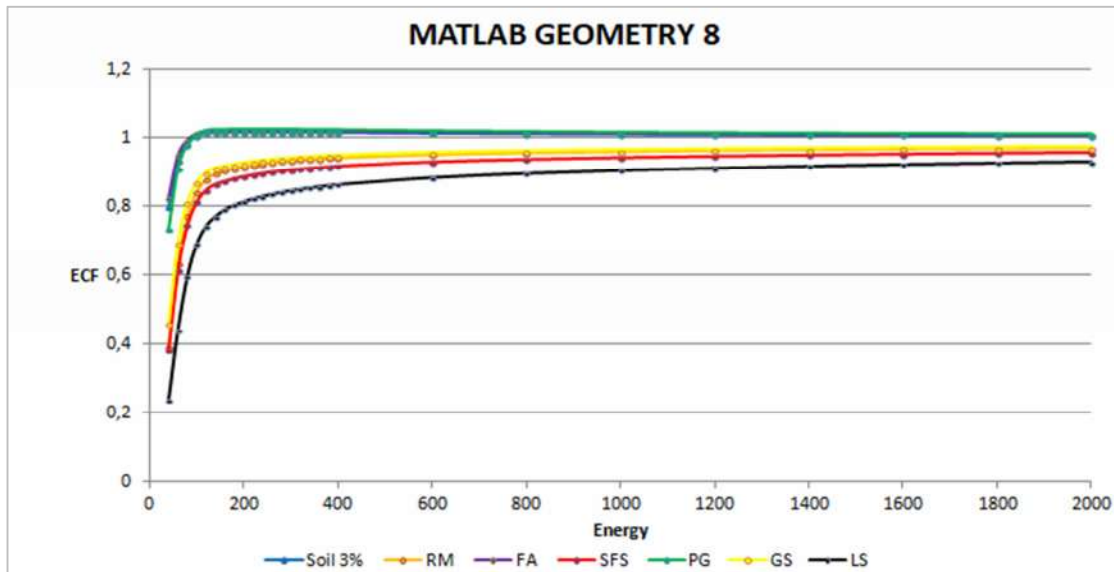


Σχήμα 6: Η εφαρμογή σε μορφή “.exe”

Στα σχήματα 7 και 8 που ακολουθούν παρατίθενται γραφήματα του συντελεστή ECF συναρτήσεως της ενέργειας των φωτονίων, για όλα τα υπό μελέτη υλικά για την ονομαστική πυκνότητα που εμφανίζεται στην οθόνη της εφαρμογής για κάθε υλικό και για τις δύο τυπικές γεωμετρίες “2” και “8”. Σε κάθε περίπτωση η τιμή του ECF όσο αυξάνει η ενέργεια τείνει προς μία σταθερή τιμή, χωρίς όμως αυτή να είναι η μονάδα (δηλαδή να μη χρειάζεται διόρθωση) για όλα τα υλικά.



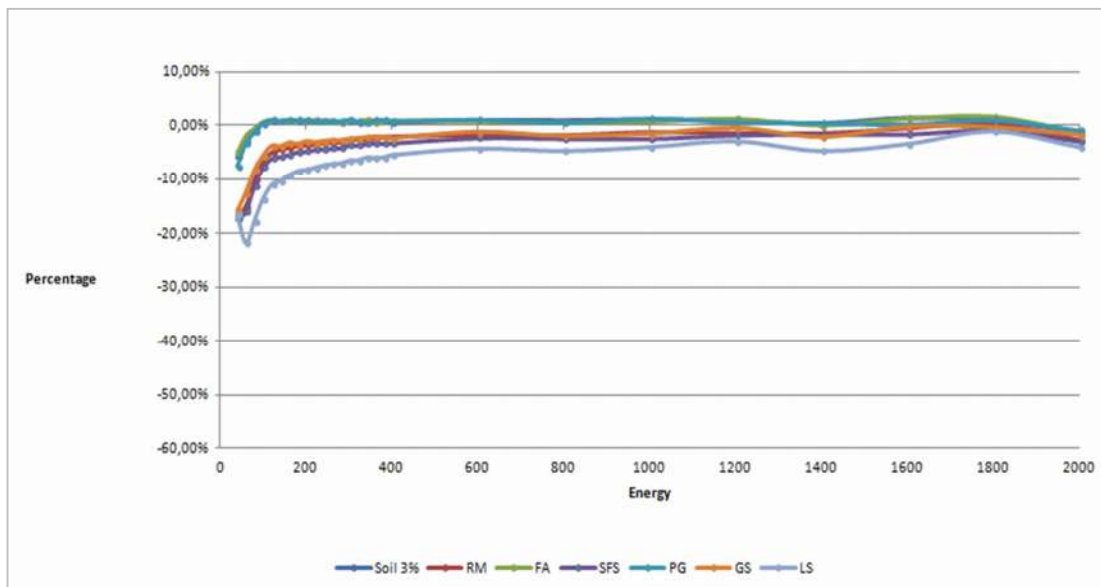
Σχήμα 7: Το διάγραμμα του ECF συναρτήσεως της ενέργειας για Geometry-2 (πάχος 69mm)



Σχήμα 8: Το διάγραμμα του ECF συναρτήσει της ενέργειας για Geometry 8 (πάχος 10mm)

Πιο συγκεκριμένα, υλικά με μικρές πυκνότητες (χώμα, φωσφογύψος) πλησιάζουν στη μονάδα, ενώ υλικά με μεγάλες πυκνότητες (lead slag) δεν φτάνουν στη μονάδα, κάτι που δείχνει ότι απαιτείται διόρθωση λόγω αυτοαπορρόφησης και για πολύ υψηλής ενέργειας φωτόνια. Για παράδειγμα η μέγιστη τιμή του ECF για lead slag είναι ίση περίπου με 0.93. Αυτό είναι συμβατό με τη βιβλιογραφία όπου αναφέρεται ότι για τις υψηλές ενέργειες και για υλικά με υψηλές πυκνότητες οι συντελεστές ECF προσεγγίζουν τη μονάδα αλλά δεν την φτάνουν [8], [33].

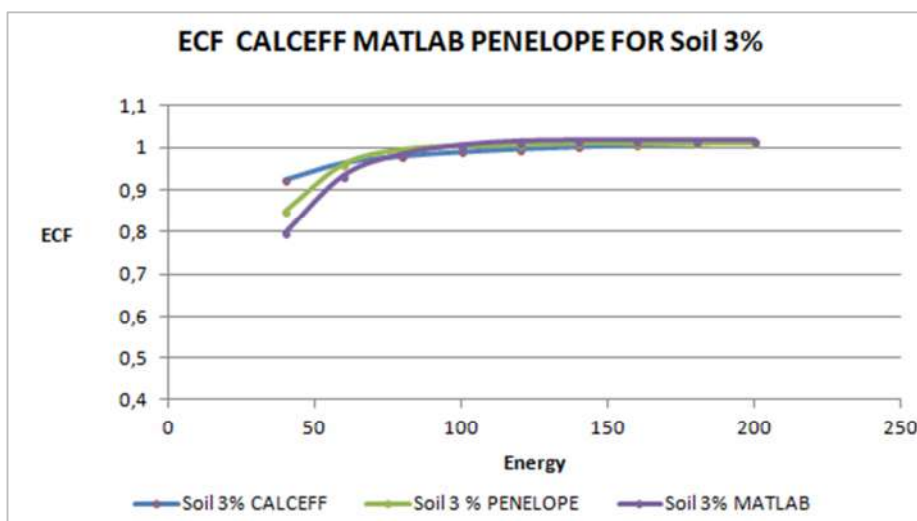
Στην συνέχεια ακολούθησε σύγκριση των νέων τιμών του ECF με τις τιμές της προσομοίωσης M-C με επέκταση μέχρι την ενέργεια των 2000keV. Οι τιμές αυτές έχουν υπολογιστεί μόνο για τη γεωμετρία “8”. Από τη σύγκριση των αποτελεσμάτων προκύπτει το διάγραμμα του παρακάτω σχήματος 9.



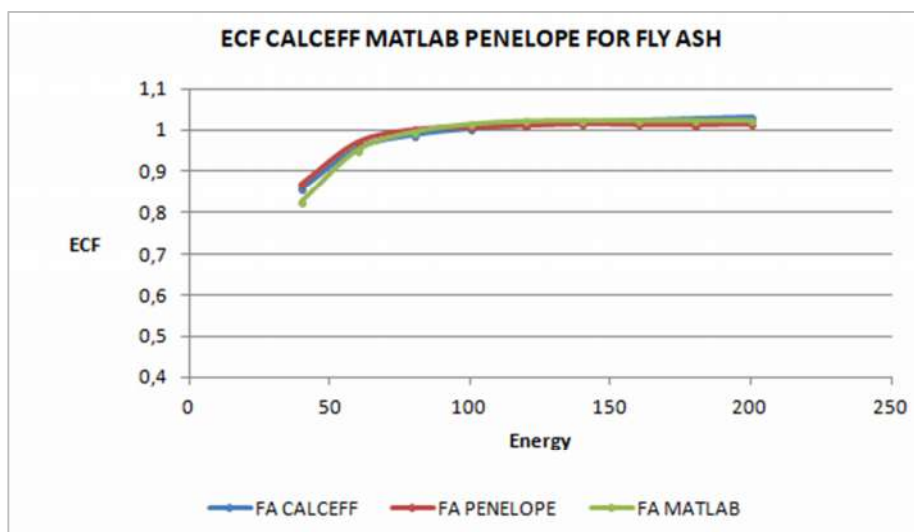
Σχήμα 9: Διαφορά % των τιμών ECF μεταξύ προγράμματος MATLAB και προσομοίωσης M-C

Όπως διαπιστώνεται η διαφορά αυτή έπεσε από το ~60%, που ήταν στην αρχή, στο 21% για το πιο βαρύ υλικό (Lead Slag) και αυτό για τις πιο χαμηλές ενέργειες. Το ίδιο ισχύει για όλα τα υλικά με τις διαφορές να έχουν πέσει κατά πολύ. Αυτό σημαίνει πως οι τροποποιήσεις που έγιναν στο πρόγραμμα έχουν σημαντική επίδραση στην ακρίβεια υπολογισμού του ECF, αλλά υπάρχει χώρος για περαιτέρω αναβάθμιση του προγράμματος αφού οι διαφορές στις χαμηλές ενέργειες σε ορισμένες περιπτώσεις έχουν ακόμα αρκετά υψηλές τιμές.

Μεγάλο ενδιαφέρον έχει επίσης η σύγκριση των αποτελεσμάτων του νέου προγράμματος με αυτά του προγράμματος calceff. Όπως αναφέρθηκε και προηγουμένως, η προηγούμενη έκδοση του προγράμματος MATLAB είχε σημαντικές διαφορές στα αποτελέσματα από το πρόγραμμα calceff. Στην νέα αναβαθμισμένη έκδοση υπάρχουν ακόμα διαφορές αλλά σε μικρότερη κλίμακα. Στα δύο σχήματα 11 και 12 που ακολουθούν φαίνονται ποιοτικά οι συγκρίσεις μεταξύ των τριών μεθόδων υπολογισμού του ECF για δυο υλικά.

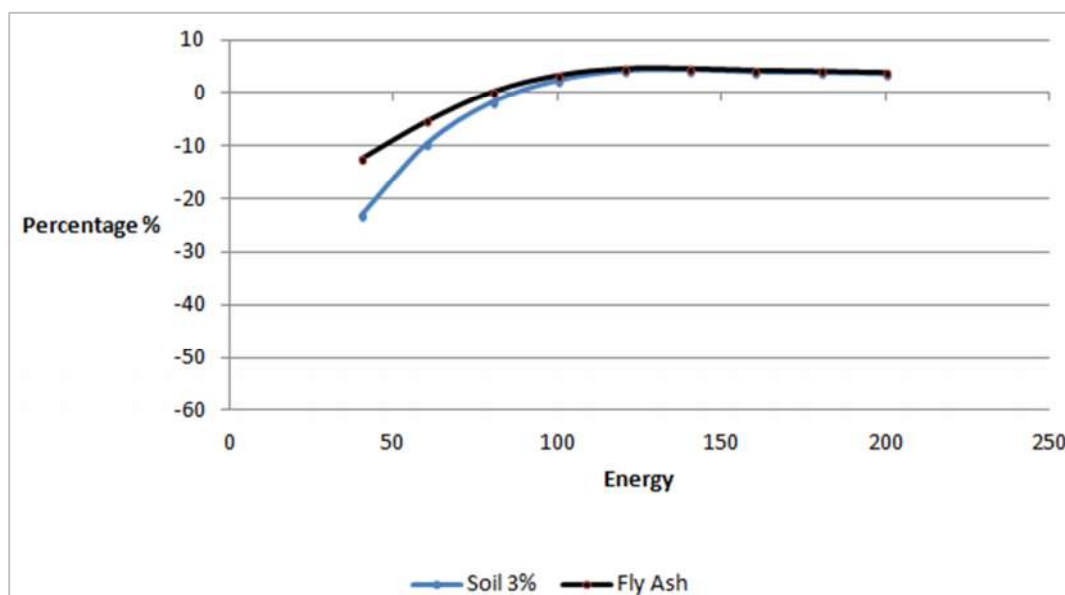


Σχήμα 10: ECF συναρτήσει της ενέργειας και με τις τρεις μεθόδους υπολογισμού για το υλικό χώμα



Σχήμα 11: ECF συναρτήσει της ενέργειας και με τις τρεις μεθόδους υπολογισμού για το υλικό ιπτάμενη τέφρα

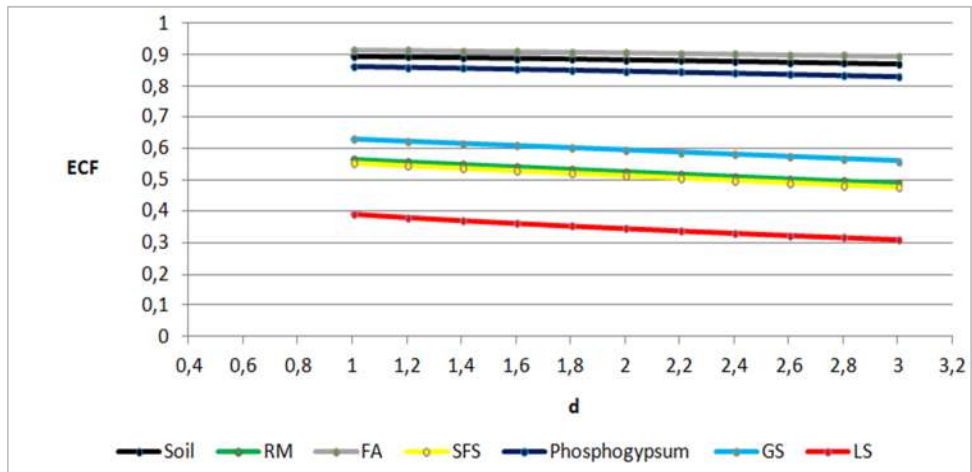
Η μέγιστη αυτή ποσοστιαία διαφορά για το χώμα φτάνει το 22% και για την ιπτάμενη τέφρα το 12%. Φυσικά, για όλα τα υλικά οι μεγάλες αυτές διαφορές βρίσκονται μόνο στις χαμηλές ενέργειες. Είναι ενδιαφέρον το γεγονός ότι οι δύο μέθοδοι που χρησιμοποιούν τις ίδιες τιμές μαζικού συντελεστή εξασθένησης (MATLAB και προσομοίωση M-C) βρίσκονται πιο κοντά από ότι τα αποτελέσματα των δύο προγραμμάτων που χρησιμοποιούν την “integral method” (MATLAB και calceff). Φυσικά το πιο σημαντικό είναι ότι τα αποτελέσματα του προγράμματος MATLAB που βελτιώθηκε στα πλαίσια της ΔΕ να είναι πιο κοντά στα αποτελέσματα της προσομοίωσης αλλά και πάλι, οι τρεις μέθοδοι φαίνεται πως στις υψηλές ενέργειες πλέον συμφωνούν, ενώ στις χαμηλές υπάρχουν αποκλίσεις για συγκεκριμένα υλικά. Στο σχήμα 12 που ακολουθεί καταγράφονται οι ποσοστιαίες διαφορές μεταξύ των προγραμμάτων MATLAB και calceff. Υπενθυμίζεται ότι στο πρόγραμμα calceff η σύσταση αυτών των δυο υλικών είναι διαφορετική σε σχέση με αυτήν που χρησιμοποιήθηκε στα δυο άλλα προγράμματα. Ενδεχομένως, οι διαφορές που εμφανίζονται στις χαμηλές ενέργειες να οφείλονται σε αυτό το γεγονός.



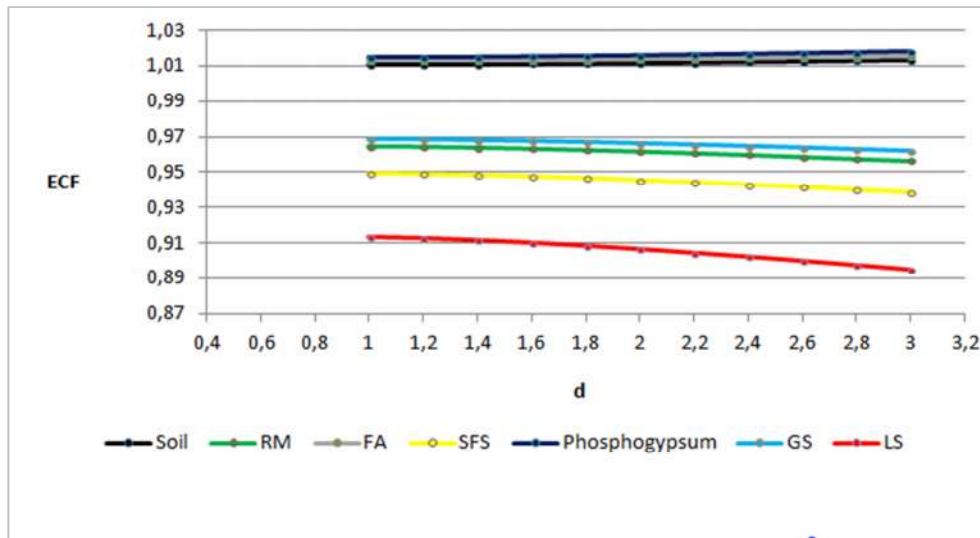
Σχήμα 12: Διαφορά % των τιμών ECF μεταξύ των προγραμμάτων MATLAB και calceff

Με το νέο πρόγραμμα ήταν πλέον πολύ εύκολο να γίνει μία παραμετρική μελέτη της επίδρασης που έχει το βάθος d στον συντελεστή διόρθωσης ECF. Για να γίνει αυτό επιλέχθηκαν δύο ενέργειες ($E=50\text{keV}$ και $E=1000\text{keV}$) και η γεωμετρία “8”. Στη συνέχεια, επιλέγοντας τιμές του d στην περιοχή 1-3 cm με βήμα 0,2cm υπολογίσθηκαν οι αντίστοιχες τιμές του ECF. Με τον τρόπο αυτό προέκυψαν τα διαγράμματα που παρουσιάζονται στα σχήματα 13 και 14. Όπως φαίνεται από τα σχήματα αυτά και για τις δύο τιμές της ενέργειας υπάρχει μια μικρή μείωση του συντελεστή ECF με το βάθος d , με τη μείωση αυτή να είναι μεγαλύτερη για τα υλικά με τη μεγαλύτερη πυκνότητα. Σαφώς λοιπόν παίζει ρόλο η κατάλληλη επιλογή του συντελεστή d για το σωστό υπολογισμό του ECF και αυτό είναι κάτι που θα πρέπει να διερευνηθεί με μεγάλη προσοχή στη συνέχεια.

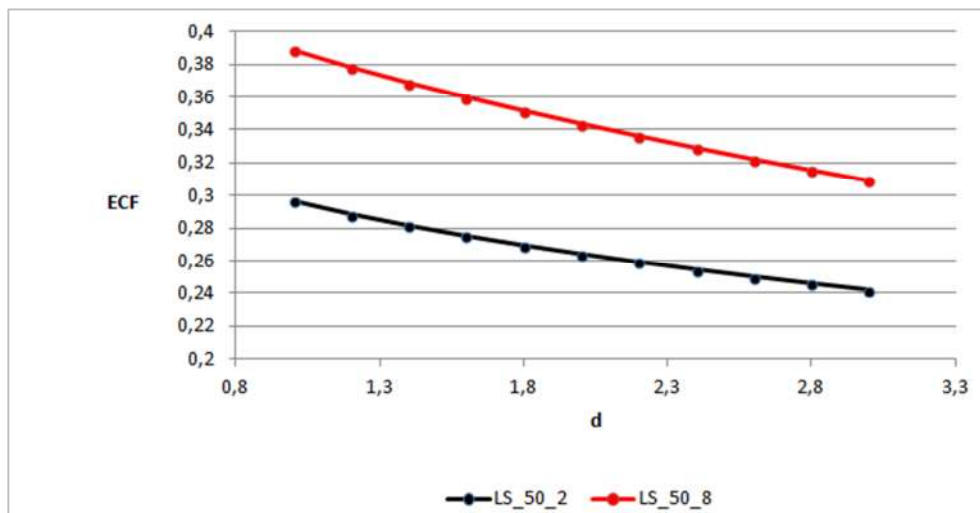
Τέλος, διερευνήθηκε η επίδραση που έχει η επιλογή του βάθους d σε συνδυασμό με τη γεωμετρία – ειδικότερα του πάχους του δείγματος – στην τιμή του συντελεστή ECF. Τα σχετικά αποτελέσματα παρουσιάζονται στο σχήμα 15 για το βαρύτερο υλικό που μελετήθηκε “lead slag”.



Σχήμα 13: ECF συναρτήσει του “d” για E=50keV και για γεωμετρία “8”



Σχήμα 14: ECF συναρτήσει του “d” για E=1000keV και για γεωμετρία “8”



Σχήμα 15: ECF συναρτήσει του “d” για το υλικό LS με ενέργεια E=50keV για τις γεωμετρίες “2” & “8”

Από τα συμπεράσματα των τριών τελευταίων διαγραμμάτων μπορούμε να έχουμε μια πιο ολοκληρωμένη εικόνα για το πως μεταβάλλεται ο συντελεστής ECF συναρτήσει του “d”.

Τελικά, όπως φαίνεται το νέο πρόγραμμα λειτουργεί με ικανοποιητική ακρίβεια στις υψηλές ενέργειες και με μικρότερη ακρίβεια στις χαμηλές. Με τις αλλαγές που έγιναν στο πρόγραμμα έχει αυξηθεί η ακρίβεια και η λειτουργικότητα του καθώς και οι δυνατότητες επιλογής του χρήστη.

Για τα χαμηλής πυκνότητας υλικά που εξετάστηκαν οι διαφορές με τα αποτελέσματα της προσομοίωσης M-C είναι ασήμαντες (1%-5%). Για τα υψηλής πυκνότητας υλικά η διαφορά από τα αποτελέσματα της προσομοίωσης μπορεί να φτάνει το 20% για ενέργειες χαμηλότερες των 200keV. Οι διαφορές αυτές θα μπορούσαν να οφείλονται στην τιμή του ενεργού βάθους αλληλεπίδρασης “d” η οποία φαίνεται να επηρεάζει σημαντικά τα αποτελέσματα. Στο σημείο αυτό θα πρέπει να εστιάσει και η μελλοντική έρευνα στο αντικείμενο αυτό, καθώς θα μπορούσε ενδεχομένως να βελτιωθεί η σχέση πάνω στην οποία βασίζεται η ολοκληρωτική μέθοδος, έτσι ώστε να λαμβάνει υπόψη την περίπτωση ανάλυσης υλικών πολύ μεγάλης πυκνότητας και την επίδραση που αυτή μπορεί να έχει σε παραμέτρους όπως, το ενεργό βάθος αλληλεπίδρασης, ή ενδεχομένως άλλα φαινόμενα, όπως η σχεδόν ελαστική σκέδαση φωτονίων⁸. Συναφώς, μεγάλο ενδιαφέρον θα έχει η μελέτη της επίδρασης της πυκνότητας των υλικών στην τιμή του συντελεστή ECF.

Πάντως, ανεξάρτητα από τις όποιες ανακρίβειες παρουσιάζονται σε ορισμένες ενέργειες και πυκνότητες, το όλο εγχείρημα της τροποποίησης του αρχικού κώδικα M-C κρίνεται ιδιαίτερα επιτυχημένο, καθώς πρόκειται για ένα επαρκώς ακριβές και ιδιαίτερα φιλικό στο χρήστη πρόγραμμα για τον υπολογισμό συντελεστών διόρθωσης αυτοαπορρόφησης σε καθημερινές εφαρμογές. Επιπλέον, η ευκολία χρήσης του προγράμματος επέτρεψε την ανάδειξη της αναγκαιότητας για χρήση συντελεστών ECF ακόμα και για πολύ υψηλές ενέργειες που πλησιάζουν τα 2000 keV.

⁸ Near elastic scattering

CHAPTER 1

INTRODUCTION

Gamma ray spectroscopy is an analytical technique used for the qualitative and quantitative determination of gamma ray emitting radionuclides in a sample. The technique is based on the analysis of the gamma ray spectrum produced by the gamma rays emitted from the sample. When a relative thick sample – like those analyzed in environmental applications – is analyzed through gamma ray spectroscopy, a part of the gamma rays which are emitted from the sample is either absorbed or scattered from the sample material itself. The result is the loss of some photons that would be otherwise recorded under the corresponding photopeak in the spectrum – a phenomenon described as “self-absorption” of the photons within the sample itself. The attenuation of the photon beam emitted by the sample, besides the sample geometrical characteristics, depends upon the density and elemental composition of the sample and the energy of the gamma radiation.

In gamma spectroscopic analysis, quite often samples of large volume and thickness need to be analyzed. In this case – especially when low energy photons are involved – the self-absorption within the sample may be significant. Since the efficiency calibration of the detector is normally performed using a calibration standard made up from material of specific type and density, the difference in self-absorption between the calibration standard material and the sample material needs to be taken into consideration. To this end several methods have been proposed in the literature [2]. The method that has been implemented and is being used at the Nuclear Engineering Laboratory of the National Technical University of Athens (NEL-NTUA) since more than 25 years, is based on the calculation of an efficiency correction factor (EFC) to take into consideration the efficiency difference between the calibration standard and the sample that is being analyzed [2], [5]. For this purpose a computer program has been developed so as to calculate (EFC) for a series of environmental materials often analyzed at NEL-NTUA, like soil, fly-ash, and bottom ash produced in coal burning power plants. For these materials it was considered sufficient at NEL-NTUA to correct for self-absorption only for low energy photons, up to the energy of 200keV, while for higher energies self-absorption was considered negligible [2].

A group of materials often analyzed the last few years using gamma spectroscopy is NORM (Naturally Occurring Radioactive Materials). These materials – mostly by-products of mining activities, metallurgical or other industrial and chemical processes – may contain large amounts of high Z elements, have high density and as a result may have very high self-absorption characteristics, especially for low energy photons. Therefore, the last few years it was deemed of great importance to extend the capabilities of NEL-NTUA to accurately analyze NORM, especially after these materials were regulated by the EURATOM Directive 59/2013 [1] that was transposed to National Legislation in Greece since late 2018. This capabilities extension had to be twofold: (i) towards the analysis of more materials, including high Z and high density materials, such as NORM and (ii) towards the extension of self-absorption corrections for higher than 200keV photons, if needed for these materials.

In [3] the first attempt to extend the capabilities of NEL-NTUA in correcting for self-absorption is presented. In that work a MATLAB computer program was developed for the calculation of ECF,

for a series of NORM, reaching photon energy of 400 keV. The results of the ECF obtained with this program were compared with similar results obtained by other means, including Monte-Carlo simulation. Although the results obtained were interesting and the program was found useful, it turned out that the program had had some weaknesses and in some cases the results were unexpected.

The aim of the present work was to extend and improve, in terms of accuracy and operation, and to thoroughly evaluate the results of the MATLAB program developed in [3] by comparing its results with other means of ECF determination. During this work the improvement of the program output at the low energy region was significant. The program was also extended to give results till the energy of 2000keV, thus providing ECF values for very important photons regularly used in gamma spectrometry – especially when analyzing NORM – like those emitted from short lived ^{222}Rn daughters like ^{214}Bi and ^{214}Pb , ^{228}Ac , ^{212}Pb and ^{40}K . This extension showed that for some materials there is a need to correct for self-attenuation for very high energies, something which in most cases is ignored. The new program is furthermore made more user-friendly, while providing more flexibility to choose between various geometries and materials.

This work consists of six chapters.

The 2nd chapter is a small introduction to gamma ray-spectrometry. It starts with the interactions of gamma rays with matter and continues with the detectors used for gamma ray spectrometry. Then the process of the detector efficiency calibration is presented and the need for self-absorption correction is demonstrated. After a short introduction to some techniques proposed for self-absorption correction, the method used at NEL-NTUA for the calculation of ECF is presented in detail. A small introduction to NORM is also given in this Chapter.

In the 3rd chapter the basic characteristics of the MATLAB program developed in [3] are presented. Typical outputs of the program are shown and comparisons with other means of ECF calculations are made. This chapter is concluded with the presentation of the program weaknesses and limitations.

In the 4th chapter the work done towards the modification, extension and thorough evaluation of the new MATLAB program is presented. The modifications made resulted to (i) more accurate determination of ECF, in a wider energy region and for more materials, (ii) ability of the user to select source to detector geometry, sample geometrical characteristics and material density, (iii) and a user friendly interface.

In the 5th chapter the new program is used for the calculation of ECF for various materials and geometries. The ECF values determined are compared with those obtained by the previous program version as well other means of calculating ECF, including Monte-Carlo simulation. In this chapter a series of graphs and figures are presented to demonstrate the new program improved results in terms of accuracy.

In the last 6th chapter the results and conclusions of this work are presented, together with comments on the new program operation, its weakness and limitations. Ideas for future extension and improvement of the program are also presented, as well as ideas for future research in this field.

CHAPTER 2

GAMMA SPECTROSCOPIC ANALYSIS OF ENVIRONMENTAL SAMPLES

In nature, the nuclei of most atoms are stable. However, certain atoms have unstable nuclei due to an excess of either protons or neutrons. These nuclei are described as radioactive and are known as radioisotopes or radionuclides.

The nuclei of radioactive atoms change spontaneously into other atomic nuclei, which may or may not be radioactive. For instance, Uranium-238 (^{238}U) changes into a succession of different radioactive nuclei – often called daughter radionuclides – until it reaches a stable form, Lead-206 (^{206}Pb). This irreversible transformation of a radioactive atom into a different type of atom is known as disintegration or decay. It is accompanied by the emission of different types of radiation, usually α -particles, or β -particles and in most cases by one or more γ -rays (photons) too. A chemical element can therefore have both radioactive isotopes and non-radioactive isotopes. For example, Carbon-12 (^{12}C) is not radioactive, while Carbon-14 (^{14}C) is radioactive. Because isotopes of the same element have the same electron structure, the chemical properties of the stable and radioactive isotopes of the same element are the same.

All radionuclides are characterized by their half-life $T_{1/2}$. Half-life indicates the time needed for half of the existing radioactive nuclei to decay to the daughter nuclei. Each radionuclide is characterized by a decay constant (λ) which is given by the formula:

$$\lambda = \frac{\ln(2)}{T_{1/2}} \quad (2.1)$$

The average decay rate of a certain number of (N) nuclei in a sample is described by:

$$\frac{dN}{dt} = -\lambda \cdot N \quad (2.2)$$

Thus, eventually the **law of radioactive decay** comes with the following equation:

$$N(t) = N_0 \cdot e^{-\lambda \cdot t} \quad (2.3)$$

which gives the number of nuclei that have not decayed yet after time t , when the number of nuclei at $t=0$ is N_0 .

The determination of a radionuclide is mostly based on the detection and analysis of the radiations which it emits. In most cases it is based on the analysis of the spectrum of its γ -rays (photons), a method called gamma-ray spectroscopy (γ -spectroscopy).

Gamma spectroscopy is a non-destructive analytical technique for the qualitative and quantitative determination of gamma emitting radionuclides. The technique is based on the collection of the spectrum of gamma rays emitted by a source, using a suitable gamma ray

detector. In most cases a high resolution detector, such as an HPGe⁹ detector is used for this purpose. Some of the photons emitted by the source deliver all their energy to the detector, thus resulting to a characteristic peak in the spectrum known as a photopeak. The photons which deliver only part of their original energy to the detector, as a result of an interaction with the detector, the source or the surroundings are recorded in the spectrum as the background continuum. Therefore, a gamma spectrum consists of photopeaks on top of a background continuum. The analysis of the gamma spectrum and the determination of the energy and the area corresponding to the photopeaks observed may result to the determination of the radionuclides emitting the photons which are detected, as well as their activity (Bq). The interactions of the gamma rays (photons) with the detector, the detector-shielding and the sample itself are of great importance to the shape of the spectrum and the size of the photopeaks especially. The most important parameter to describe the interactions of gamma rays with materials in general is the *linear attenuation coefficient* μ , which expresses the probability per unit length of photon track, for a photon to interact with a material. The linear attenuation coefficient strongly depends on the material type and density as well as the photon energy. It is therefore to be expected that different materials having different μ values will result to a different attenuation of photons.

2.1 Interactions of gamma rays with matter

Gamma rays refer to electromagnetic radiation (no rest mass, no charge) of very high energies which are very penetrating into matter. They are emitted by unstable nuclei in their transition from a high energy state to a lower state, usually after a previous beta or alpha decay.

Gamma rays interact with matter through a series of interactions. Although a large number of possible interactions are known, there are four key interaction mechanisms with matter: the Photoelectric Effect, the Compton Scattering, the Elastic Scattering and Pair Production. All four of them are briefly described in the following paragraphs. It should be noted here that, X-rays, which are also electromagnetic radiation as gamma rays yet of different origin, have the very same characteristics as gamma rays and interact with matter with the very same mechanisms.

2.1.1 Photoelectric Effect

In the photoelectric effect, a photon undergoes an interaction with an electron which is strongly bound in an atom (e.g. a K-shell electron). In this interaction the incident photon completely disappears and an energetic electron (often call photoelectron) is ejected from one of its bound shells. The kinetic energy of the ejected photoelectron (E_e) is equal to the incident photon energy ($h \cdot \nu$) reduced by the binding energy of the photoelectron in its original shell (E_b).

$$E_e = h \cdot \nu - E_b \quad (2.4)$$

⁹ High Purity Germanium detector

Therefore, photoelectrons are only emitted by the photoelectric effect when photon energy exceeds a threshold - the binding energy of the electron in the shell. For low energy gamma rays and for high Z materials the photoelectron is the dominant interaction of photons with matter.

Following a photoelectric interaction, an ionized atom is created with a vacancy in one of its bound shells. This vacancy will be quickly filled by an electron from a shell with a lower binding energy (outer shell) resulting to the emission of a characteristic X-ray. The rearrangement of electrons from other shells creates another vacancy, which, in turn, is filled by an electron from an even lower binding energy shell. Therefore a cascade of more characteristic X-rays can be also generated (Fig. 2.1).

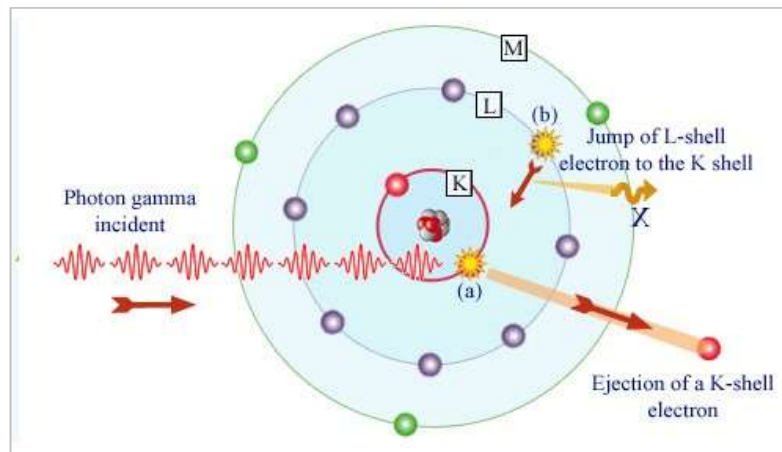


Figure 2.1: Photoelectric interaction

Since the electrons and the low energy X-rays emitted after a photoelectric interaction are not very penetrating, it is very probable that the total energy of the original photons is deposited locally. As a result, when a photon interacts with a detector through photoelectric interaction, the original photon energy will be most likely fully absorbed within the detector.

2.1.2 Compton scattering

Compton scattering is the inelastic scattering of a photon (which may be an X-ray or gamma ray photon) by an electron of the outer shells, loosely bound in the atom. In Compton scattering, the incident gamma ray loses energy and is deflected through an angle (θ) with respect to the original photon direction. The photon energy lost is transferred to an electron. This energy can vary from zero to a large fraction of the incident gamma ray energy, because all angles of scattering are possible. The Compton Scattering was observed by A.H. Compton in 1923 at Washington University in St. Louis. Compton earned the Nobel Prize in Physics in 1927 for this new understanding about the particle – nature of photons.

When a photon suffers a Compton scattering, only part of its energy will be deposited locally (mainly that carried by the recoil electron), while the rest of the energy carried by the scattered photon will be most probably deposited elsewhere (Fig. 2.2).

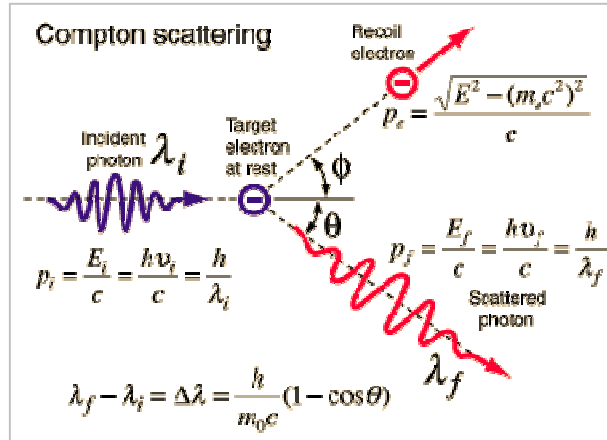


Figure 2.1: Compton Scattering

2.1.3 Rayleigh elastic scattering

In Rayleigh scattering, the photon is scattered by bound atomic electrons, without causing atomic excitation or ionization and therefore no energy loss (Fig. 2.3). In essence, Rayleigh scattering is a scattering by the atom as a whole. Therefore the charge distribution of all electrons in an atom must be simultaneously considered. This kind of scattering occurs mainly with very low energy photons, when a photon does not have enough energy to ionize the specific atom shell.

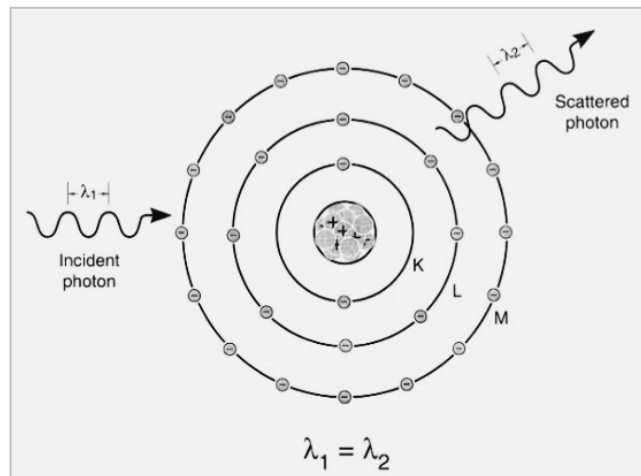


Figure 2.3: Rayleigh Elastic Scattering

2.1.4 Pair Production

In general, pair production is a natural phenomenon where energy is directly converted to matter. The phenomenon of pair production can be viewed in two different ways. One way is a particle-antiparticle production and the other is particle-hole production. The particle-antiparticle production is the result of the interaction of a package of electromagnetic energy (high energy gamma ray or X-ray) travelling through matter. It is one of the possible ways in which gamma rays interact with matter and at high energy this interaction dominates.

In order for an electron-positron pair production to occur, the photon energy must exceed a threshold energy, which is equivalent to the rest mass of the two particles ($1,02\text{MeV}=2\cdot 0,511\text{MeV}$). The excess energy above 1,02 MeV will be equally shared between the two particles as kinetic energy (Fig. 2.4). The presence of an electric field of an atom is essential in order to satisfy conservation of momentum and energy. In order to satisfy both conservation of momentum and energy, the atomic nucleus must receive some momentum. Therefore a photon pair production in free space cannot occur. Pair production is most probable for high energy photons and high Z materials.

Since positron is the anti-particle of the electron, when the positron comes to rest, after losing its kinetic energy, it interacts with another electron, resulting in the annihilation of the both particles and the complete conversion of their rest mass back to pure energy in the form of two oppositely directed 0,511MeV gamma rays. The pair production phenomenon is therefore related with the creation and destruction of matter in one reaction.

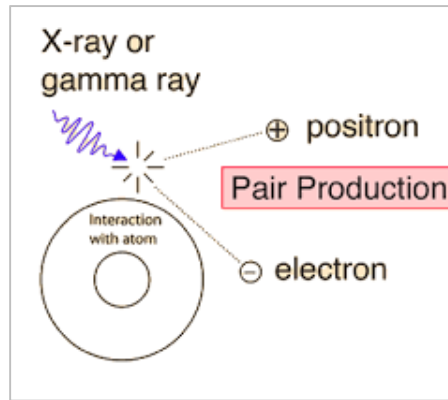


Figure 2.4: Pair Production simple schematic

2.1.5 Linear and mass attenuation coefficients

All the interactions described in the previous paragraph – with the exception of the elastic scattering – result to the loss of the original photon energy (photoelectric effect and pair production) or reduction of its energy and change in its direction (Compton scattering). Therefore, the original photon beam emitted by the source is attenuated (lost or scattered) as a result of these interactions.

A measure of the probability of an interaction to occur with an atom is the cross section. The total cross section is a measure of the probability of any interaction to occur with the atom and is equal to the sum of all cross sections:

$$\sigma = \sigma_f + \sigma_c + \sigma_p + \sigma_e \quad (2.5)$$

where:

- σ_f : Photoelectric effect cross section
- σ_c : Compton scattering cross section
- σ_p : Pair production cross section
- σ_e : Elastic scattering cross section

In most cases elastic scattering is ignored and therefore σ_e is considered equal to zero.

Depending on the gamma ray energy and the absorber material, one of the three remaining partial cross sections may become the dominant one as can be seen in Figure 2.5. At low energies, the photoelectric effect dominates. Compton scattering dominates at intermediate energies and for low Z materials. Finally, electron–positron pair production dominates at high energies.

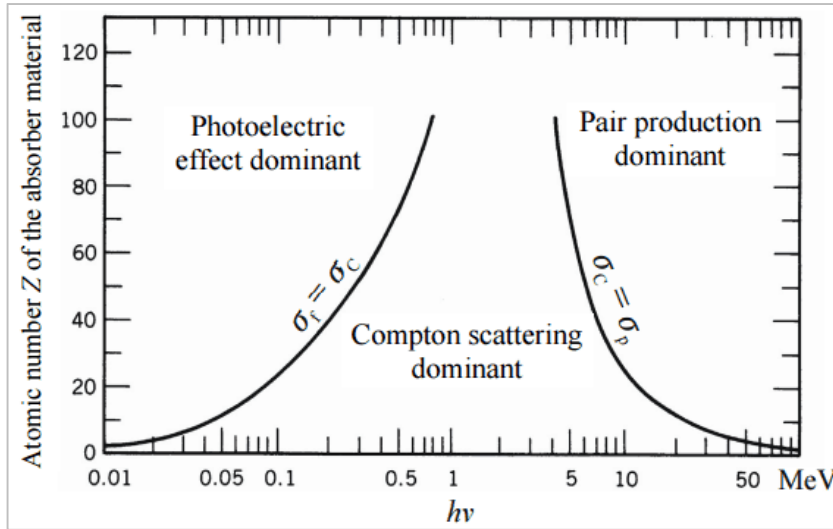


Figure 2.5: The relative importance of various processes of gamma radiation with matter

For a monoenergetic narrow photon beam with intensity I (photons/cm²·s) falling on a slab with thickness dx , the attenuation of the photon beam as a result of the interaction of the photons with the slab material is given by the formula:

$$-dI = I \cdot \mu \cdot dx \quad (2.6)$$

where:

dI : the number of photons removed from the photon beam as a result of any interaction

I : the number of photons in the original photon beam (photons/cm²·s)

dx : the slab thickness (cm)

μ : the probability per unit length of a photon to interact with the slab with any interaction, known as the **linear attenuation coefficient**,

The attenuation of gamma radiation can be then described by the following equation, which is known as the **exponential law of photon attenuation** through a slab of thickness x (Fig. 2.6):

$$I = I_0 \cdot e^{-\mu \cdot x} \quad (2.7)$$

Where I_0 and I are the original and the attenuated photon beam intensities respectively.

The linear attenuation coefficient μ is the sum of the attenuation coefficients for all interactions:¹⁰

$$\mu = \tau_{photo} + \sigma_{Compton} + \kappa_{PP} \quad (2.8)$$

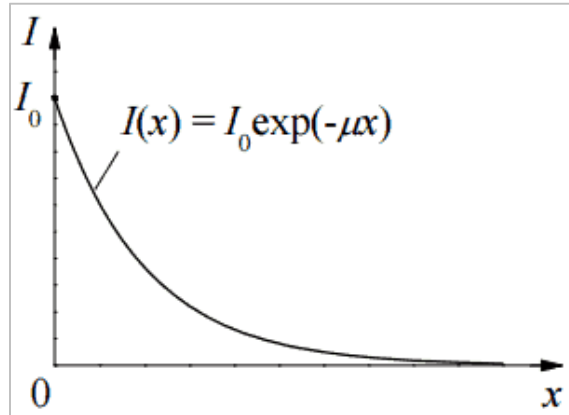


Figure 2.6: The exponential law of photon attenuation

The linear attenuation coefficient depends on the photon energy, the material type and the material density ρ . When characterizing a material for its absorbing properties, the mass **attenuation coefficient** μ_m is also used. The mass attenuation coefficient is defined as the ratio of the linear attenuation coefficient and the absorber density (μ/ρ) and its units are [$\text{cm}^2 \cdot \text{g}^{-1}$]. The attenuation of gamma radiation can be then described by the following formula:

$$I = I_0 \cdot e^{-\mu_m \cdot x \cdot \rho} \quad (2.9)$$

Where ρ is the material density, μ_m is the mass attenuation coefficient and the product $x \cdot \rho$ is the **mass thickness** of the slab. By definition, the mass attenuation coefficient depends only on the material and photon energy and is independent of material density.

2.2 Basics of gamma ray spectrometry

Gamma ray spectrometry is an analytical method that allows the identification and quantification of gamma emitting radionuclides in a variety of matrices. Applications of gamma ray spectrometry include: nuclear physics, radioecology, monitoring in nuclear facilities, health physics, nuclear medicine etc. In one single measurement and with little or no sample preparation, gamma ray spectrometry allows the detection and quantification of several gamma emitting radionuclides in the sample. The result of the measurements is the gamma spectrum (Fig. 2.7) where a series of lines can be observed over a continuous background. Each line corresponds to the photons of a specific energy (photopeak) emitted by the source, which have deposited all their energy to the detector.

¹⁰ Each coefficient corresponds to the probability per unit length that a photon interacts with the specific interaction.

The whole process in a gamma spectroscopic analysis is briefly described next. The radionuclides in the analyzed sample emit one or more gamma rays with characteristic energies. These gamma rays may reach the detector and interact with it. The signal produced as a result is detected by the detector, treated by the electronic setup and then presented in the form of a spectrum. In more detail, first the photons interact with the detector material in the ways described in the previous chapter (chapter 2.1) and their energy is converted in kinetic energy of charged particles (electrons “e⁻” and possibly positrons “e⁺”). Then, depending on the detector type, electron–ion pairs, electron-hole pairs and excited molecular states are produced as a result of the interactions of the charged particles with the detector material.

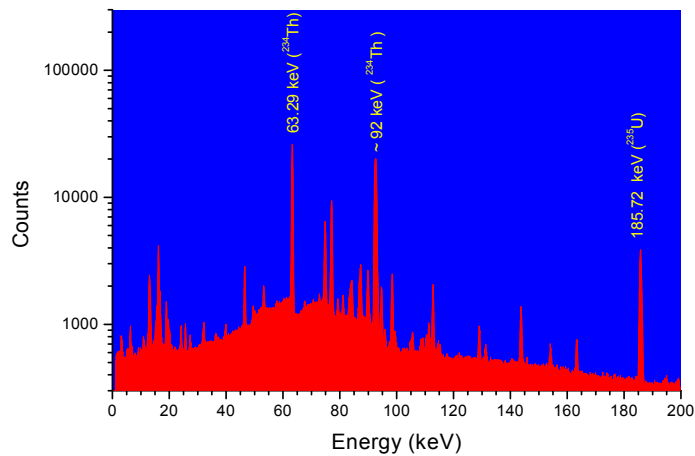


Figure 2.7: Typical gamma spectrum with a Low Energy Germanium detector

In the case of HPGe detectors (Fig. 2.8) which are mainly used in gamma spectroscopy applications, the charge carriers are electron–hole pairs. The collection of the charge carriers by the system electronics result to the signal (pulse) produced by the photon interaction with the detector. There are many components in the gamma spectrum, but two of them are the most important. The first one is the Full Energy Peak (FEP) which is basically the result of detecting full energy events. The second one is the background continuum which is the result of the partial deposition of the original photon energy to the detector.



Figure 2.8: High Purity Germanium detector (HPGe) at NED-NTUA

The position of the photopeak in the spectrum reflects to the photon energy and may result to the emitting radionuclide detection. The net area under the photopeak (Fig. 2.9) corresponds to the total number of photons recorded under the photopeak during measurement and may result to the detected radionuclides quantification.

A gamma ray spectrometer is a gamma ray detector and consists of three parts. The first one is the detection system that includes the energy sensitive detector and the shielding which is very important – especially for low activity measurements. The second one comprises the electronics that analyze the pulses produced by the interaction of photons with the detector and process the detector signals, like the multi – channel analyzer (MCA). The final part is the data analysis system which includes the gamma analysis software. The most important information in a gamma spectrum is the photopeaks detected. The net¹¹ area under a photopeak corresponds to the photons of a specific energy E that have been detected during spectrum collection.

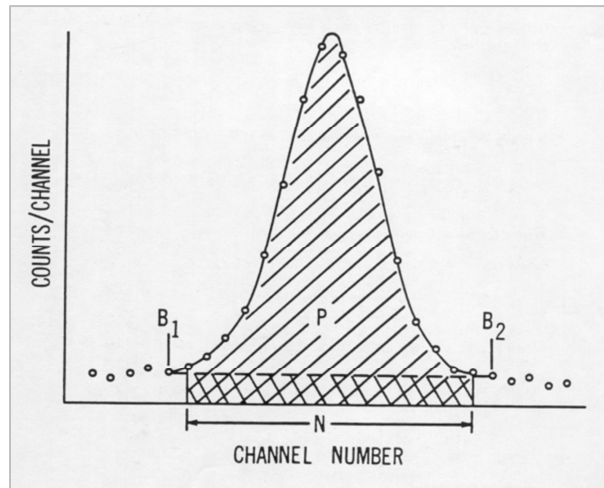


Figure 2.9: The photopeak in a typical gamma spectrum

This number of photons is related to the activity of the respective radionuclide with the following formula:

$$activity = \frac{area}{time \cdot yield \cdot efficiency} \quad (2.10)$$

where:

time : is the duration of spectrum collection

yield : is the emission probability of the photons of the specific energy

efficiency: is the full energy peak efficiency of detection of the energy E photons

As it is made clear from formula 2.10, full energy peak efficiency is a key factor in gamma spectroscopy and a correlation between the efficiency and the photon energy for the specific source-to-detector geometry used, has to be determined prior to any analysis. This

¹¹ The area (P) above the background

correlation is determined either experimentally or using other techniques, such as Monte-Carlo simulation. It is very important to notice that this correlation is valid for the material of the calibration source. For a material of a different type or density the efficiency may not be the same, due to the different interactions of the photons between the two materials, and therefore due to the different photon attenuation. This problem of the different attenuation within the source, known as self-absorption is more pronounced for high Z and dense materials, thick samples, and low energy photons.

2.2.1 Low Energy Germanium Detectors

For the detection and the spectroscopic analysis of low energy photons (e.g. below 200keV or even lower) a specific type of detector may be used. These detectors have a special configuration that allows the detection of these low energy photons with higher efficiency than conventional HPGe detectors (Fig. 2.10). The Low Energy Germanium Detector (LEGe) is in all aspects optimized for performance at low and moderate energies and has specific advantages over conventional planar or coaxial detectors. The LEGe detector is fabricated with a thin front and side contact, thin dead layer and also a window typically made of Be, or carbon fibers. The area of the rear electric contact of the detector is less than the whole detector area, which gives a lower detector capacitance compared to a planar detector of similar size. Since preamplifier noise increases with detector capacitance, the LEGe detector affords lower noise than any other detector geometry and consequently better energy resolution¹² at low and moderate energies. This characteristic is of particular importance, since in the low energy region – besides the gamma rays – a large number of X-rays of different origins are normally detected too, resulting to a complicated spectrum. Therefore, LEGe detectors are preferable in low energy gamma spectroscopy, for the detection for radionuclides like: ^{210}Pb (46.52keV), ^{234}Th (63.29keV) and ^{241}Am (59.54keV).

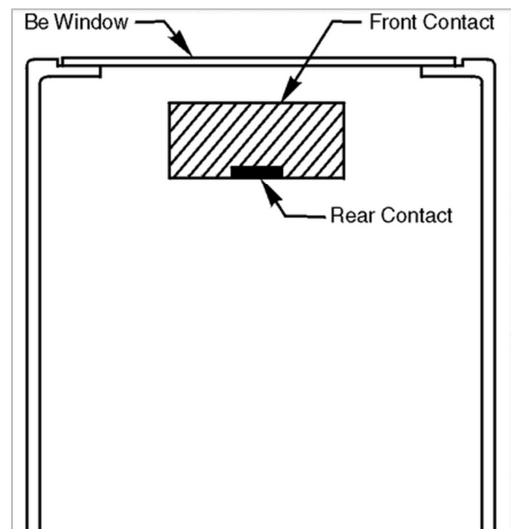


Figure 2.10: LEGe Schematics.

¹² Energy resolution is an expression of the ability of the detector to resolve between photopeaks of similar energy and is usually expressed as the Full Width at Half Maximum of a photopeak (FWHM)

2.2.2 Efficiency Correction Factor in Low energy gamma spectrometry

As previously mentioned, one of the problems in gamma ray spectroscopy is the different attenuation of the photons inside the source used for efficiency calibration and the material of the analyzed sample. As a result, the counting efficiency during the analysis of samples can be significantly affected by this different self-absorption, particularly when a radionuclide emits low-energy photons. Self-absorption may be defined as the absorption of photons by the sample emitting them. These absorbed photons do not reach the detector and, if appreciable, counting efficiency can be significantly reduced. Self-absorption depends on the photon energy, the sample composition, namely its effective atomic number and its density; furthermore it depends on sample geometry – especially sample thickness.

The importance of self-absorption increases as the energy of the photons decreases and the density of the sample gets higher. Several radionuclides detected in environmental samples emit photons in the low-energy region below 80keV, like: ^{210}Pb (46,52keV), ^{234}Th (63,29keV) and ^{241}Am (59,54keV). For this reason, it is generally accepted [2] that corrections are needed below about 200keV. As it will be shown in this work, there are cases where correction is needed for much higher energies. This work will be focused on photon energies between 40keV and 2000keV.

In general, to take into consideration the difference between the efficiency obtained during efficiency calibration, and the actual efficiency of the detector during the analysis of a specific sample, an efficiency correction factor (ECF) “ η ” [5] may be used. This factor may be defined as the ratio:

$$\eta = \frac{eff_{sample}}{eff_{cal_std}} \quad (2.11)$$

Where:

eff_{sample} : the efficiency of photon detection for the sample material

eff_{cal_std} : the efficiency of photon detection for the calibration source material

If the efficiency of the detector for a specific source-to-detector geometry and material is known – e.g. from a previous experimental calibration – and ECF is also known, then the actual efficiency during the analysis of a sample is determined as the product:

$$eff_{sample} = eff_{cal_std} \cdot \eta \quad (2.12)$$

In the literature, a small number of methods that can be applied for the determination of ECF may be found.

One such method involves Monte Carlo simulation. If for a specific source-to-detector geometry, both eff_{sample} and eff_{cal_std} are determined for the same energy, then, formula 2.11 gives ECF. One might claim that in this case there is no need for ECF calculation since eff_{sample} is already known. It should be emphasized however that, in case the detector geometry is not known with good accuracy, then, the efficiency correction factor calculated as the ratio of the two efficiencies determined via simulation, tends to rule out the inaccuracy introduced due to the detector geometrical characteristics. The ECF calculated this way should be then

used to correct the experimentally determined detector efficiency. Another good reason to calculate ECF using M-C simulation is to compare with the results of other methods.

Another method for the determination of ECF is based on the measurement of the attenuated and the non-attenuated photon beam which is produced by an external photon source put over the sample vessel. This method is based on the following formula¹³ proposed in [25].

$$I = I_0 \cdot \frac{1 - e^{-\mu \cdot x}}{\mu \cdot x} \quad (2.13)$$

where:

I_0 : is the non-attenuated photon beam. In this case the source is put over an empty sample vessel

I : is the attenuated photon beam through the specific sample

μ : is the linear attenuation coefficient of the material

x : is the sample thickness

The ECF is calculated as the ratio of the values of I/I_0 determined for both the sample and calibration source. This method correlates the attenuation of an external photon beam through the sample, to the self-absorption of the photons emitted within the sample. However, this technique has a limited accuracy and is applicable for a specific range of sample thickness [25] and it will not be used in this work. For this purpose no more details will be given.

A third method for the calculation of ECF is based on a formula that was introduced by [4]. This method simply known as the “Integral Method” has been used by [5] in order calculate the efficiency correction factor that is being used at NEL-NTUA for self-absorption corrections, when analyzing environmental samples using low energy photons, below 200keV. For this purpose a FORTRAN computer program named calceff has been developed and is integrated within the gamma spectroscopic analysis code SPUNAL used at NEL-NTUA.

2.2.3 The Integral Method for the determination of ECF

The “Integral Method” was developed as an analytical way to calculate the efficiency correction factor due to the different self-attenuation properties of two materials – the calibration standard and the sample that is being analyzed – provided that the source-to-detector geometries are identical. The method is based on the assumption that **“all photons emitted by the calibration standard and the sample that is analyzed are absorbed by a “fictitious” point detector, situated inside the actual detector at a specific depth”** (Figure 2.11). The fictitious point detector lays at a depth d_e inside the actual detector, which is known as **“effective interaction depth”** that has to be experimentally determined, applying a process that will be described in the next paragraph.

¹³ It is often reported as the “self-absorption formula”

In formula 2.14 one can identify two parts:

- one part which is purely geometry specific and should be the same regardless of the sample material, and
- one part which includes information about the attenuating properties of the material through μ , which in general is differs between calibration source and sample. This second part is given by the formula:

$$J(\mu) = \int_0^R \int_0^t \frac{e^{-\mu z}}{r^2 + (x+d)^2} \cdot r \cdot dx \cdot dr \quad (2.17)$$

It is therefore obvious, that the efficiency correction factor η between the sample material and the calibration standard material can be calculated by the formula:

$$\eta = \frac{\varepsilon_{v, sample}}{\varepsilon_{v, cal_std}} = \frac{J(\mu_{sample})}{J(\mu_{cal_std})} \quad (2.18)$$

where:

μ_{cal_std} : calibration source linear attenuation coefficient

μ_{sample} : sample source linear attenuation coefficient

As shown from the previous formulas, for a specific detector, “ η ” depends on the linear attenuation coefficient of the calibration source, the linear attenuation coefficient of the sample material and on the geometry characteristics of the sample. Needless to say, this method is applicable only for cylindrical sources.

2.2.4 The detector effective interaction depth

As the photons emitted from the volume source are not absorbed in the surface of the actual detector but instead at different depths inside the detector, the “fictitious” point detector should be positioned in a place where it would produce the same results with the actual detector. Therefore the effective interaction depth d_e corresponds to the average depth of interaction of photons within the actual detector. The depth d_e should depend on the photon energy and the type and geometry of the detector.

The effective interaction depth for a specific detector and photon energy should be experimentally determined, following the procedure described in [4]. This procedure requires the positioning of a point source which emits photons of the energy of interest along the axis of the actual detector and in various distances from it, and recording the count rate of the photons detected for each distance. Then, taking into consideration the inverse square law, with a simple graph of the recorded count-rates it is easy to determine the effective interaction depth.

By applying this technique, the effective interaction depth for the LEGe detector installed at NEL-NTUA [2] has been estimated equal to:

- 1.00 cm ± 1.4%, for 59.54 keV photons
- 1.34 cm ± 0.9%, for 122.06 keV photons
- 1.33 cm ± 1.33% for 661.66keV photons

However, a value of 1cm for d_e has been used so far for efficiency correction for all energies. In the present work the effect of using different values for d_e on ECF calculation is also investigated.

2.3 Naturally Occurring Radioactive Materials (NORM)

All minerals and raw materials contain trace amounts of radionuclides of natural origin. The most important radionuclides – from the radiation protection point of view – are the radionuclides of the Uranium (^{238}U) series (Fig. 2.12), Thorium (^{232}Th) series (Fig. 2.13) and (^{40}K). For most human activities involving minerals and raw materials, the levels of exposure to these radionuclides are not significantly greater than normal background levels and are of no concern from the radiation protection point of view. However, certain work activities can give rise to significantly enhanced exposures that may need to be controlled by regulation. A material giving rise to these enhanced exposures has become known as Naturally Occurring Radioactive Material ¹⁴(NORM).

The NORM acronym potentially includes all naturally radioactive elements found in the environment. However, the term is used more specifically for all naturally occurring radioactive materials where human activities have increased the potential for exposure, compared with the unaltered situation. Concentrations of actual radionuclides may or may not have been increased; if they have increased, the term technologically - Enhanced NORM (TENORM) may also be used.

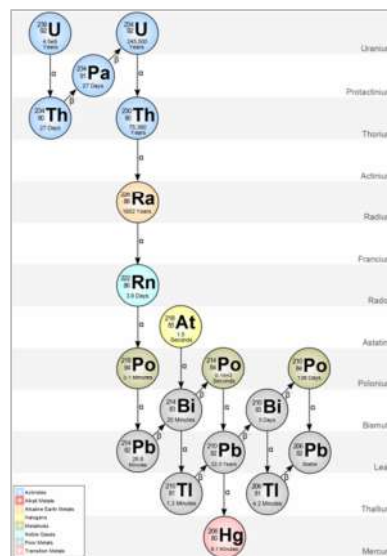


Figure 2.12: Uranium series

¹⁴ "World Nuclear Association" (<https://www.world-nuclear.org/information-library>)

Long lived radionuclides such as ^{238}U , ^{232}Th and ^{40}K and any of their decay products, such as radium and radon isotopes are examples of radionuclides found in NORM. These radionuclides have always been present in the Earth's crust and atmosphere and are concentrated in some places, such as uranium ore bodies which may be mined. The term NORM is used also to distinguish "natural radioactive material" from anthropogenic sources of radioactive material, such as those produced by nuclear power plants or used in nuclear medicine.

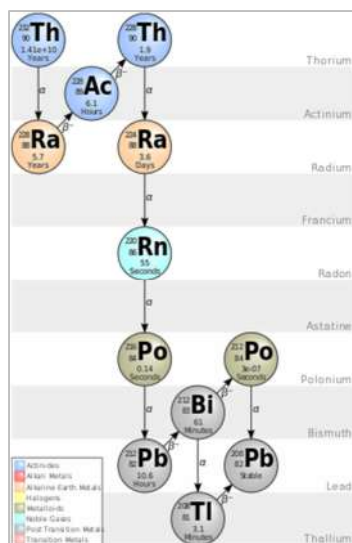


Figure 2.13: Thorium series

By-products, or waste produced during a series of industrial activities, such as smelting, metal production industry, fertilizer industry, fossil fuel burning for electricity production, oil extraction, geothermal energy production etc, are quite often characterized as NORM. This particular group of NORM may have high density and contain significant amounts of high Z elements. As a result, when analyzing these materials using gamma spectrometry techniques, the problem of photon self-absorption may become much more significant compared to that observed in other environmental materials such as soil or sediments.

In this work, a series of NORM was examined with regard to their photon absorbing properties and the need to use an efficiency correction factor, when applying gamma spectroscopic techniques for their analysis. Six typical NORMs were analyzed for their photon self-absorption properties. As the matrix of many calibration sources is 4M HCl solution, the absorbing properties of this material were also examined. Another material that was also analyzed – mainly for comparison reasons – was a typical soil with 3% humidity content. All these materials – with the exception of 4M HCl – are considered as typical environmental materials and typical weight composition and density tables for them are listed in the (ANNEX V). Finally, water was also examined as a sample material, since the analysis of water samples is a routine type of analysis at NEL-NTUA. The materials examined during this work are:¹⁵

¹⁵ The code names used during this work for the materials is in parentheses

- Soil with 3% moisture [**Soil 3%**]
- Red Mud (waste generated in Bayer process) [**RM**]
- Fly Ash [**FA**]
- Phosphogypsum [**PG**]
- Lead Slag [**LS**]
- Granulated Slag [**GS**]
- Shaft furnace slag [**SFS**]
- 4M HCl solution (Calibration Material) [**4M HCl**]
- Water [**Water**]

In the paragraphs that follow more details on the materials examined are provided.

2.3.1 Soil

Soil (Fig. 2.14) is simply a porous medium consisting of minerals, water, gases, organic matter and microorganisms. A traditional definition for soil is: *“soil is a dynamic natural body having properties derived from the combined effects of climate and biotic activities, as modified by topography, acting on parent materials over time”* [52].



Figure 2.14: Natural soil

In more detail, the largest component of soil is the mineral portion, which makes up approximately 45% to 49% of the volume. Soil minerals are derived from two principal mineral types. Primary minerals, such as those found in sand and silt are those soil materials that are similar to the parent material from which they formed. They have often round or irregular shape. Secondary minerals, on the other hand, result from the weathering of the primary minerals, which release important ions and more stable mineral forms such as silicate clay. The texture of soil is based on the percentage of sand, silt and clay found in that soil. The identification of sand, silt and clay is based on size. Water is the second basic component of soil. Water can make up approximately 2% to 50% of the soil volume. The capacity of a soil to hold water is largely dependent on soil texture. The more small particles in soil, the more water the soil can retain. The next basic component of soil is organic matter

which is found in soils at levels of approximately 1% to 5%. Organic matter is derived from dead plants and animals and as such has a high capacity to hold onto and/or provide the essential elements. The last component found in soils is gases or air. Because air can occupy the same spaces as water, it can make up approximately 2% to 50% of the soil volume. Oxygen is essential for root and microbe respiration.

2.3.2 Red Mud

Red mud is a by-product of the Bayer process used for the production of alumina from bauxite. It is usually stored in dams, where the possibility of accidents cannot be excluded (Fig. 2.15). Its composition depends upon its parent material (bauxite) from which it is produced. It is present in the form of slurry, having 10-30% solid materials and high pH. Red mud contains a large amount of Al and Fe oxides.



Figure 2.15: Red Mud accident in Hungary

2.3.3 Fly Ash

Fly ash is a coal combustion by-product (Fig. 2.16). It is among the by-products that make up the most abundant waste materials worldwide. If not collected, this waste material is released with the flue gas in a coal fired power plant. Fly ash exists after fossil fuel combustion because ash adheres to coal, making up between 1–15% of its weight. Moreover it is composed of tiny, airborne particles and is thus considered to be a type of a particulate matter or particle pollution.

To prevent the ash from escaping when the coal is burned, electrostatic precipitators (ESP) are used to reduce the emission of fly ash to the atmosphere. Additionally, other stack filtration devices such as bag houses and scrubbers are used to reduce the emission of fly ash. These methods are able to catch most, but not all, of the fly ash as they are unable to capture particles that are less than a micrometer in diameter. These small particles escape the flue stacks into the air. Fly ash is a typical NORM analyzed for its chemical composition and radionuclide content. Along with the health and environmental impacts of fly ash, an additional issue is that it exists in massive quantities. Fly ash may be recycled and used in the production of cement, concrete and asphalt.

Fly ash can have different chemical makeup, depending on where the coal was mined. This ash can contain lead, arsenic, mercury, cadmium, uranium, thorium and their decay products. The U.S. Environmental protection Agency¹⁶(EPA) has found that significant exposure to fly ash and other components of coal ash increases the risk of cancer and other respiratory diseases development.



Figure 2.16: Fly ash piles

2.3.4 Phosphogypsum

Phosphogypsum is a by-product from the processing of phosphate rock in plants producing phosphoric acid and phosphate fertilizers. The wet chemical phosphoric acid treatment process, or “wet process”, in which phosphate ore is digested with sulfuric acid, is widely used to produce phosphoric acid and calcium sulfate as by-product.

The world production of phosphogypsum annually is estimated to about 300Mt. This by-product contains various impurities, both chemical and radioactive and is usually stockpiled within special areas (Fig. 2.16). The problem of phosphogypsum has already been recognized as an international ecological problem. For example, huge amounts of phosphogypsum have accumulated in Florida, Europe, Canada, Morocco, Togo, India, China, Korea, Israel, Jordan, Syria, Russia and other parts of the world.

The building materials industry seems to be the largest among all the industries which is able to reprocess amounts of this industrial by-product. However, only 15% of world phosphogypsum production is recycled in building materials industry – mainly in the manufacture of Portland cement – while the rest 85% is disposed off without any treatment. Disposed phosphogypsum is usually dumped in large stockpiles occupying considerable land areas and causing serious environmental damage due to both chemical and radioactive contamination.

The key problem restraining the utilization of phosphogypsum in construction is its radioactivity content – mainly ²²⁶Ra content – and the possible effect on human health. The remaining impurities can be extracted relatively easily.

¹⁶ EPA regulation on website : (<https://www.epa.gov/coalash/coal-ash-rule>)



Figure 2.17: Phosphogypsum pile

2.3.5 Slags

Many metal processing industrial activities produce various types of slags as by-products. Typical slag types examined in this work are:

Lead Slag

Lead slag is a by-product of lead production process, originating mainly from two pathways: lead ore smelting and waste lead-acid battery recovery [23]. The production of primary lead is a process of extracting lead from lead sulfide concentrate by smelting. Smelting process mainly includes sinter plant–blast furnace route and direct smelting reduction process, including oxidation, reduction, and refining. Lead slag has a black color and a glassy appearance. The density of lead slag varies between 2.5 and 3.9 g/cm³. In this work a typical lead slag density of 2.645g/cm³ is considered. The particle size of lead slag is between 0.1 and 4 mm [24].



Figure 2.18: Lead Slag

The main disposal methods of lead slag are landfill and stockpiling; these methods occupy massive land and may result to a series of environmental problems. The environmental stability of lead slag depends on various factors: pH, mineral phase in the slag, influence of environmental conditions and the interaction time between slag and water. Lead slag is

easier to release Zn, Fe and Ca under acidic conditions, and it is easily weathered by water. The presence of oxygen in the open air enhances oxidative weathering, and promotes the formation of secondary oxide and carbonate phases, which are easier to release toxic elements. With the weathering and rainfall, toxic elements, such as Pd, Zn, in the slag may penetrate the soil, thus resulting in toxic elements pollution. Because the toxic elements in the soil are not decomposed by microorganisms, they will migrate to the plant body and impact the surrounding plants and animal growth.

Granulated Slag

Granulated Slag is an amorphous, coarse sand-sized material. Although average granule size of granulated slag depends on many factors such as its source it is about 1 - 1.5 mm.

Granulated slag has off-white or near-white color and it exhibits excellent cementitious properties, when finely ground and combined with Portland cement (PC). Its density is about 2.90. The fineness of granulated slag is a very important parameter and it is measured by its specific surface area that controls its reactivity [26]. In general, increased fineness results in better strength development, but in practice, fineness is limited by economic and performance considerations and factors such as setting times and shrinkage.



Figure 2.19: Granulated Slag

Shaft Furnace Slag

It is the slag produced in shaft furnace. In this work the shaft furnace slag considered consists mainly of the following: Silicon (Si), Aluminum (Al), Iron (Fe), Magnesium (Mg), Calcium (Ca), Sodium (Na), Potassium (K), Titanium (Ti), Manganese (Mn) and Oxygen (O).

CHAPTER 3

A MATLAB PROGRAM FOR THE CALCULATION OF THE EFFICIENCY CORRECTION FACTOR

For the gamma spectroscopic analysis of environmental samples at the Nuclear Engineering Laboratory of the National Technical University of Athens (NEL-NTUA) a home developed computer code named SPUNAL is used for more than 30 years. This code was originally developed in FORTRAN, runs under UNIX and has been expanded over the years to include new capabilities in spectrum analysis. Especially for the analysis in the low energy region, where the problem of self-absorption is significant, the code performs automatically self-absorption corrections. For this purpose an efficiency correction factor (ECF) based on the integral formula is calculated and used. For detector energy and efficiency calibration, the program “calceff” – one of the SPUNAL components – is used. This program, among other things, calculates the efficiency correction factor, for very specific materials (soil, fly-ash and bottom ash) usually analyzed at NEL-NTUA, covering the energy region below 200keV. When this program was first developed it was considered that there was no need for efficiency corrections above this energy.

Besides the calculation of the efficiency correction factor by calceff program, it was deemed useful to develop another program for efficiency correction factor calculations that can be used independently. A program like this has the advantage of being easily adaptable and expandable, to cover more materials and a wider energy range. One such program was program “factor” that was developed under UNIX environment and it was written in FORTRAN. The original version of this program covered the same materials and the same energy region as program calceff.

In 2017 an effort was undertaken to develop a completely new program, based on the same philosophy of calculating the efficiency correction factor and a new program was developed in MATLAB¹⁷ [3]. The heart of MATLAB is “MATLAB language”, a matrix based language, allowing the most natural expression of computational mathematics. The language apps and built-in math functions enable to quickly explore multiple approaches to arrive at a solution. This program expanded the capabilities of program “factor” originally developed under Unix environment, to a wider energy region and it could provide efficiency correction factors for more materials. The reason for this expansion was the need to analyze NORM, which in many cases have high density. For these new high density materials the need for self-attenuation corrections for energies higher than 200 keV had to be investigated. Though the first version of this program [3] gave useful results and lead to interesting conclusions, it turned out that it had some weaknesses and limitations.

Aim of the present work was to:

- i. modify the original MATLAB program in order to give more accurate results,

¹⁷ Version MATLABR2015a-64bit.

- ii. make it more user-friendly and flexible, by introducing new capabilities, geometries and densities, and
- iii. expand its capabilities to cover new materials, a wider energy range and new source-to-detector geometric characteristics.

The modifications with regard to the accuracy of the code, as described in the chapters to follow, have to do mainly with the linear attenuation coefficient values used. In this chapter, the original code (ANNEX I) and its results are presented and thoroughly examined so as to explain the need for the changes that will be presented in the following chapter.

3.1 MATLAB source code basics and execution

The original code was operating in the MATLAB command window and the MATLAB software should have been previously installed in the computer used. When running the program, the user was firstly prompted to select the sample geometry. There were two cylindrical geometries that could be selected, “geometry 2” and “geometry 8” both of them based on the plastic cylindrical beaker presented in figure 3.1. Though the radius of the beaker slightly increases with height, for simplicity, the radius is considered constant with height and equal to 3.65cm. For geometry “2” the beaker is completely filled up to the height of 6.9cm, while for geometry “8” the beaker is filled up to the level of 1.077cm.

The distance d between the source (cylindrical beaker base) and the fictitious point detector that is used in the integral method has been set to 2cm [5].



Figure 3.1: The beaker considered in “geometry 2” and “geometry 8”

Figure 3.2 presents the part of the MATLAB program where the sample geometry is selected, while figure 3.3 presents dialogue for the geometry selection by the user.

After the geometry selection, the user was prompted to select the sample material from a list of available materials. It should be noted that the calibration standard material is fixed to be a 4M HCl solution, which is a typical matrix for mixed radionuclides liquid calibration sources used for efficiency calibration at NEL-NTUA. It should also be noted that for each material the density [g/cm^3] was fixed. Figure 3.4 presents the dialogue for material selection by the user.

```

% 2. Sample geometry
prompt='Geometry [2/8] : ';
geom=input(prompt);

if geom==8
r=3.6; % Radius of the sample [cm]
t=1.077; % Thickness of the sample [cm]
end

if geom==2
r=3.6; % Radius of the sample [cm]
t=6.9; % Thickness of the sample [cm]
end

```

Figure 3.2: Configuration of geometry in the code

```

Command Window
>> old_code
fx Geometry [2/8] : |

```

Figure 3.3: Sample geometry selection in commend window

```

Command Window
>> old_code
Geometry [2/8] : 2

MATERIAL

1:Soil
2:Red Mud
3:Fly Ash
4:SF Slag
5:Phosphogypsum
6:G Slag
7:L Slag
fx |

```

Figure 3.4: User was asked to choose a certain material

The next piece of information required for the calculation of the efficiency correction factor is the linear attenuation coefficient for both the calibration standard and the sample material. This information is automatically calculated by the code, for the photon specific energy (in keV) which is inserted by the user (Figure 3.5).

The linear attenuation coefficient for the specific energy requested by the user is calculated as the product of the mass attenuation coefficient for this energy and the fixed material density. To this end, for each material, a series of values for the mass attenuation coefficient, covering the energy region between 40-1000 keV had been included in a vector "v_mi".



Figure 3.5: The user was asked to input the desired energy

Another vector “x_en” contained the corresponding photon energies. All mass attenuation coefficient values were obtained using the program MuPlot¹⁸. In the case the user selects an energy included in the vector “x_en”, the corresponding mass attenuation coefficient value from vector “v_mi” is considered; otherwise the mass attenuation coefficient is calculated by a simple formula of the form:

$$\ln(\mu) = A \cdot \ln(E)^2 + B \cdot \ln(E) + C \quad (3.1)$$

which is equivalent to:

$$\mu = e^{A \cdot \ln(E)^2 + B \cdot \ln(E) + C} \quad (3.2)$$

Formulas of this form had been externally determined for each material and incorporated in the code, using the data included in vectors “x_en” and “v_mi”.

Figure 3.6 presents, the “if” statement used for the selection of a mass attenuation value for the first material (Soil 3%), where the vectors containing the energy and the mass attenuation coefficient can be seen. If the user input “1” in the command window, the code chooses the appropriate parameter values (A, B, C) for the material “soil” and the appropriate energy and mass attenuation coefficient vectors. These three parameters are then imported in formula (3.2) to determine the mass attenuation coefficient for the selected energy, if this energy is not included in vector “x_en”. To decide whether the requested energy is contained in vector “x_en”, the MATLAB function “ismember” is used as a logical statement.

After the mass attenuation coefficient is chosen or calculated (Figure 3.7), it is multiplied by the fixed density for this material to give the linear attenuation coefficient needed for the integral calculation. The same procedure is also followed for the calibration material (4M HCl).

¹⁸ MuPlot has been developed by the University of Bologna and allows the computation of mass attenuation coefficient for a material defined as a mixture of compounds or elements.

```

if mat==1 % Soil
ro=1.000; % Density of the sample [g/cm^3]
x_en=[30 40 50 60 80 100 150 200 300 400 500 600 800
1000];
v_mi=[1.3647 0.67714 0.42883 0.31624 0.2212
0.18221 0.14283 0.12509 0.10562 9.40E-02 8.59E-
02 7.98E-02 7.12E-02 6.54E-02];
A=0.265;
B=-3.4735;
C=8.79645;
end

```

Figure 3.6: If statement for Soil 3%

```
mi_m=exp(A*(log(energy))^2+B*log(energy)+C);
```

Figure 3.7: The function calculating the mass attenuation coefficient if not present in “x_en”

Finally, having all the variables needed, the computation of the double integrals required for the implementation of the “Integral Method” follows, as described in (Chapter 2.2.3). The double integral (formula 2.17) is calculated for both the material selected by the user and also for the calibration material which is fixed to 4M HCl. Finally, the efficiency correction factor is calculated by computing the ratio between the integral for the selected material and that of the calibration source (formula 2.18), and the efficiency correction factor is displayed in the command window.

3.2 Efficiency Correction Factor results

By using the MATLAB code for the two geometries “8” and “2” for all available materials and several photon energies, the efficiency correction factor values had been calculated in [3], covering the energy region [40, 400] keV, as presented in the following tables (Table 3.1 & Table 3.2).

A first look on the results of these tables shows that they seem reasonable – not necessarily correct – with values more or less around one, which in most cases tend to reach one, as the energy increases. This is to be expected, since efficiency correction is considered significant for low energies, usually lower than 200 keV. It is interesting to notice that in some cases, for very low energies, the efficiency correction factor has a very low value, of the order of 0.2-0.3 indicating that a significant efficiency correction is needed in these cases. Furthermore, it is clear that for some materials, like Lead Slag (LS) – a high Z, high density material – efficiency correction is required even for energies higher than 400 keV.

Another interesting conclusion is that the ECF calculated for geometry “2” is higher than that calculated for geometry “8”. This is to be expected since geometry “2” is a much thicker sample geometry, for which self-absorption within the sample is expected to be higher. These reasonable results however yet needed to be tested for their accuracy. For this purpose other means for the calculation of ECF were also used in [3] for comparison purposes, specifically:

- i. calculation of ECF using Monte-Carlo simulation, and
- ii. calculation of ECF using the program calceff of code SPUNAL,

as presented in the paragraphs that follow.

Table 3.1: Efficiency correction factor values for geometry “8” obtained with the original MATLAB program [3]

Efficiency Correction Factor – Geometry 8							
keV	Soil 3%	RM	FA	SFS	PG	GS	LS
40	0.8019	0.3952	0.8311	0.3911	0.7436	0.4662	0.2413
60	0.9432	0.6440	0.9591	0.6279	0.9230	0.7041	0.4534
80	0.9873	0.7761	0.9976	0.7525	0.9833	0.8157	0.6005
100	1.0030	0.8390	1.0108	0.8124	1.0056	0.8662	0.6917
120	1.0000	0.8458	1.0085	0.8194	1.0028	0.8700	0.7056
140	1.0068	0.8755	1.0141	0.8496	1.0114	0.8948	0.7496
160	1.0110	0.8960	1.0174	0.8709	1.0166	0.9119	0.7816
180	1.0137	0.9108	1.0195	0.8864	1.0199	0.9241	0.8054
200	1.0139	0.9157	1.0185	0.8893	1.0219	0.9267	0.8149
220	1.0167	0.9300	1.0218	0.9069	1.0235	0.9401	0.8377
240	1.0175	0.9363	1.0223	0.9139	1.0244	0.9454	0.8489
260	1.0181	0.9413	1.0226	0.9194	1.0250	0.9495	0.8578
280	1.0184	0.9453	1.0228	0.9238	1.0253	0.9528	0.8651
300	1.0135	0.9319	1.0173	0.9080	1.0211	0.9402	0.8455
320	1.0187	0.9510	1.0228	0.9302	1.0255	0.9575	0.8758
340	1.0186	0.9530	1.0227	0.9326	1.0255	0.9592	0.8798
360	1.0186	0.9546	1.0226	0.9345	1.0253	0.9605	0.8830
380	1.0185	0.9559	1.0224	0.9360	1.0251	0.9616	0.8857
400	1.0132	0.9405	1.0166	0.9187	1.0201	0.9478	0.8624

Table 3.2: Efficiency correction factor values for geometry “2” obtained with the original MATLAB program.

Efficiency Correction Factor – Geometry 2							
keV	Soil 3%	RM	FA	SFS	PG	GS	LS
40	0.7213	0.3232	0.7571	0.3197	0.6539	0.3840	0.1962
60	0.8893	0.4989	0.9184	0.4832	0.8540	0.5606	0.3315
80	0.9705	0.6212	0.9942	0.5927	0.9617	0.6727	0.4359
100	1.0075	0.6933	1.0279	0.6557	1.0144	0.7347	0.5119
120	0.9999	0.6962	1.0228	0.6578	1.0074	0.7340	0.5187
140	1.0190	0.7340	1.0403	0.6924	1.0324	0.7673	0.5579
160	1.0326	0.7629	1.0526	0.7190	1.0501	0.7927	0.5888
180	1.0425	0.7855	1.0616	0.7399	1.0629	0.8123	0.6136
200	1.0427	0.7965	1.0576	0.7466	1.0689	0.8190	0.6285
220	1.0552	0.8176	1.0730	0.7699	1.0792	0.8401	0.6502
240	1.0592	0.8291	1.0766	0.7807	1.0844	0.8500	0.6637
260	1.0622	0.8384	1.0792	0.7896	1.0882	0.8580	0.6748
280	1.0645	0.8459	1.0811	0.7968	1.0909	0.8644	0.6841
300	1.0451	0.8189	1.0586	0.7687	1.0721	0.8377	0.6581
320	1.0671	0.8571	1.0834	0.8075	1.0942	0.8739	0.6982
340	1.0679	0.8611	1.0840	0.8114	1.0950	0.8773	0.7034
360	1.0682	0.8643	1.0843	0.8146	1.0954	0.8800	0.7078
380	1.0684	0.8669	1.0844	0.8171	1.0955	0.8821	0.7114
400	1.0465	0.8316	1.0593	0.7822	1.0725	0.8493	0.6753

3.3 Calculation of ECF using Monte Carlo simulation

As previously mentioned, one method for the calculation of an ECF is through Monte-Carlo simulation. For this purpose two simulations have to be performed for the same energy and source-to-detector geometry. One simulation for the calibration standard material (e.g. 4M HCl) and one simulation for the material of interest (e.g. soil). It is implied that the detector will have to be characterized¹⁹ prior to simulations. The ratio of the efficiencies calculated from the two simulations is the required efficiency correction factor.

3.3.1 The Monte Carlo simulation code PENELOPE

Monte Carlo simulation code PENELOPE was used to determine ECF values for the NEL-NTUA LGe detector and for the materials calculated by the MATLAB program. PENELOPE is a computer code system that performs Monte Carlo simulations of coupled electron–photon transport in arbitrary materials for a wide energy range. Photon transport is simulated by means of the standard, detailed simulation scheme that considers Rayleigh scattering, Compton scattering, pair production and photoelectric effect. This code is widely used at NEL-NTUA for simulation of various problems of interactions of photons and electrons with mater, such as detector simulations.

3.3.2 Results and comparisons

In order to check the MATLAB program [3] PENELOPE code was used as previously described, to calculate ECF for the photon energies of Tables 3.1 and 3.2. Figure 3.8 presents the results for ECF obtained through M-C simulation for geometry “8” and Figure 3.9 the percentage differences between ECF values obtained using MATLAB and M-C simulation with PENELOPE. The respective values are presented in the (ANNEX V).

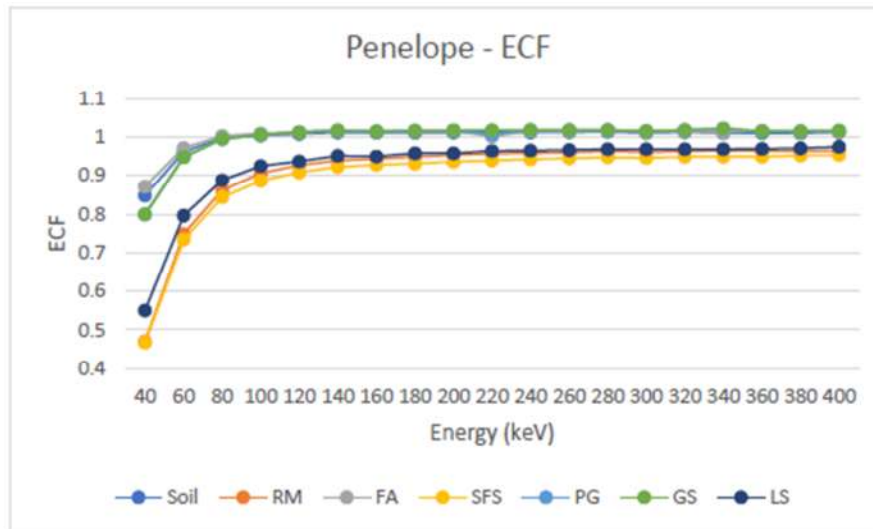


Figure 3.8: ECF values obtained using M-C simulation for geometry “8” [3]

¹⁹ Detector characterization is the process of obtaining the detector geometrical characteristics which are necessary for detector simulation. This process is a combination of experimental work and Monte-Carlo simulation [27].

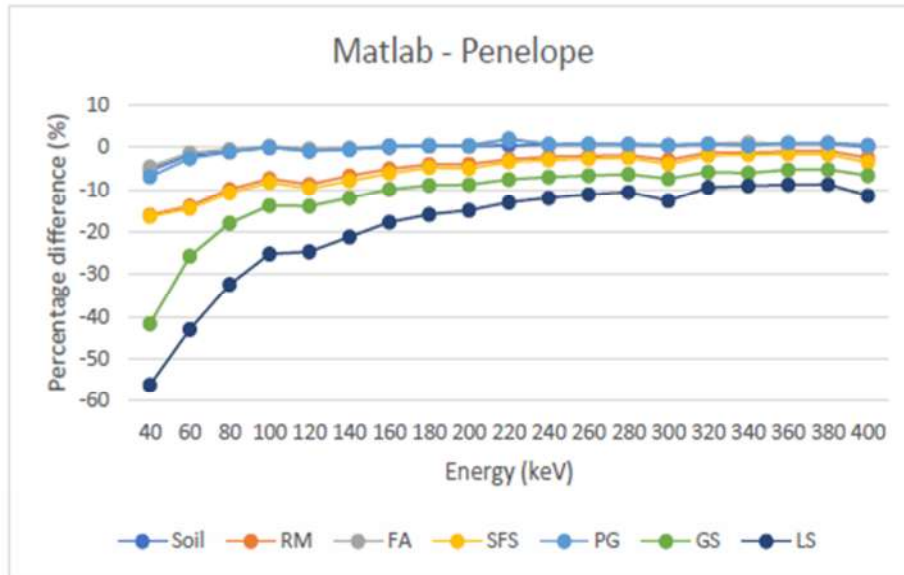


Figure 3.9: Percentage difference between the ECF values obtained with MATLAB and M-C simulation for geometry "8" [3]

From figures 3.8 & 3.9 a series of very interesting conclusions are drawn:

- The only case where the result of the two methods satisfactorily converge (difference close to 0%) is for fly-ash and soil and for energies above 80keV. For all other materials and energies the differences may be as high as 60%.
- Differences are higher for lower energies
- Differences are higher for high density materials like lead slag (LS)
- Though differences for a specific material appear to follow a smooth line, there are some unexpected deviations (e.g. 300 keV for most materials, and 120 keV for lead slag).

Possible explanations for the results of Figure 3.9 could be:

- Difference in the mass attenuation coefficient values used by MATLAB program and PENELOPE code. In MATLAB program the linear attenuation coefficient is obtained, as previously mentioned from MuPlot, while PENELOPE on the other hand calculates its own values.
- The formula that is used to fit mass attenuation coefficient values in MATLAB program is not adequate, as seen in figure 3.10. Another formula could be used to better fit mass attenuation coefficient values. It is clear from this figure that the first experimental point, corresponding to the energy of 30keV, is not well fitted to the correlation. It is useful to remind in this point that MATLAB program uses experimental points from vector (x_en) where available, and fitted from the formula were not available. This could also explain the deviations observed in specific energies (e.g. 300 and 400 keV).
- Other reasons.

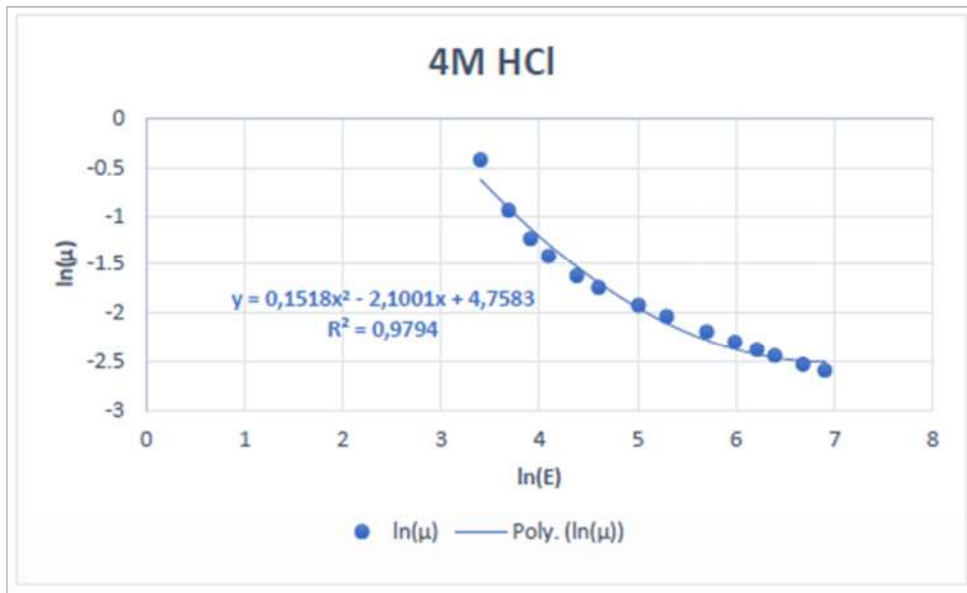


Figure 3.10: Plot of the natural logarithm of the mass attenuation coefficient over the natural logarithm of the energy for the 4M HCl solution presented as an example.

3.4 Calculation of ECF using program calceff

As mentioned before, the program “calceff” is used at NEL-NTUA, for the determination of ECF. This program has also been used by [3] for the determination of ECF values and comparison with the results of MATLAB program. With “calceff” it is possible to calculate efficiency correction factors only up to 200keV and only for soil, fly-ash and bottom-ash.

The program “calceff” requires as input the sample material and density, sample geometry, type of detector and the photon energy. As output it provides the efficiency for the calibration source (4M HCl), the efficiency for the selected material and the ECF using the “Integral Method”. The linear attenuation coefficient values are calculated from a correlation of the form $\mu = f(d,E)$ for the materials: soil, fly-ash and bottom-ash. These correlations have been produced from experimentally determined μ values for various densities and energies, for each material, as described in [2]. It should be noted however that the composition of the materials used to produce these correlations is not known – this is something to be taken into consideration when comparing ECF values given by the program “calceff” with those calculated with MATLAB program or through M-C simulation.

Using program calceff in [3] ECF values were determined for fly-ash and soil, as presented in Table 3.3.

Figures 3.11 and 3.12 present the efficiency correction factors as calculated in [3] with the three different techniques²⁰, for soil and fly-ash, for energies in the region 40-200 keV. From these two figures it is made clear that:

²⁰ Program calceff, MATLAB program, and through M-C simulation

- For soil all methods converge satisfactorily above 80 keV.
- Below that energy the differences increase. For fly-ash all methods converge satisfactorily even for photon energy as low as 40 keV.

Table 3.3: ECF values calculated with program calceff

keV	Soil 3%	Fly Ash
40	0,925	0,857
60	0,965	0,956
80	0,981	0,988
100	0,991	1,003
120	0,998	1,012
140	1,003	1,018
160	1,008	1,023
180	1,012	1,027
200	1,016	1,031

It should be reminded that, while MATLAB program and M-C simulation calculate ECF for materials (soil and fly-ash) having the very same composition, calceff calculates ECF for materials soil and fly-ash for which their composition is not known, therefore any comparison of ECF values obtained by calceff, with those obtained with MATLAB code and M-C simulation should be considered of limited value. It should also be reminded that the use of ECFs is of particular importance for low energies.

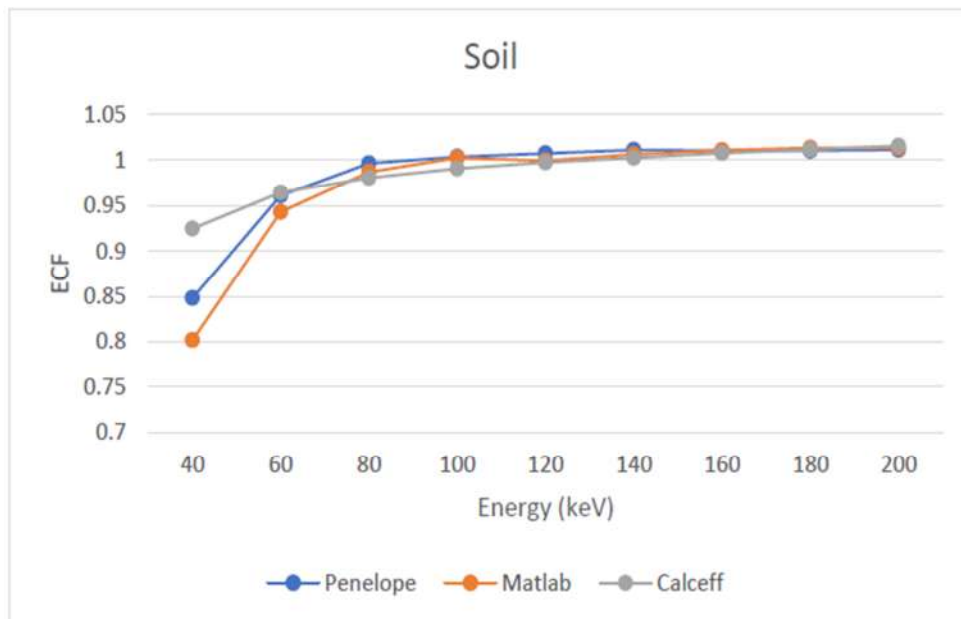


Figure 3.11: ECF trend for soil obtained with MATLAB, M-C simulation and program calceff [3].

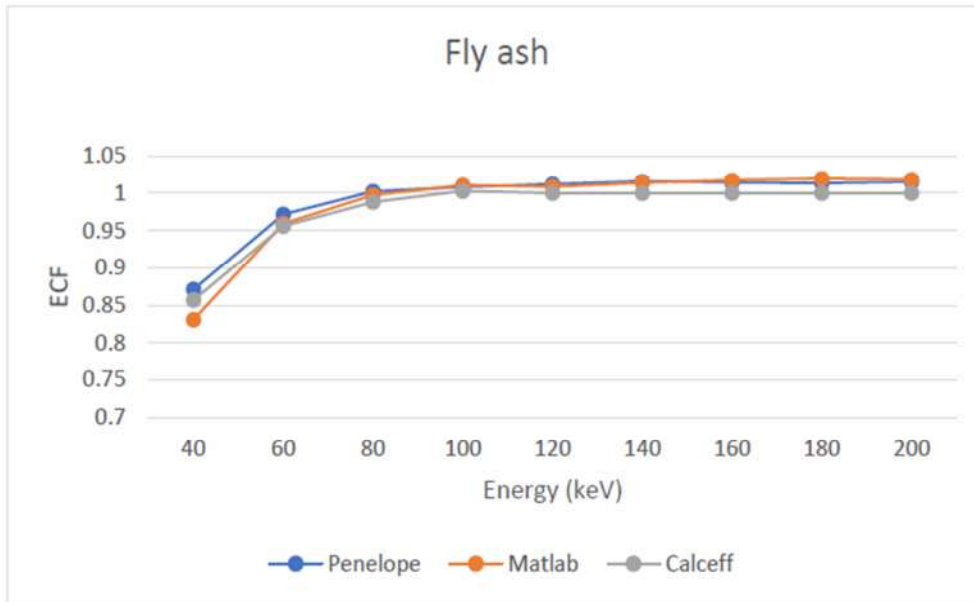


Figure 3.12: ECF trend for FA obtained with MATLAB, PENELOPE and calceff [3].

3.5 Conclusions

As it turns out from what has been presented in the previous paragraphs, the original MATLAB program is well made and executed, but there is plenty of room of improvement. As previously mentioned the difference between the results of this code and M-C simulation is relatively high for the low energy photons and it is worthwhile trying to reduce it, if MATLAB program is to be trusted for its results. In order to do so, the first variable that needs to be revised is the mass attenuation coefficient and the way it is calculated. The formula used to fit the available data in this early code appears not to be the best possible choice. Furthermore, after securing that the mass attenuation coefficient is calculated in the highest possible accuracy, the calculations should be extended to higher energies. There are several cases of important photons used in gamma spectrometry in energies above 400keV, almost reaching 2000keV like those emitted by very important isotopes like: ^{214}Bi (609 keV, 1120 keV, and 1764 keV), ^{228}Ac (911 keV) and ^{40}K (1460 keV). Though for materials such as soil and fly-ash it seems that corrections are not needed for these very high energies, for some materials, like NORM – especially lead slag – it is possible that corrections are needed for high energies, especially for thick samples. In addition, after a lot of research in the literature, several articles were found [28], [8] reporting that the efficiency correction factor calculated using various techniques never reaches unit. This fact needs to be cross-checked with the results obtained with the MATLAB program. In this thesis, it was decided that the program should be extended to 2000keV, while new results of the ECF were calculated using M-C simulation for the same energy spectrum, for comparison reasons.

Another main limitation of the original program is the fact that the user can only choose between two certain geometries with a fixed effective interaction depth and fixed densities. This clearly becomes a problem when the user wants to change those variables. It is of great importance to give to the user the flexibility to change all parameters involved in the

“Integral Method” so as to have the most accurate efficiency correction factor for all these materials. As a result these variables will be required as inputs in the final version of this program. This will also allow the investigation of the effect of material type and material density in an independent way, to find out whether the use of efficiency correction factors based only on the material density is a good practice.

Finally, the original program is only accessible through MATLAB which is expensive and difficult to use by users who are not familiar with this particular interface. Someone should have knowledge on how to use MATLAB and how to write a basic code. It was therefore deemed of great importance to turn MATLAB program to a user friendly standalone application under windows, accessible by anyone.

CHAPTER 4

MODIFICATIONS AND EXTENSION OF MATLAB CODE

In this chapter are presented the efforts that were made in this work in order to make the original MATLAB program more accurate, user friendly and applicable in a wider energy region, for more sample geometries and material densities. As a first step, the linear attenuation coefficient was recalculated for all materials. It was decided that, in order to make a straight fair comparison between MATLAB and M-C simulation results, there was a need for a common database of the mass attenuation coefficient to be used. To this end, all mass attenuation coefficient values were obtained from PENELOPE code, for energies between 30keV to 2000keV. Then, the focus was turned on how these values would be better fitted in order to obtain more accurate μ_m values for the energies where no data were available. Again, after a thorough investigation, the appropriate correlations were found, giving much better results, compared with that of the original program. A series of changes were made to the program to make it more flexible by allowing the user to select the source geometrical characteristics as well as the material density and the effective interaction depth "d". All these modifications are presented in detail. Finally, the procedure to produce an executable MATLAB program to run in any windows system is described.

4.1 Mass Attenuation Coefficient with PENELOPE

The mass and linear attenuation coefficients used in the original MATLAB program [3] were obtained from program MuPlot. However, if the results of the program are to be compared with those of Monte-Carlo simulations using PENELOPE code, it would be important to ensure that the mass attenuation coefficient data used in both cases were the same. So, the first modification of the program was to use the mass attenuation coefficient values for every material and energy that were calculated by PENELOPE code.

At first, PENELOPE was used to calculate the mass attenuation coefficient for the seven materials of this Thesis (ANNEX IV). These calculations were made for 14 energy levels between 30keV and 2000keV. Especially for Lead Slag though, it seemed wise to obtain more (27) energy levels; so in this way there are more data to be fitted to the appropriate correlation. Since the user of MATLAB program must give as input an energy value to obtain the efficiency correction factor of a certain material, it is important to develop correlations of the form $\mu_m = f(E)$ for each material.

There was a thorough investigation to find the best correlation to fit to the data (E, μ_m). The first formula that was tested and adopted by [3] was:

$$\ln(\mu_m) = A + B \cdot \ln(E) + C \cdot (\ln(E))^2 \quad (4.1)$$

However, this formula is not adequate for a wide energy region, especially for high energies and very low energies, as can be seen in Figure 4.1 for Lead Slag.

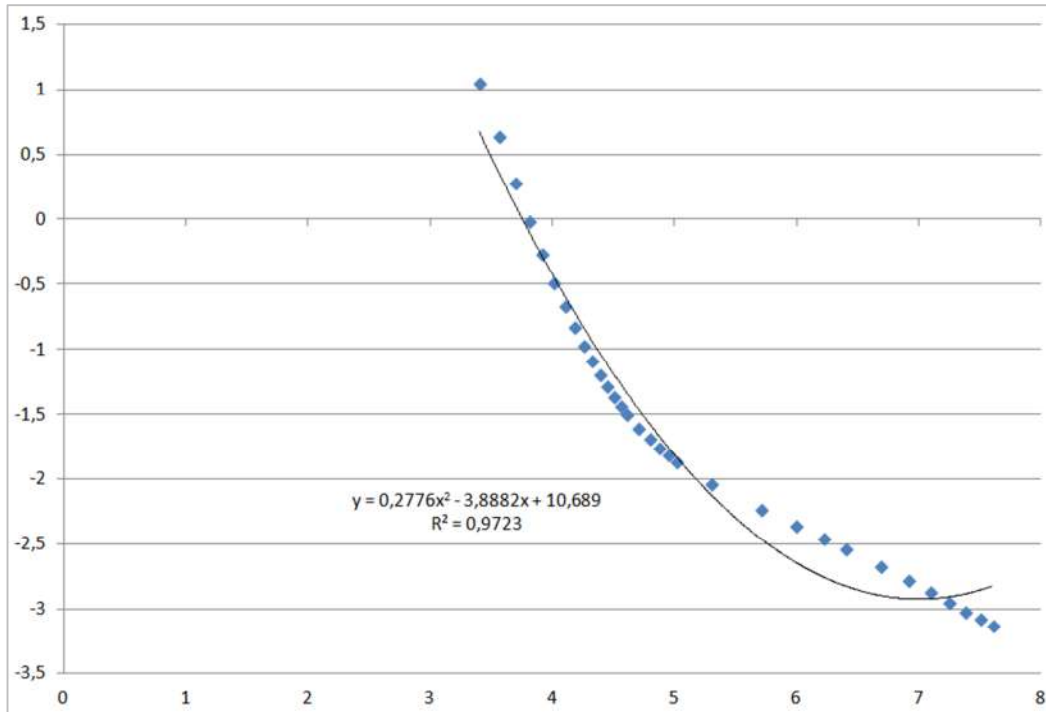


Figure 4.1: Plot of the natural logarithm of the mass attenuation coefficient μ_m over the natural logarithm of the energy for the Lead Slag presented as an example with a second degree polynomial

The second formula tested in this work was higher order polynomials (third) giving better results, both in low and high energies, yet not of acceptable accuracy.

$$\ln(\mu_m) = A \cdot (\ln(E))^3 + B \cdot (\ln(E))^2 + C \cdot \ln(E) + D \quad (4.2)$$

As shown in the following plot (Fig. 4.2), even though the third order polynomial fits very well in low energy region, for high energies the fitting is not so good.

Following, it was clear that a better way to deal with this problem, in both low and high energy region, was to split the energy region in two sub-regions and use two third order polynomials to cover each part. It was found that the best solution was to split the energy region 30-2000keV at the energy of 150keV (Fig. 4.3). These two 3rd order polynomials give a correlation coefficient better than 0,9998 for both energy regions. This procedure was followed for all materials involved. In Figure 4.3, on the y-axis is the mass attenuation coefficient calculated by PENELOPE and on x-axis energy is presented. Overall, fourteen correlations were produced. In [ANNEX V] the correlations for all materials are represented.

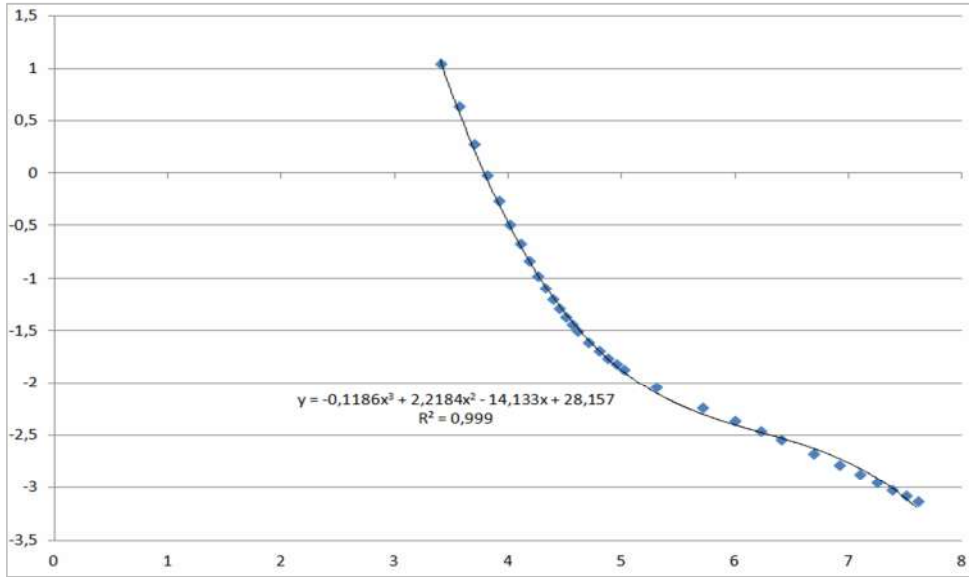


Figure 4.2: Plot of the natural logarithm of the mass attenuation coefficient over the natural logarithm of the energy for the Lead Slag presented as an example with a third order polynomial.

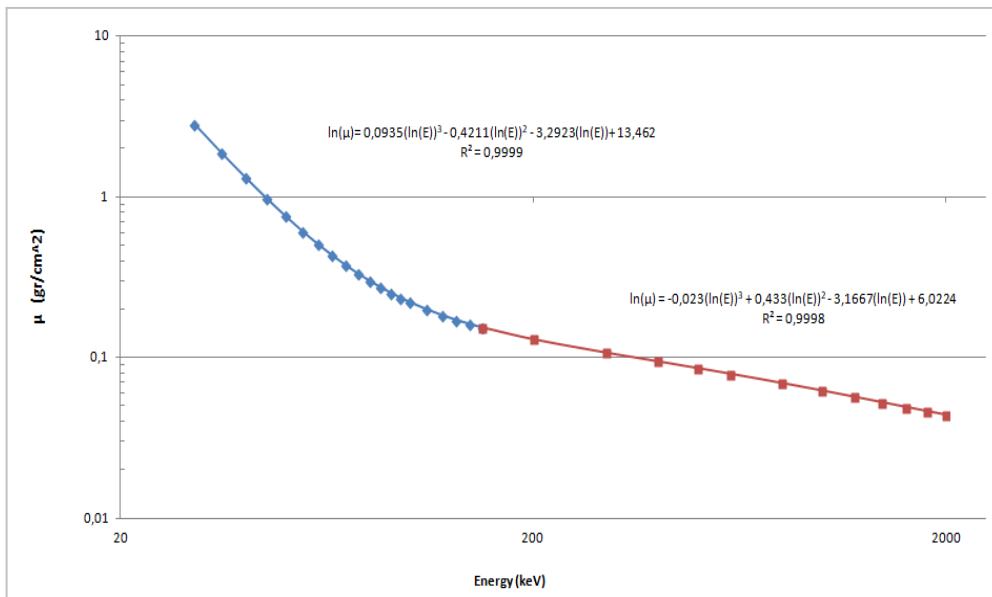


Figure 4.3: Plot of the natural logarithm of the mass attenuation coefficient over the natural logarithm of the energy for the LS presented as an example with two third order polynomials

Hence, the equation used by the MATLAB program to calculate the mass attenuation coefficient for any energy is:

$$\mu_m = e^{[A \cdot (\ln E)^3 + B \cdot (\ln E)^2 + C \cdot \ln(E) + D]} \quad (4.3)$$

For each material two sets of A, B, C, D values, one for each energy range are determined, as presented in Tables 4.1 and 4.2.

Table 4.1: Correlation parameters for the low energy region (30-150keV)

Material	A	B	C	D	R ²
4M HCl	-0,2998	4,347	-21,38	33,82	1
Soil 3%	-0,1166	2,23	-13,91	26,45	0,9999
RM	0,05843	0,03045	-5,118	15,65	0,9999
FA	-0,1312	2,41	-14,61	27,27	0,9999
SFS	0,0233	0,4741	-6,893	17,81	0,9999
PG	-0,04834	1,394	-10,68	22,69	0,9999
GS	0,003599	0,7292	-7,954	19,19	0,9999
LS	0,0935	-0,4211	-3,292	13,46	0,9999
Water	-0,2567	3,54	-16,56	24,49	1

Table 4.2: Correlation parameters for the high energy region (150-2000keV)

Material	A	B	C	D	R ²
4M HCl	-0,002213	0,000239	-0,1725	-0,757	1
Soil 3%	-0,009175	0,1466	-1,194	1,518	1
RM	-0,01837	0,3375	-2,511	4,532	1
FA	-0,008551	0,1338	-1,107	1,316	1
SFS	-0,01615	0,2912	-2,189	3,788	1
PG	-0,01202	0,2064	-1,611	2,488	1
GS	-0,01488	0,2652	-2,013	3,393	1
LS	-0,023	0,433	-3,167	6,022	1
Water	7,263e-05	-0,0478	0,1627	-1,517	1

Figure 4.4 presents the difference between the mass attenuation coefficient values obtained by the correlation and the original data for the material Lead Slag. As it turns out, the percentage difference, even for the material with the highest density, is very small ($\geq 1\%$). For the rest of the materials the differences were even lower.

Eventually, it was decided that in the new MATLAB code all mass attenuation coefficient values will be calculated using the new correlations obtained.

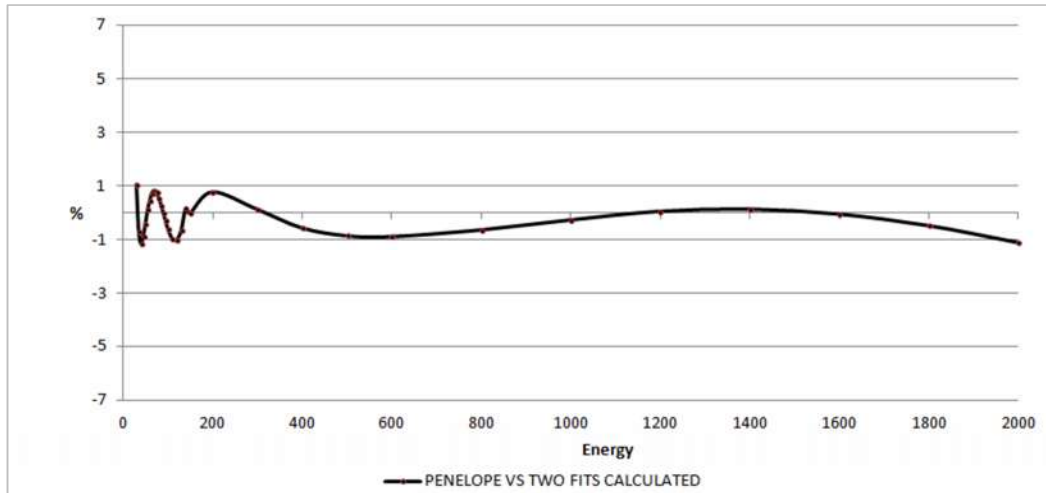


Figure 4.4: LS percentage difference calculated values of μ vs experimental.

4.2 MATLAB program modifications

One of the first modifications made in the source program is the way the linear attenuation is calculated as thoroughly mentioned in the previous paragraph. So the first change in the code is the conditional statement “if” where the constants are defined depending on the material chosen. Then, in this statement there is one more condition statement which is used to choose the constants depending on the energy given. For each material there are two different groups of constants (shown in Figure 4.5).

```

if mat==1 % Soil
%rho=1.000; % Density of the sample [g/cm^3]
x_en=[30 35 40 45 50 60 80 100 150 200 300 400 500 600 800 1000];
y_mi=[1.3986 0.94829 0.69336 0.53746 0.43687 0.32054 0.22286 0.18346 0.14449 0.12715 0.1078 0.09582 0.08719 0.080498 0.070568 0.063378];

if energy<150
A=-0.1166;
B=2.23;
C=-13.91;
D=26.45;
end

if energy>150
A=-0.009175;
B=0.1466;
C=-1.194;
D=1.518;
end

if energy == 150
mi_m = 0.1449;
end

end

```

Figure 4.5: If statement in the new code, defining the constants for mass attenuation coefficient

Another modification in the code is the formula calculating the mass attenuation coefficient μ_m of the selected material. This change is shown in Figure 4.6.

As mentioned before, it is decided to use only the calculated values of the mass attenuation coefficient. So the vectors are only used as a reference in the new MATLAB program. With this in mind, the “ismember” command in the code should be deleted; so when the user inputs an energy, the code will calculate the mass attenuation coefficient using the equation (Figure 4.6), with the only exception the energy at the midpoint 150keV, where μ_m value is taken from the corresponding vector.

```
if energy ~=150
mi_m=exp(A*log(energy)^3 + B*log(energy)^2 + C*log(energy) + D);% it calculates the  $\mu$ 
end
```

Figure 4.6: Calculation of the mass attenuation coefficient μ_m

According to the “Integral Method”, the fictitious point detector setup is inside the actual detector, at a depth called “effective interaction depth”[4]. In the original code the effective interaction depth of the detector was a fixed value of 1 cm [5] and the total distance from the typical cylindrical source used at NEL-NTUA to the point detector was 2cm. This fixed value of “d” corresponds to a cylindrical sample positioned over the NEL-NTUA Low Energy Germanium Detector .

During this work it was deemed necessary that the user is free to insert the value of the effective interaction depth (Fig. 4.7), which must have been previously experimentally determined for the detector and photon energy of interest. Actually, to give the user more flexibility, the program requires as input the total distance between the source and the point detector²¹ and not the depth inside the detector. With this modification it is possible to use the MATLAB program for a parametric study of the effect of the effective interaction depth on the ECF calculation as well as the source to detector distance. Such a study is presented in the next chapter.

```
% 1. Source - detector setup
prompt='Input interaction depth (in cm):';
d=input(prompt);
```

Figure 4.7: Command for the input of effective interaction depth

Another major change in the program is the selection of the material density, which in the original version of the program was fixed. The user may select the material density, while typical values for each material are provided in the screen to assist the user. This, besides the flexibility that gives to the program, allows the parametric study of the effect of density on ECF.

If the program is to be widely used, it should not be limited to specific sample geometries. In the original version the program was able to calculate ECF for two of the commonly used sample geometries at NEL-NTUA, geometry “2” and geometry “8”. In the new version the user is still able to select between these two geometries, but he can also select another cylindrical geometry, by simply giving its height and radius.

²¹ It is the sum of the distance of the source from the detector and the effective interaction depth inside the detector.

Finally, the material “Water” was added in the list of materials. It is interesting to note that, water may be seen both as a material to be analyzed and as a calibration standard material, since, in some cases water solutions may be used as a calibration standard. In this case, if water is to be considered as the calibration standard material, the code will have to be used twice: once to determine ECF between the material to be analyzed and 4M HCl, and once to determine ECF between water and 4M HCl. Finally, ECF considering water as calibration standard material will be the product of the two ECFs. The modifications made to include “water” in the MATLAB code is presented in Figure 4.8.

```

if mat==8 % Water
%rho=1.000; % Density of the sample [g/cm^3]
x_en=[30 35 40 45 50 60 80 100 150 200 300 400 500 600 800 1000];
v_mi=[0.37808 0.30952 0.27011 0.24513 0.22824 0.20686 0.18425 0.17113 0.15067 0.13711 0.11866 0.10614 0.096845 0.89541 0.078607 0.070644];

if energy<150
A=-0.2567;
B=3.54;
C=-16.56;
D=24.49;
end

if energy>150
A=7.263e-05;
B=-0.0478;
C=0.1627;
D=-1.517;
end

if energy == 150
mi_m = 0.15067;
end

```

Figure 4.8: If statement in the new code for water, defining the constants for mass attenuation coefficient

4.3 MATLAB and Graphical User Interface

Graphical user interfaces (GUIs), also known as apps, provide point-and-click control of software applications, eliminating the need for the user to learn a language or type commands in order to run the application. These apps can be both, used within MATLAB and also as standalone desktop or web apps. In this work the MATLAB GUI is converted into a standalone desktop application in the form of “.exe”. This will make the calculation of the ECF value much easier and accessible for any user no matter if MATLAB is installed in the users computer or not.

4.3.1 MATLAB guide command

At first, before the app is created, it is important to make a graphical user interface inside the MATLAB source code. In order to do that, the first step is to open MATLAB. Then in a new script, enter the command “guide” in the “command window” (Fig. 4.9). This is the command that opens the editing layout of the app that will be created later.



Figure 4.9: How to open “guide” in MATLAB

Then the first pop up page is the one that is asking to create and save a specific MATLAB app. The pop up window is the one presented in Figure 4.10. The user should choose the “Blank GUI” and create a new one.

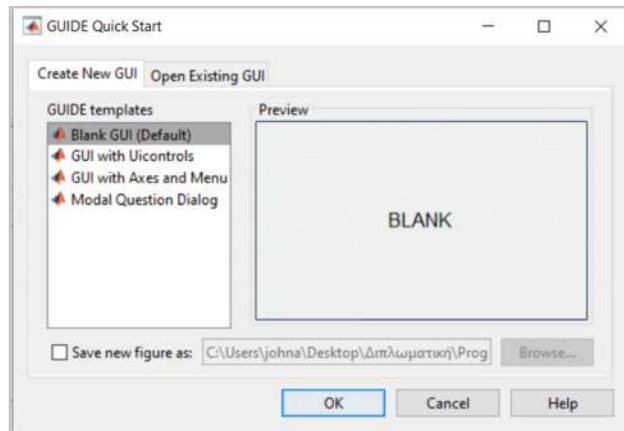


Figure 4.10: Opening guide – first page

The edit window page will pop up where the user can create the layout of the app (Fig. 4.11). There are many different options, including buttons, sliders, list boxes, toggle buttons edit and static texts and panels. In this work there is a need for five different steps. First the user must choose one of the available materials and its density in the “Material” panel. Then, the user can manually input the effective interaction depth. Following, there will be two different standard geometry sample options available for the user, as used in the previous source code. As an additional option in this version the user can manually choose the radius and the thickness of the sample, thus constructing any cylindrical sample geometry.

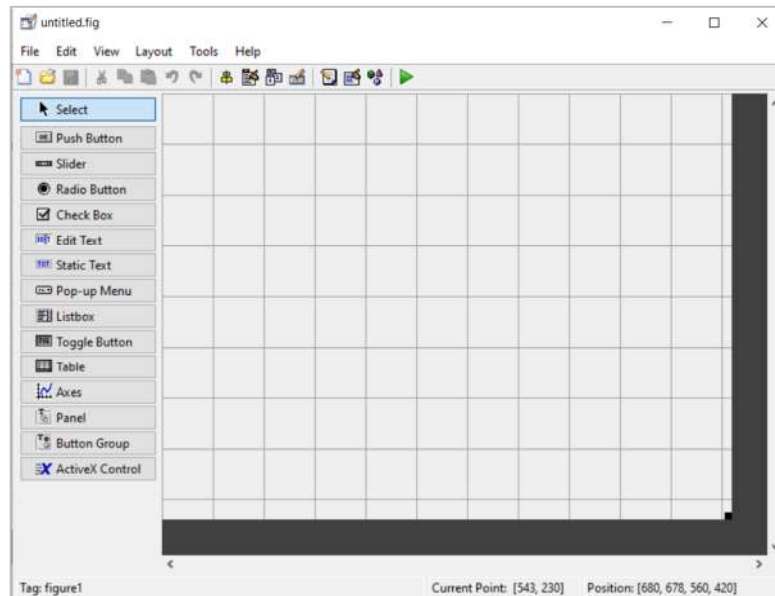


Figure 4.11: Edit windows page of GUI

Finally, the energy of the photons is requested in a certain range which is [30, 2000] keV and also the density of the sample material. Pressing the button “Calculate ECF”, the efficiency

correction factor as well as the mass attenuation coefficient μ_m for the material and photon energy selected are shown on the screen. Eventually, with the push of a button the user will be able to calculate the ECF value for the chosen variables requested. The five different inputs are set in the GUI as “Edit Text” while next to these variable boxes the requests will be set in forms of “Static Text”. The “Edit texts”, in general, are the editable texts where the user can input what the “Static Texts” are asking to.

For instance, when the variable asked is the density of the sample there should be a static text asking the user to input this variable in g/cm^3 and then an edit text where the user will be able to input the desired value (Figure 4.12).



Figure 4.12: First static and editable text

By double clicking in each window the “property inspector” opens up so as to change the “string” of these texts, the size, the font and also the tag of each window. It is important to remember the tag later in the program. The final layout of the app is shown in the next figure (Figure 4.13).

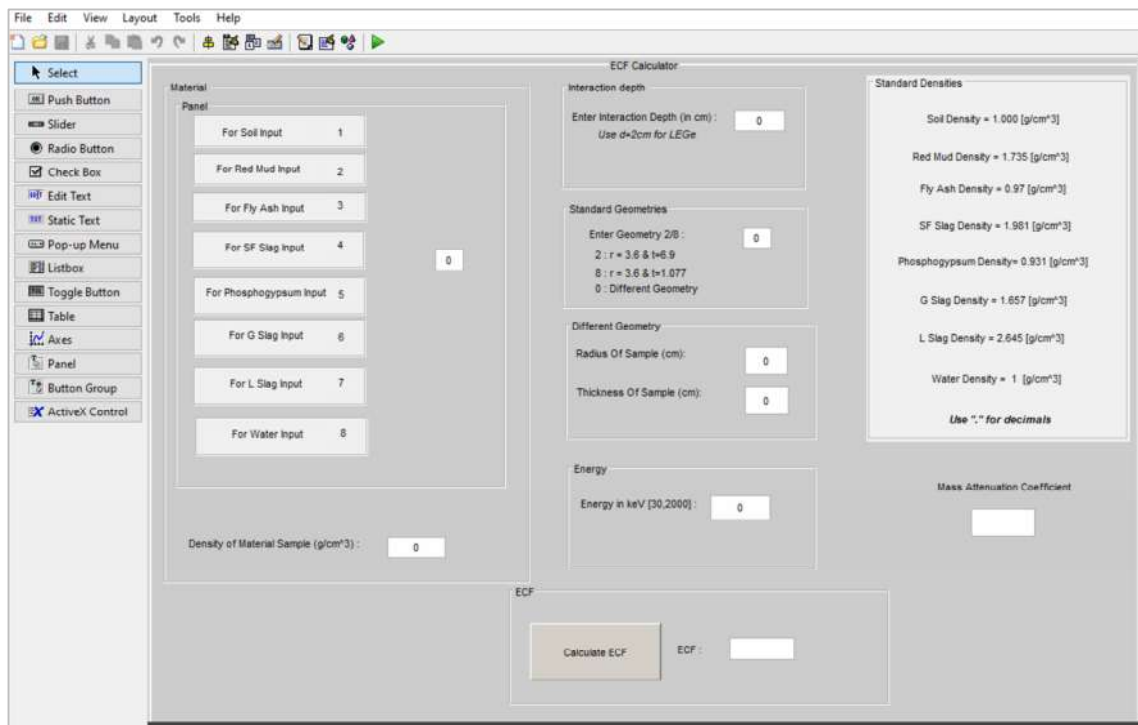


Figure 4.13: Editing Layout of the app

While each button is created, MATLAB creates a script containing all the “Callbacks” of “Edit Texts” and “Static Texts”. For now, these windows are just a “Showcase” of the actual program. In order to make these windows functional, they should be assigned in certain

commands. These commands are called “Callbacks”. It is fairly easy to find the callbacks of each button simply by right clicking in one of them.

In the next figure, the buttons’ callbacks are presented with the appropriate changes (Figure 4.14). As it is clear with this new code, all variables are available and easy to change.

```
d=str2double(get(handles.d,'String'));
geom=str2double(get(handles.geom,'String'));
mat=str2double(get(handles.mat,'String'));
energy=str2double(get(handles.energy,'String'));
r=str2double(get(handles.r,'String'));
t=str2double(get(handles.t,'String'));
ro=str2double(get(handles.ro,'String'));
```

Figure 4.14: Pushbutton callback

These seven commands set the inputs in certain variables. These inputs are provided by the user with the “Edit Text”. For instance, the first command (Figure 4.14) sets in variable “d” the input of the user through the “Edit Text” tagged as “d”. Also the “str2double” command changes the “String” variable (text variable) into a “Double” variable (number variable).

Furthermore, the program after these input commands are given follows the same principles as the basic MATLAB source code. The only difference is that this program does not give feedback. For example, if the user inputs geometry number which is not “2” or “8”, the program does not give a warning message to the user. In contrast, the app will not run at all. In addition, if the user wants to input different sample geometry, the number “0” should be presented the “Standard Geometry” window.

It is very important to mention that, while this application allows the user to input the desired density of the sample material on the right side of the window, all the standard densities are available as a comment. These densities are the ones that have been used in all calculations during this work.

In figure 4.15 the app is running for the following user selected values:

- Material: Soil 3%
- Geometry : “2”
- Photon energy : 1000keV
- Distance d: 2 cm

The result is displayed by pressing the “Calculate ECF” button. All decimals should be inputted using the “.”.

In this work all calculations of ECF values were made using this application. With this application the calculation of ECF is fast and makes the whole procedure easier and more user-friendly. The complete code of this application can be found in the (ANNEX II). As an additional change, the mass attenuation coefficient value is shown on the right hand side of the window. It was found very useful during our calculation to know the mass attenuation coefficient value every time a calculation of the ECF was made. In fact, this app can also be used as a mass attenuation coefficient calculator for these materials and this particular

energy range. As mentioned on (Chapter 4.1), the mass attenuation coefficient values calculated are less than $\pm 1\%$ different than the real values calculated with PENELOPE, especially in low energy values.



Figure 4.15: Running the application with example

4.3.2 GUI application in form of .exe

The next step into making the GUI more user-friendly is the creation of an application outside MATLAB user interface. MATLAB is not open to public users and needs to be purchased so as to be used. In this paragraph, the step by step procedure is presented on how this GUI became a standalone application in the form of “.exe”.

As a first action the “MATLAB Compiler” should be used with the command: “deploytool”. Doing that, the following pop up window is shown on the screen (Figure 4.16) where the user should choose the option “Application Compiler”.

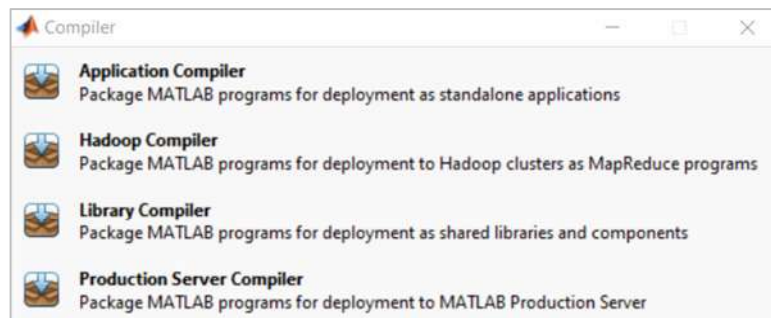


Figure 4.16: MATLAB compiler

Then, MATLAB asks for a description of the application that the user wants to create and some basic information like the “Author Name”, “Company” etc. After completing the appropriate fills the next step is to add a “Main File” on the top left of the pop up window (Figure 4.17), where MATLAB compiler asks for the particular GUI that the user wants to make a standalone application.

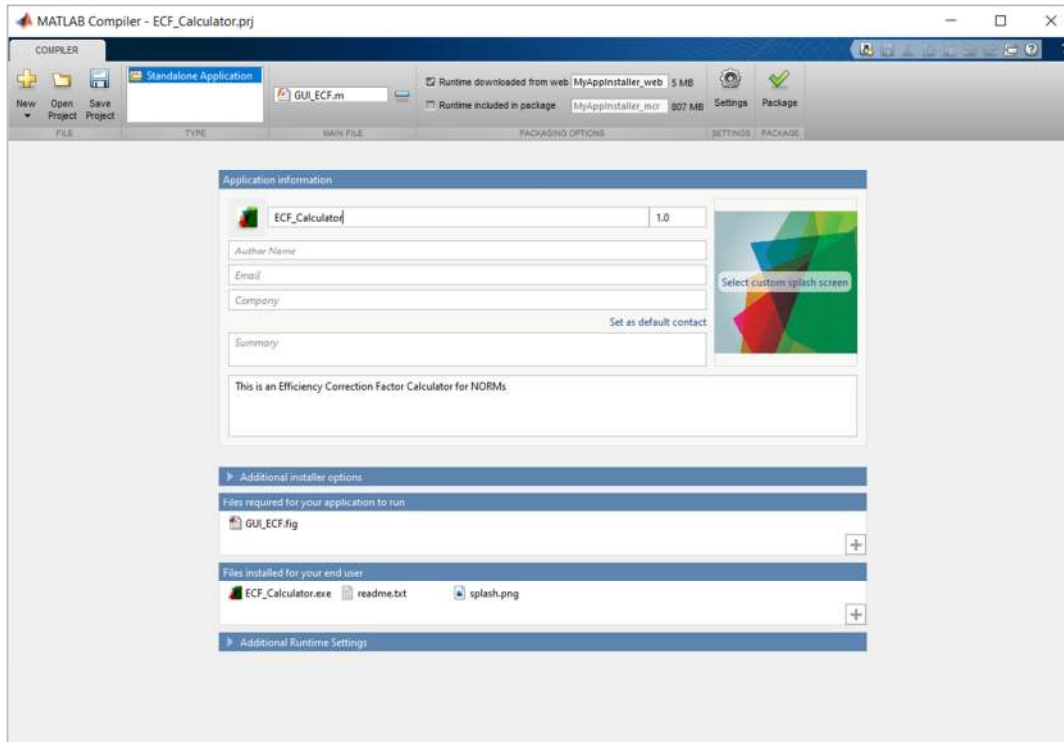


Figure 4.17: Basic information about the standalone application

By pressing the “Package” button, the GUI will be converted into a standalone application in the file specified by the user. Then, opening the file containing the application, the user can run the application without the need of MATLAB to be installed in his computer.

CHAPTER 5

CALCULATION OF EFFICIENCY CORRECTION FACTORS WITH THE NEW MATLAB PROGRAM

In this chapter all the results obtained with the new MATLAB program will be presented and compared to the results calculated by M-C simulation and the program calceff. It is important to mention that with all the changes made as presented in Chapter 4, it was very easy to calculate the ECF by changing the density and the effective interaction depth, to obtain massive results.

The main goal of the changes made in the MATLAB program was to minimize the difference between MATLAB and PENELOPE results, and to investigate the effect of various parameters on ECF.

In the first part of this chapter, the results of ECF in the energy region 30-2000 keV as calculated using the new MATLAB program are presented. Then, comparisons are made with M-C simulation results, which were also extended up to 2000keV. Calculating ECF for these high energies, we get a better picture on how the ECF changes at high energies. It was very important to find out that for some of the materials examined, ECF does not reach one (ECF=1) regardless of the way of calculation. The results of comparing these two methods look more promising than before, which means that all the changes made – in the mass attenuation coefficient correlation mostly – had a great impact. Then, a short comparison with the results of program calceff is presented, where again the results are much better than they were with the previous version of the program. Finally, at the end of this chapter, there is thorough investigation on how the ECF changes when the effective interaction depth and density changes, leading to very interesting conclusions.

5.1 ECF results obtained with the new MATLAB program

The main goal of this Thesis is the calculation of the efficiency correction factor for seven natural radioactive materials and water. Using the MATLAB program (ANNEX II), the values presented in the following tables (Table 5.1 and Table 5.2, Figure 5.1 and Figure 5.2) were obtained. Table 5.1 and Figure 5.1 show the ECF values for Geometry “2” ($r = 3,6$ and $t = 6,9$ cm) and Table 5.2 and Figure 5.2 show the ECF values for Geometry “8” ($r = 3,6$ and $t = 1,077$ cm). These results were obtained for the typical densities of the materials used by the code, which are presented in (ANNEX V). Similar tables and figures may be produced for any other geometry and material density.

It should be noted that for comparison reasons, the ECF values are not properly rounded, since no estimation of the uncertainty of ECF values was made in this work. From previous works [2] the uncertainty of ECF when calculated by the integral method is estimated to 1-2%.

Table 5.1: New MATLAB code ECF results for geometry “2” for seven materials

keV	Soil 3%	RM	FA	SFS	PG	GS	LS
40	0,712	0,320	0,750	0,316	0,647	0,381	0,194
60	0,873	0,490	0,904	0,472	0,84	0,551	0,325
80	0,965	0,617	0,990	0,587	0,959	0,670	0,435
100	1,015	0,701	1,036	0,662	1,025	0,745	0,514
120	1,040	0,751	1,058	0,706	1,059	0,787	0,564
140	1,048	0,775	1,065	0,726	1,070	0,806	0,591
160	1,049	0,785	1,067	0,735	1,071	0,812	0,611
180	1,052	0,795	1,069	0,744	1,075	0,820	0,623
200	1,054	0,803	1,070	0,752	1,078	0,827	0,633
220	1,055	0,810	1,076	0,759	1,080	0,833	0,642
240	1,056	0,816	1,072	0,764	1,081	0,837	0,649
260	1,057	0,820	1,073	0,768	1,083	0,841	0,656
280	1,057	0,825	1,073	0,772	1,083	0,845	0,661
300	1,058	0,8285	1,073	0,776	1,083	0,848	0,666
320	1,058	0,8315	1,073	0,779	1,084	0,851	0,670
340	1,059	0,834	1,073	0,782	1,083	0,853	0,674
360	1,058	0,836	1,072	0,785	1,083	0,855	0,678
380	1,058	0,839	1,072	0,787	1,083	0,857	0,681
400	1,057	0,841	1,071	0,789	1,083	0,859	0,684
600	1,054	0,854	1,067	0,804	1,078	0,870	0,704
800	1,051	0,862	1,063	0,814	1,072	0,877	0,717
1000	1,047	0,868	1,059	0,821	1,068	0,883	0,727
1200	1,045	0,873	1,055	0,828	1,064	0,887	0,736
1400	1,043	0,877	1,053	0,834	1,061	0,891	0,744
1600	1,041	0,881	1,050	0,839	1,058	0,895	0,752
1800	1,039	0,885	1,048	0,844	1,056	0,899	0,759
2000	1,038	0,889	1,046	0,849	1,053	0,902	0,765

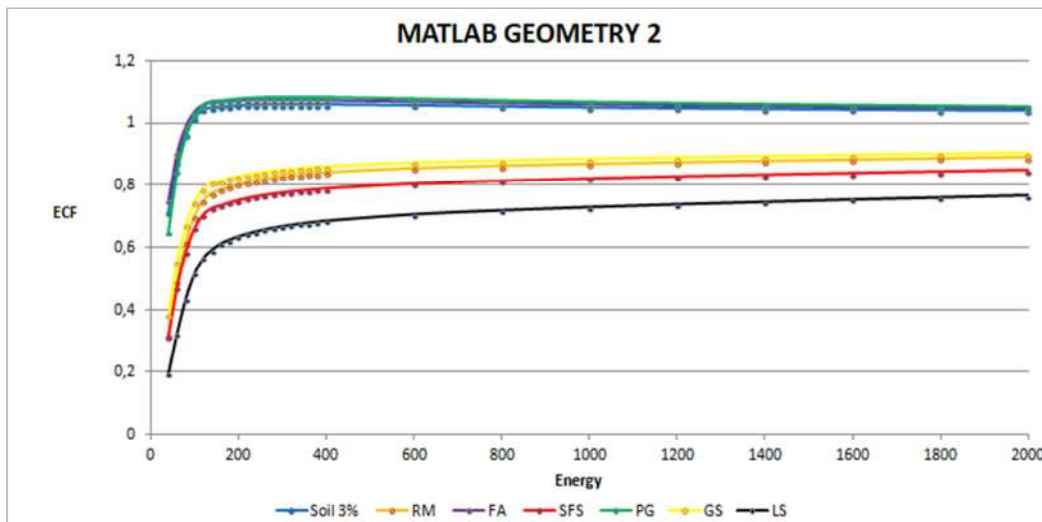


Figure 5.1: ECF calculated with MATLAB code for geometry “2” and seven materials

Table 5.2: New MATLAB code ECF results for Geometry "8" for seven materials

keV	Soil 3%	RM	FA	SFS	PG	GS	LS
40	0,798	0,392	0,825	0,386	0,738	0,463	0,239
60	0,934	0,635	0,952	0,617	0,916	0,696	0,445
80	0,985	0,773	0,996	0,747	0,982	0,814	0,599
100	1,006	0,843	1,014	0,816	1,010	0,872	0,692
120	1,015	0,879	1,021	0,851	1,021	0,901	0,745
140	1,017	0,896	1,023	0,868	1,025	0,914	0,772
160	1,017	0,904	1,023	0,876	1,024	0,919	0,792
180	1,017	0,912	1,023	0,884	1,025	0,924	0,805
200	1,018	0,917	1,023	0,890	1,025	0,929	0,815
220	1,018	0,922	1,023	0,895	1,025	0,933	0,824
240	1,018	0,926	1,023	0,890	1,025	0,936	0,831
260	1,018	0,929	1,022	0,903	1,025	0,939	0,837
280	1,018	0,932	1,022	0,907	1,025	0,941	0,843
300	1,018	0,934	1,022	0,910	1,025	0,943	0,847
320	1,017	0,937	1,022	0,912	1,024	0,945	0,852
340	1,017	0,939	1,021	0,915	1,024	0,947	0,855
360	1,017	0,940	1,021	0,917	1,024	0,948	0,859
380	1,017	0,942	1,021	0,919	1,024	0,949	0,862
400	1,016	0,943	1,020	0,920	1,023	0,951	0,865
600	1,014	0,953	1,018	0,933	1,020	0,959	0,885
800	1,013	0,958	1,016	0,940	1,018	0,963	0,898
1000	1,011	0,962	1,014	0,945	1,016	0,967	0,906
1200	1,010	0,965	1,013	0,949	1,015	0,969	0,913
1400	1,010	0,967	1,012	0,953	1,013	0,971	0,919
1600	1,009	0,969	1,011	0,956	1,013	0,973	0,924
1800	1,008	0,971	1,010	0,958	1,012	0,975	0,928
2000	1,008	0,972	1,010	0,961	1,011	0,976	0,932

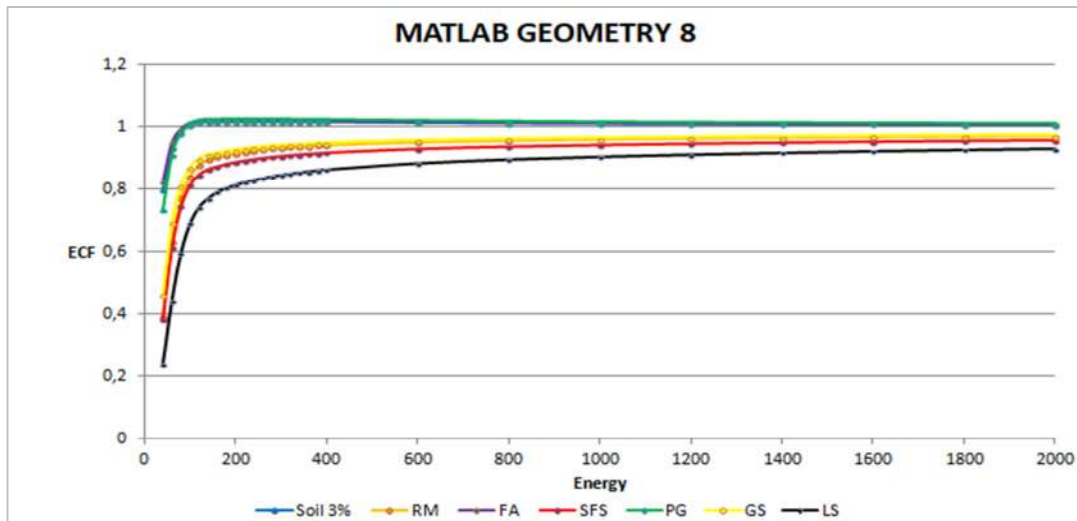


Figure 5.2: ECF calculated with MATLAB code for geometry "8" and seven materials

From the previous figures and tables some very useful conclusions are drawn:

- For low energies there is a need for significant self-attenuation correction, for both geometries, especially for high density materials such as Lead Slag and Granulated Slag.
- While the energy increases the efficiency correction factor tends asymptotically to a value.
- For geometry “8”, which is a relatively thin geometry (1cm thick) this value is very close to “1” for most materials, with the exception of Lead slag, taking into consideration any uncertainties.
- For geometry “2” this value in most cases is far from being equal to “1” for most materials. That means there is a need for self-attenuation corrections for high energy photons. This is a very important issue and there has been plenty of research regarding the need for corrections for very high energies.

It should be emphasized that the results previously presented correspond to the materials and the densities examined in this work. If the material density is significantly changed, then the conclusions will be different.

5.1.1 New MATLAB program and Monte-Carlo simulation results coherence

As previously mentioned, in this work the results of ECF obtained through M-C simulation were extended to higher energies (up to 2000keV). In Table 5.3 and Figure 5.3 the ECF values obtained with M-C simulation are presented, for geometry “8”, for all the materials under investigation and for the typical density. The uncertainty of these values is estimated to be lower than 1%.

From table 5.3 and Figure 5.3 similar conclusions are drawn, as with the MATLAB program calculated values. For most materials ECF values are reaching the value of “1”, within experimental uncertainties.

Figures 5.4 and 5.5 present the results for the ECF calculated both from MATLAB code and through M-C simulation, for phosphogypsum and Lead Slag respectively. From these figures it is made clear that the results for phosphogypsum are very similar, while for Lead Slag the differences are higher, with ECF values calculated from MATLAB code being systematically lower.

One useful comparison that needs to be made is between ECF calculated with MATLAB program and M-C simulation, for the various materials and photon energies. Such a comparison is presented in Figure 5.6. From this comparison the following, very useful, conclusions are drawn:

- For fly-ash and soil, both methods appear to give the same results above 100 keV
- For all other cases MATLAB code gives lower values than PENELOPE, which for energies above 400keV are of the order of 5%, while for energies in the region 40-400keV may be as much as 20%
- The highest the material density, the largest the difference of the results of the two methods

Table 5.3: ECF obtained by PENELOPE for Geometry 8

keV	Soil 3%	RM	FA	SFS	PG	GS	LS
40	0,848	0,471	0,871	0,468	0,799	0,551	0,286
60	0,961	0,748	0,972	0,734	0,948	0,796	0,568
80	0,997	0,862	1,002	0,844	0,995	0,888	0,728
100	1,004	0,906	1,008	0,886	1,006	0,925	0,801
120	1,008	0,927	1,012	0,908	1,011	0,937	0,837
140	1,011	0,939	1,016	0,923	1,017	0,951	0,860
160	1,011	0,944	1,014	0,928	1,013	0,950	0,873
180	1,011	0,949	1,014	0,931	1,016	0,958	0,880
200	1,012	0,953	1,015	0,936	1,017	0,958	0,889
220	1,012	0,957	1,014	0,939	1,017	0,964	0,894
240	1,012	0,958	1,015	0,942	1,017	0,965	0,898
260	1,012	0,960	1,015	0,945	1,017	0,966	0,902
280	1,013	0,963	1,017	0,947	1,017	0,969	0,906
300	1,010	0,961	1,012	0,946	1,015	0,968	0,907
320	1,012	0,963	1,014	0,949	1,017	0,969	0,912
340	1,010	0,965	1,012	0,949	1,021	0,969	0,910
360	1,010	0,964	1,015	0,949	1,014	0,969	0,914
380	1,009	0,964	1,013	0,952	1,015	0,971	0,917
400	1,012	0,964	1,012	0,953	1,016	0,974	0,915
600	1,006	0,970	1,010	0,956	1,010	0,971	0,925
800	1,005	0,977	1,011	0,965	1,013	0,983	0,942
1000	1,002	0,978	1,008	0,971	1,004	0,983	0,944
1200	1,003	0,979	1,001	0,968	1,009	0,974	0,941
1400	1,007	0,983	1,012	0,970	1,010	0,993	0,965
1600	0,997	0,975	0,999	0,973	1,011	0,976	0,957
1800	1,001	0,969	0,995	0,968	1,002	0,979	0,939
2000	1,021	1,001	1,024	0,991	1,021	0,995	0,971

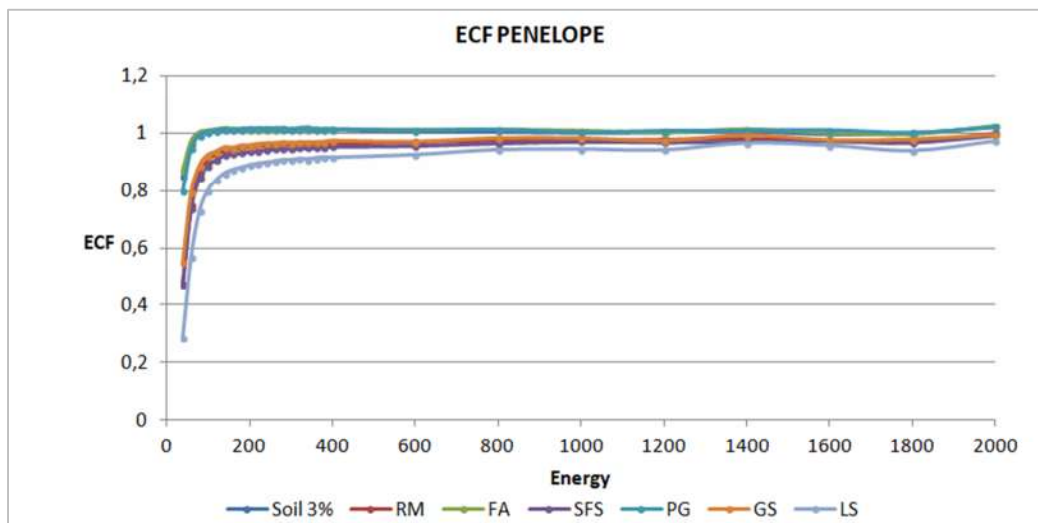


Figure 5.3: ECF – Energy for Geometry 8 / PENELOPE

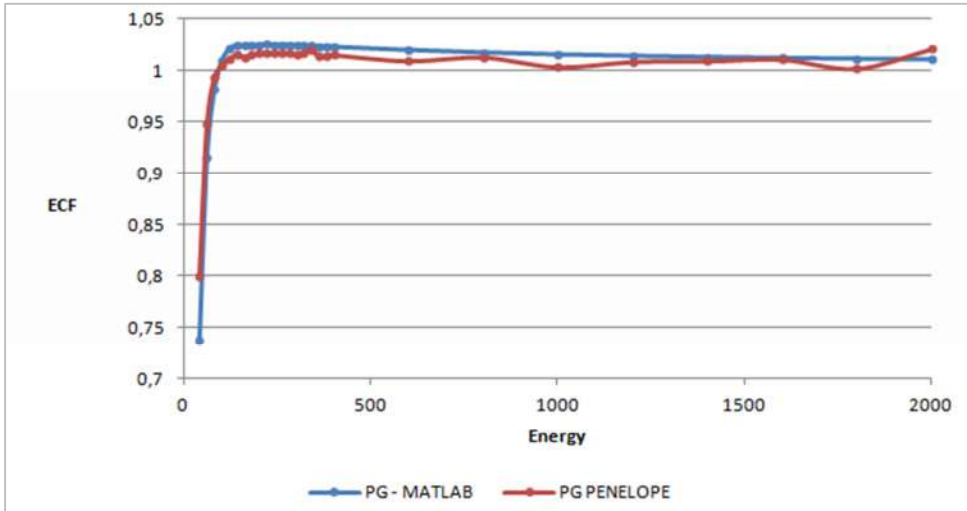


Figure 5.4: ECF of PG with MATLAB and M-C simulation

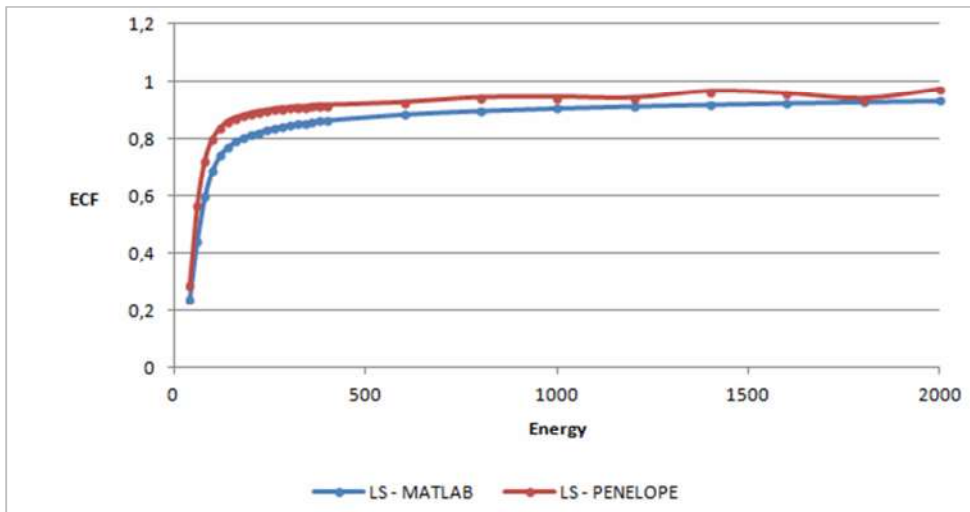


Figure 5.5: ECF of LS with MATLAB and M-C simulation

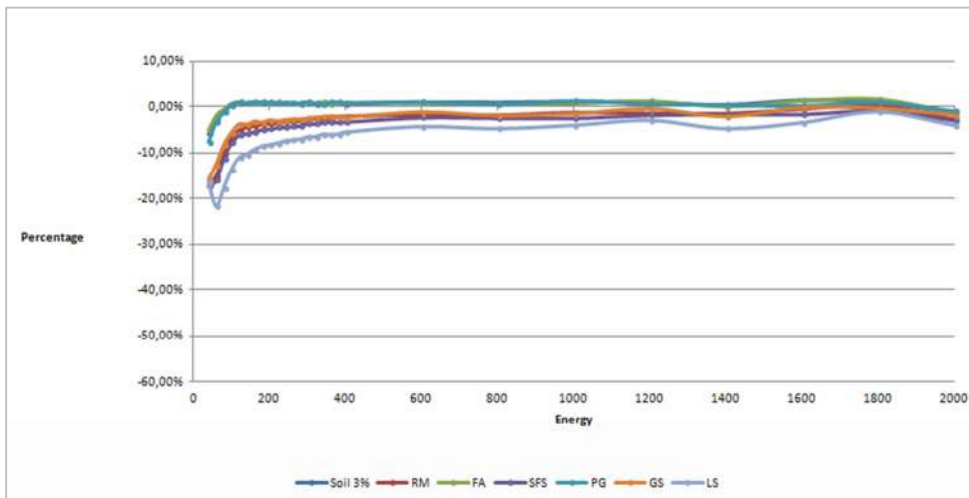


Figure 5.6: Percentage difference between MATLAB and M-C simulation

From the results previously presented it is evident that the results obtained with the new version of MATLAB program are much more consistent with the results of M-C simulation, than the results of the original MATLAB program. This is clear evidence that the new program gives much more accurate results. However, the results are not satisfactory in the full energy region and for all materials. If the MATLAB program is to be as accurate as possible, an investigation of the possible causes of the different results must be undertaken following the previous conclusion. During this work the following two possible sources of different results were examined:

- The effective interaction depth used for the various materials and energies is not constant but energy and possibly material/density specific.
- The integral method can provide accurate results for medium and low densities, while for high densities maybe other corrections are also required. So, it is of great interest to check the ECF for high dense materials, like lead slag, for lower densities as well.

No matter the changes and checks, the results remain the same in low energies for Lead Slag. It seems particularly odd, due to the fact that this new MATLAB program uses the linear attenuation values as calculated by PENELOPE, so the results should had been close.

As it turns out this MATLAB program calculates with great accuracy the ECF values for low dense materials and for energies above 250keV. There may be room for corrections on the Integral equation of the “Integral Method” so as to increase the accuracy, but for now this code is as accurate as possible.

Before this investigation, it is interesting to simultaneously compare the results of all three methods: MATLAB program, M-C simulation and calceff program, where possible. This comparison is presented in the following paragraph.

5.1.2 MATLAB code and CALCEFF results coherence

Although calceff program uses experimental data for the compositions of the materials, it is interesting to make a comparison with MATLAB program and M-C simulation results, for certain energies. The efficiency correction factor as obtained by calceff for soil and fly-ash and for nine energy levels in the region 40 – 200 is presented in the Figure 5.7.

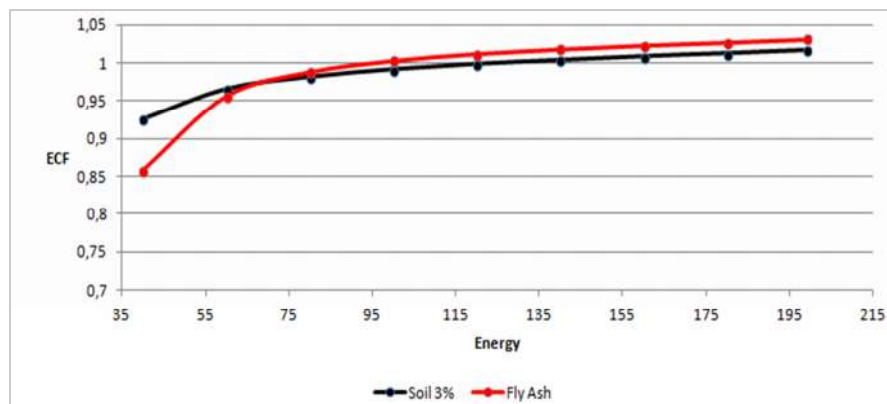


Figure 5.7: ECF values obtained with calceff

In figures 5.8 and 5.9 are presented the ECF values calculated using all three methods, for soil and fly-ash. As it is observed, for soil and energies higher than 80 keV all methods give the same results, while for lower energies the results differ, with the difference increasing as energy decreases. The highest difference is observed between the results of calceff and MATLAB program. This is an interesting result taking into consideration that the materials used in all methods do not have exactly the same composition, as calceff program uses experimental results.

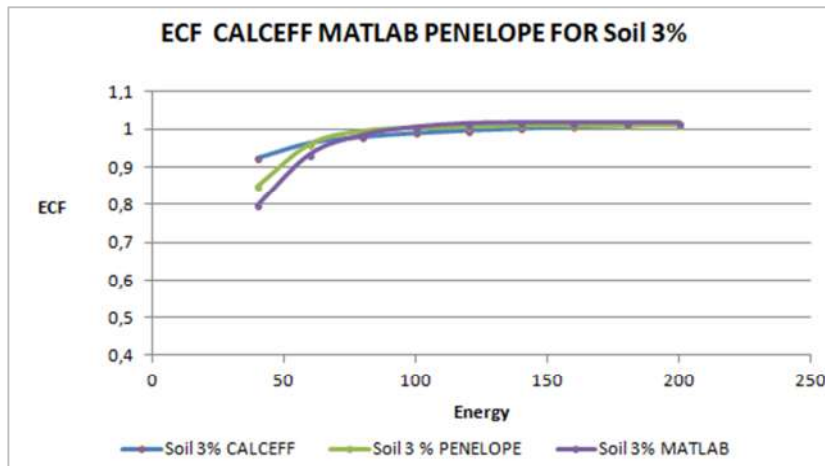


Figure 5.8: ECF plot of soil for calceff, MATLAB and M-C simulation

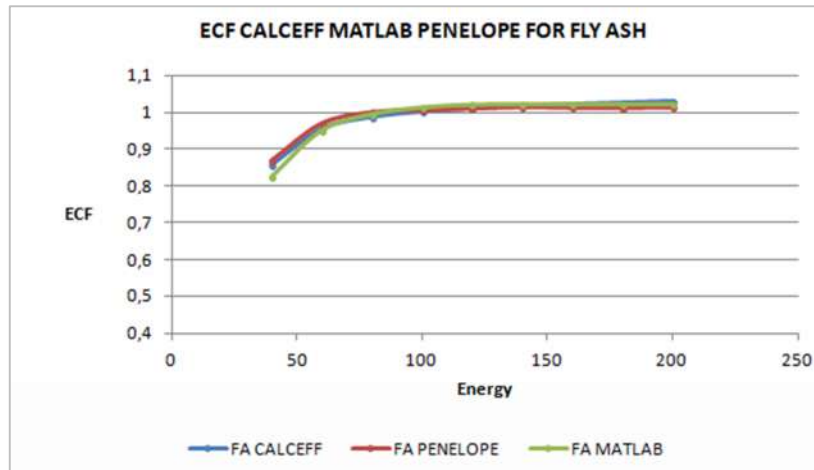


Figure 5.9: ECF plot of fly ash for calceff, MATLAB and M-C simulation

As seen from Figure 5.10 the maximum percentage difference for Soil is at 22% and for Fly Ash is at 12%. As expected these maxima only exists in low energies. Using the old MATLAB program the maximum percentage difference exceeded 25% for Soil and 20% for FA. This

means that the new code with new fitting of the linear attenuation coefficient is closer to calceff than the old code used to.

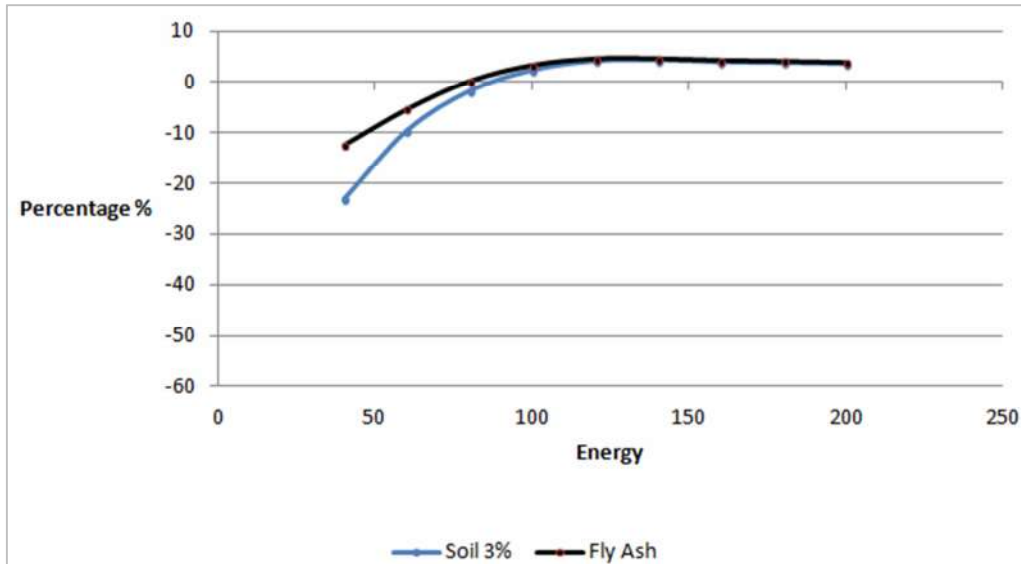


Figure 5.10: Percentage difference of ECF for soil between MATLAB and calceff

5.2 The effect of the detector effective interaction depth

There was a question raised in paragraph 5.1.1 with regard to the effect of selection of the detector's effective interaction depth, and subsequently the distance "d" between the sample and the "fictitious" point detector on the ECF values determined with the modified MATLAB code. That was the reason to modify the program in order to allow the user to select "d" instead of a fixed value. This modification allowed for a thorough investigation of the effect of "d". The results of this investigation are presented in figures 5.11 and 5.12, for geometry "2" and for the energy of 50 and 1000 keV and in figures 5.13 and 5.14 for geometry "8" for 50keV and 1000keV respectively.

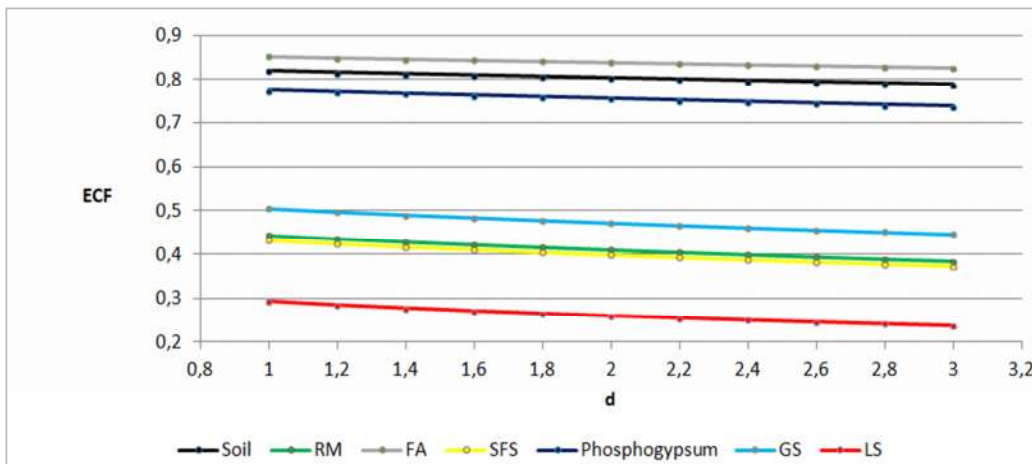


Figure 5.11: ECF from MATLAB program over "d", for geometry "2" and E=50keV

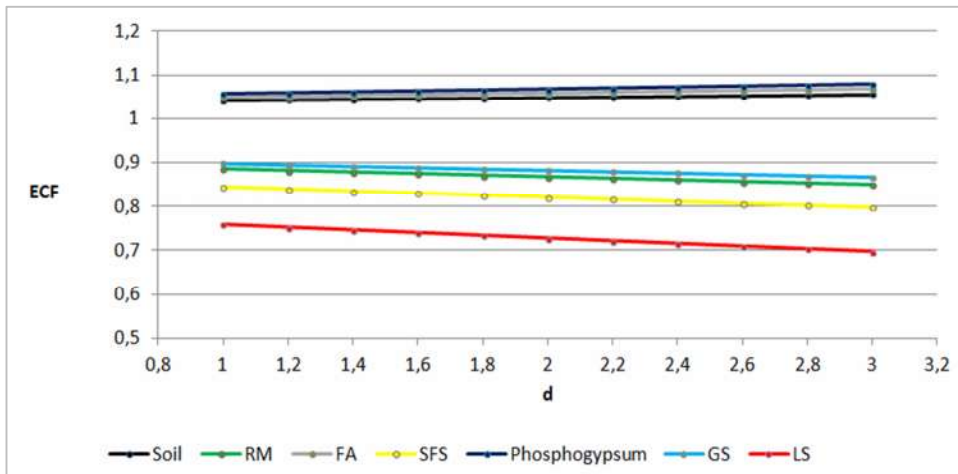


Figure 5.12: ECF from MATLAB program over “d” for geometry “2” and E=1000keV

It is clear that ECF depends on “d” for every material. For those materials where ECF is lower than 1, ECF is slightly reduced with “d”, regardless of the photon energy and the sample geometry.

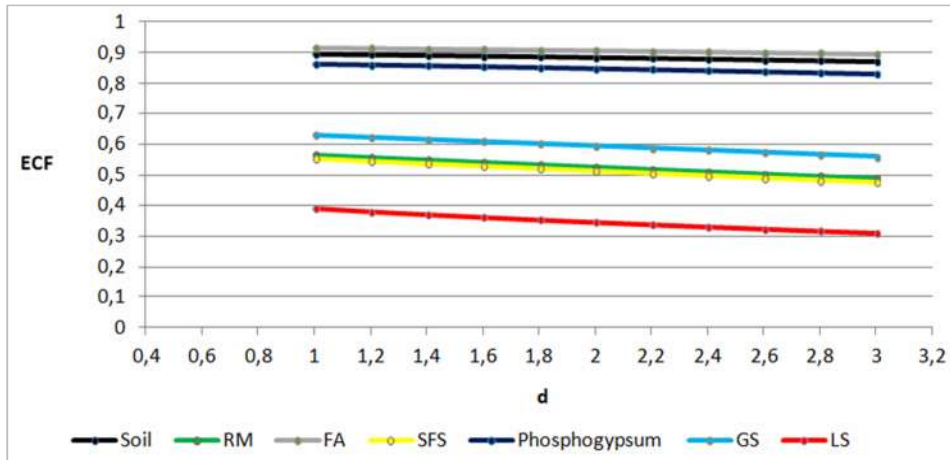


Figure 5.13: ECF over the change in the effective interaction depth for geometry “8” & E=50keV

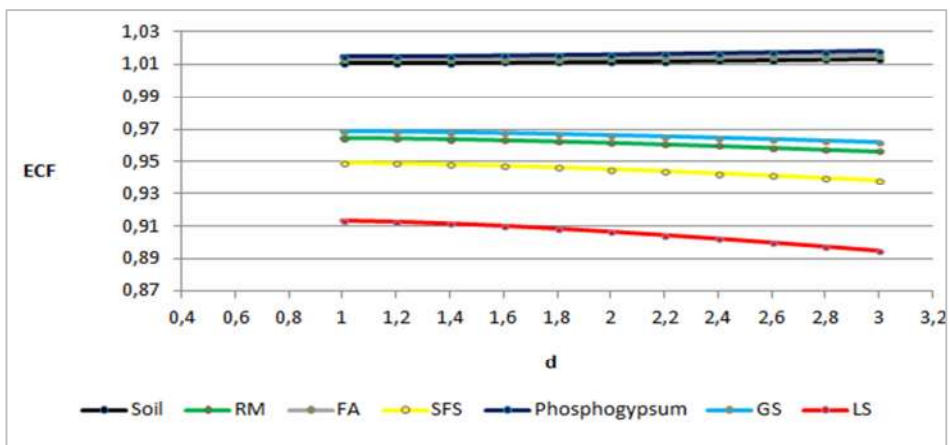


Figure 5.14: ECF over the change in the effective interaction depth for geometry “8” & E=1000keV

In the next two figures (Fig. 5.15 and 5.16) two different plots are presented. In figure 5.15 the plot of ECF values for lead slag – the material with the highest density – for 50keV and for the two geometries “2” and “8” are presented. In figure 5.16 the plot of ECF values for soil – the relatively low density material – for 50keV and for the two geometries “2” and “8” are presented. As shown, the two different graphs follow the same linear course with the same rate of decrease. The only difference is that the geometry 8 – graph shows higher values of ECF.

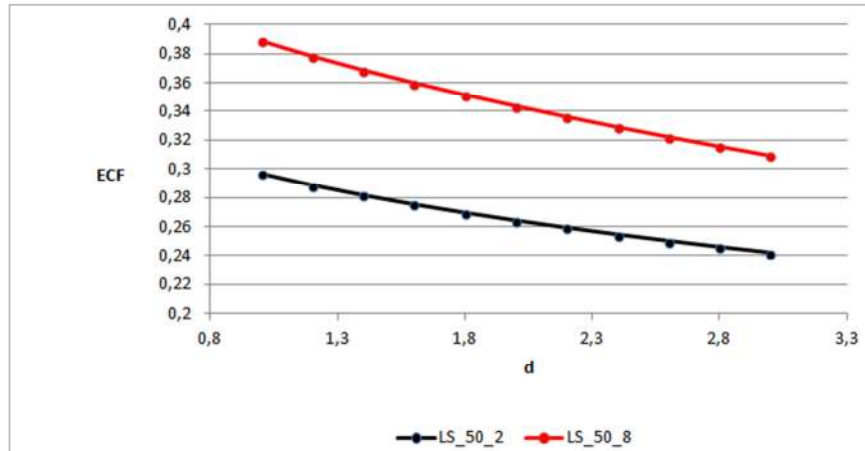


Figure 5.15: ECF over the change in the effective interaction depth for LS, E=50keV and geometry “2” & “8”

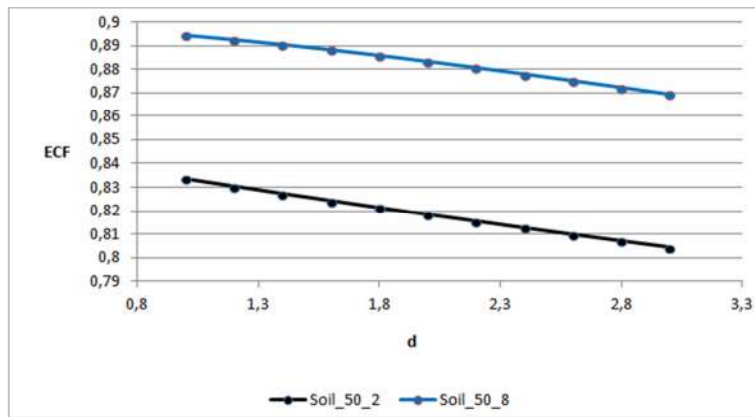


Figure 5.16: ECF over the change in the effective interaction depth for Soil, E=50keV and geometry “2” & “8”

Analyzing figures 5.15 and 5.16 one gets a complete picture on how the ECF changes with the distance “d”. For example, the linear reduction of ECF value for lead slag is reduced by about 20% between d=1,5cm and d=2cm. This means that by reducing “d”, the ECF values calculated from MATLAB program could come closer to PENELOPE values of ECF. So, in order to check this assumption, the plot presented in figure 5.17 was produced. This plot shows the percentage difference between the ECF values calculated by MATLAB and PENELOPE M-C simulation, using as effective interaction depth the values d=2cm and d=1,5cm, for the sample material of lead slag. From this Figure the following conclusions are drawn:

- For energies above 400 keV there is no effect of “d”
- For energies below 400, there is a clear effect of “d”, with the difference decreasing as “d” decreases.
- It is not clear why a difference is observed at the energy of 1400keV – the possibility of erroneous calculation cannot be excluded.

So, clearly the selection of “d” could affect the consistence between the results of MATLAB code and M-C simulation. If the M-C results are considered as more accurate, then a series of correlations of the form $d=f(E,\rho)$ for each material could be produced, to provide “d” values that could be introduced in MATLAB program. These correlations may be produced by running the MATLAB program for various materials, densities and photon energies, and for “d” values that would give ECF close to that of M-C simulation.

By doing so the MATLAB program would give results coherent with M-C simulation ECF values. In this case “d” would no longer be just a value to be obtained experimentally, depending on photon energy, but instead, it would be more like a parameter to be adjusted in order to take more accurate results, besides photon energy, material type and density.

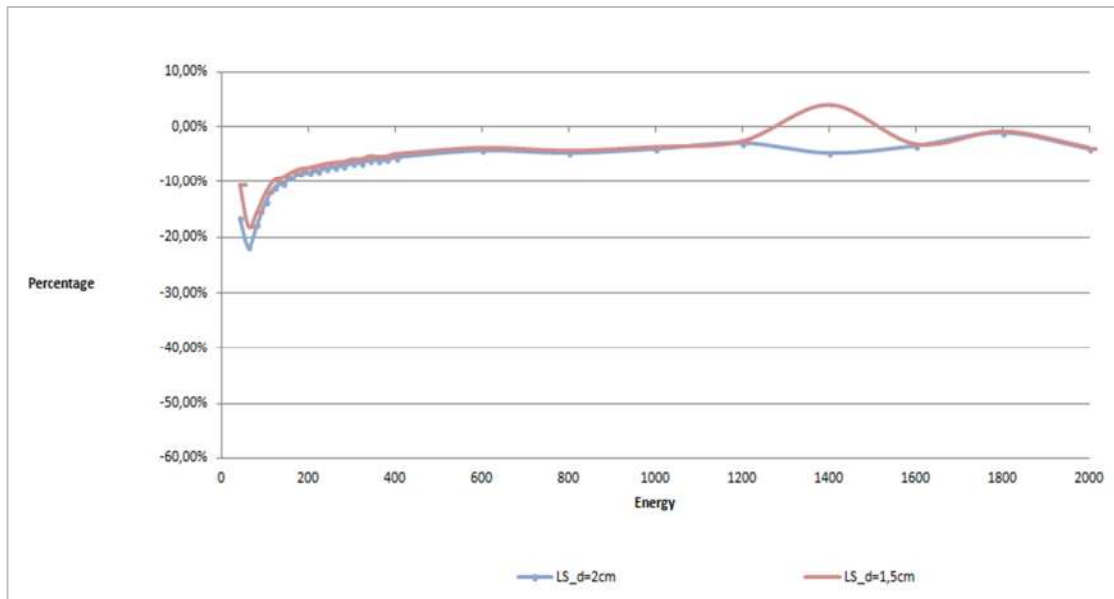


Figure 5.17: Percentage difference MATLAB and M-C simulation with d=2cm and d=1,5cm for lead slag

CHAPTER 6

CONCLUSIONS

Aim of this Thesis was to improve the performance and extend the capabilities of a MATLAB program for the determination of an efficiency correction factor (ECF) in gamma spectrometry applications, and especially when analyzing environmental materials, where the self-absorption of low energy photons becomes important. The program to be improved had been previously developed in another Thesis [3]. Three methods of determining ECF were compared. One of them was based on Monte Carlo simulations and the other two were based on the “Integral Method” that was implemented in (a) a MATLAB program, and (b) a computer program named “calceff” that is being used at NEL-NTUA for about 30 years. The efficiency correction factors were calculated for eight different materials (Soil, Fly Ash, Red Mud, Phosphogypsum, three different slags and water). This Thesis focused mainly on the MATLAB program and how it would become more accurate and user friendly.

The MATLAB program calculating ECF was originally created by [3], giving good results but also with plenty of room for improvement. More specifically, analyzing the original code it was found out that there was a major problem in low energies for high dense materials such as the three different slags. In these low energy values (below 250keV) there was a large difference between MATLAB and Monte-Carlo simulation results (more than 60%). After analyzing the way the linear attenuation coefficient was calculated it turned out the formulas used were not the most appropriate. After fixing this issue the results between MATLAB and M-C simulation converged and the percentage difference dropped to 20% for the higher density materials and 5% for low density materials. Moreover for energies up to 200keV and for materials: Soil and Fly Ash, it was possible to verify the results with the calceff program. In this case too, the results were more promising than before.

In this early MATLAB program there was a relatively small energy range available for the calculation of the ECF (30-400keV). After thorough research it was found out an efficiency correction factor – especially for high dense materials and thick big geometry samples – is needed for high energies too. In this work the energy range was extended to reach 2000keV. In an effort to make the code as accurate as possible, it was investigated the way the effective interaction depth of the detector affects ECF values for all materials and in the whole energy range. Until now the effective interaction depth was fixed at 2cm. From the investigation made, it turned out that, as the effective interaction depth is getting smaller, the ECF results MATLAB program converge to that of M-C simulation for low energies. In fact, there is a 20% reduction on the difference between these two methods when the effective interaction depth is set to 1,5cm.

Although these results in low energies were acceptable, in high energies the difference increases. This means that the effective interaction depth should be energy specific. Besides trying to make the program more accurate than the original one, significant modifications

were made on the flexibility of the program as well. Until now, this program was not available to everyone. In order to run this program and calculate the ECF, the user should have had installed MATLAB. One of the main goals of this Thesis was to make this program accessible to everyone and more user-friendly. In order to do so, the program was turned into a standalone application which is easy to use and calculate the efficiency correction factor with one button and several desired inputs. In this new application the user is now able to choose several geometric parameters and calculate ECF for any cylindrical geometry, choose the density for each material and finally choose the effective interaction depth of the detector. Thanks to these changes it was very easy and fast to obtain the ECF values and make the comparisons between different methods.

The new application that was developed gives very promising results; however there is still room for improvements. These improvements could be made in the accuracy of the results in low energies for dense materials where the difference between these three different methods investigated is maximum. Until now the accuracy of the code is very high for energy values higher than 200keV, so it is recommended to use this code mainly in the range 200-2000keV. Furthermore, it is very easy for the user to introduce new materials, standard geometries and detectors or extend the energy range to higher energies simply by following the instructions included in this thesis. It is also very easy to change the layout of the application so as to make it more user-friendly.

By using the new application for several materials and photon energies some very important conclusions were drawn, namely:

- Corrections for self-absorption may be required for energies much higher than 200keV, contrary to what is commonly believed. This is of great importance for the determination of several natural radionuclides like ^{214}Bi , ^{214}Pb , ^{228}Ac , ^{40}K , of great importance for the analysis of NORM.
- The effective interaction depth plays an important role in ECF calculation. Thorough investigation is required in this field.
- The integral method may not be sufficient when applied for high density materials.

In the future it would be very interesting to investigate the equations and the integrals of the “Integral Method” and run more M-C simulations in order to reduce the differences between these methods more consistent and make the new application more accurate. The introduction of new parameters or the investigation of the energy dependence of others – like the effective interaction depth – may be required in order to improve accuracy, provided that this is adequately theoretically justified.

BIBLIOGRAPHY

- [1] EU COUNCIL DIRECTIVE 2013/59/EURATOM. *“Laying down basic safety standards for protection against the dangers arising from exposure to ionizing radiation, and repealing Directives”* 89/618/Euratom, 90/641/Euratom, 96/29/Euratom, 97/43/Euratom and 2003/122/Euratom. EU, 2013.
- [2] Anagnostakis M.J. *“Gamma-spectroscopic analysis of low radioactivity samples, in the low energy region”*. PhD Thesis, NTUA. Athens 1998 - in Greek.
- [3] Tugnoli F. *“Analysis of the vertical distribution and the size fractionation of natural and artificial radionuclides in the soil in the vicinity of hot springs”*. Master Thesis-NTUA, 2017.
- [4] Debertin K., Helmer RG. *“Gamma spectroscopy with semiconductor detectors”*. Amsterdam: Elsevier Science Publisher B.V., ISBN 0444 871071, 1988.
- [5] Anagnostakis M.J., Simopoulos SE. *“An experimental/numerical method for the efficiency calibration of low-energy photons germanium detectors”*. Environment International Volume 22-1, pp 93-99, ISSN 0160-4120, 1996.
DOI: [https://doi.org/10.1016/S0160-4120\(96\)00094-3](https://doi.org/10.1016/S0160-4120(96)00094-3)
- [6] W.H. McMaster, N. Kerr del Grande, J.H. Mallett and J.H. Hubbell. *“Compilation of X-ray cross-sections”*. Lawrence Livermore National Laboratory Report UCRL-50174, Sect. 2, (Rev. 1), 1969.
- [7] Petropoulos N.P., Anagnostakis M.J., Simopoulos SE., *“Photon attenuation, natural radioactivity content and radon exhalation rate of building materials”*. Journal of Environmental Radioactivity Volume 61-3, pp 257-269, ISSN 0265-931X, 2002.
DOI: [https://doi.org/10.1016/S0265-931X\(01\)00132-1](https://doi.org/10.1016/S0265-931X(01)00132-1)
- [8] Jodłowski P. *“Self-absorption correction in gamma-ray spectrometry of environmental samples. An overview of methods and correction values obtained for the selected geometries”*. Nukleonika 51 (Suppl. 2), S21–S25, 2006.
- [9] Ford, J. (Ed.). *“Radiation, people and the environment”*. International Atomic Energy Agency (IAEA)-Division of Public Information, Vienna, 2004.
- [10] M. F. Attallah, N. S. Awwad and H. F. Aly. *“Environmental Radioactivity of TE-NORM Waste Produced from Petroleum Industry in Egypt: Review on Characterization and Treatment”*. Natural Gas - Extraction to End Use, Sreenath Borra Gupta, IntechOpen, 2012.
DOI: 10.5772/39223.

- [11] INTERNATIONAL ATOMIC ENERGY AGENCY. *“Regulatory and management approaches for the control of environmental residues containing naturally occurring radioactive materials (NORM)”*. IAEA-TECDOC-1484, IAEA, VIENNA, 2006.
- [12] Fernandez J.E., Molinari V.G. *“X-ray Photon Spectroscopy Calculations”*. Advances in Nuclear Science and Technology, vol 22. Springer, Boston MA, 1991
DOI: https://doi.org/10.1007/978-1-4615-3392-4_2
- [13] Vichi S. *“Caratterizzazione di un rivelatore portatile CZT per applicazioni di spettrometria gamma in medicina nucleare”*. Master Thesis - University of Bologna, 2012/2013.
- [14] Jaeger R.G., Blizard E.P., Chilton A.B., Grotenhuis M., Honig A., Jaeger T.A., Eisenlohr H.H., *“Engineering Compendium on Radiation Shielding. Shielding Materials (2)”*. Springer-Verlag Berlin Heidelberg, 1975. ISBN: 978-3-642-65003-1
- [15] Liu Y, Lin C, Wu Y. *“Characterization of red mud derived from a combined Bayer Process and bauxite calcination method”*. Journal of Hazardous Materials, Volume 146 -(1-2), pp 255-261, 2007.
DOI: <https://doi.org/10.1016/j.jhazmat.2006.12.015>
- [16] Zuo Y., Nedeljković M., Ye G., *“Pore solution composition of alkali-activated slag/fly ash pastes”*. Cement and Concrete Research, Volume 115, 2019.
DOI: <https://doi.org/10.1016/j.cemconres.2018.10.010>
- [17] Bumanis G. Zorica J., Bajare D., Korjakins A. *“Technological properties of phosphogypsum binder obtained from fertilizer production waste”*. Energy Procedia, Volume 147, pp 301-308, 2018.
DOI: <https://doi.org/10.1016/j.egypro.2018.07.096>
- [18] Mikodaa B, Kuchaa H., Potyszb A., Kmiecika E. *“Metallurgical slags from Cu production and Pb recovery in Poland Their environmental stability and resource potential”*. Applied Geochemistry – Elsevier, Volume 98, pp 459-472, ISSN 0883-2927, 2019.
DOI: <https://doi.org/10.1016/j.apgeochem.2018.09.009>
- [19] Hubbell, J.H. *“Photon Mass Attenuation and Energy-Absorption Coefficients”*. International Journal of Applied Radiation and Isotopes, Volume 33-11, 1982.
DOI: [https://doi.org/10.1016/0020-708X\(82\)90248-4](https://doi.org/10.1016/0020-708X(82)90248-4)
- [20] Hubbell, J.H. *“Photon Cross Sections, Attenuation Coefficients, and Energy Absorption Coefficients from 10 keV to 100 GeV”*. NSRDS-National Bureau of Standards 29, Washington, D.C., 1969.
- [21] Nuclear Energy Agency (OECD). *“PENELOPE-2006: A Code System for Monte Carlo Simulation of Electron and Photon Transport”*. Workshop Proceedings, Barcelona, Spain, ISBN: 92-64-02301-1, 2006.
- [22] Padovani S., Mitsios I., Anagnostakis M., Mostacci D. *“Analysis of the vertical distribution and size fractionation of natural and artificial radionuclides in soils in the vicinity of hot springs, Radiation Effects and Defects in Solids”*, Taylor and Francis Online, Volume 173-(9-10), pp 794-806, 2018.
DOI: <https://doi.org/10.1080/10420150.2018.1528605>

- [23] Ettler V., Johan Z. *“12 years of leaching of contaminants from Pb smelter slags: Geochemical/mineralogical controls and slag recycling potential”*. Applied Geochemistry - Elsevier, Volume 40, pp 97-103, ISSN 0883-2927, 2014.
DOI: <https://doi.org/10.1016/j.apgeochem.2013.11.001>
- [24] Barna R., Moszkowicz P., Gervais C. *“Leaching assessment of road materials containing primary lead and zinc slags, Waste management”*. Elsevier Volume 24-9, pp 945-955, ISSN 0956-053X, 2004.
DOI: <https://doi.org/10.1016/j.wasman.2004.07.014>
- [25] Chouak A., Vuister P., Paic G., Berrada M., Csikai J. *“Determination of U and Ra in Rock Samples by Gamma-Spectroscopic Method”*. Journal of Radioanalytical Chemistry 45, pp 445-451, 1978.
DOI: <https://doi.org/10.1007/BF02519612>
- [26] Pal S.C., Abhijit M., Pathak S.R. *“Investigation of Hydraulic Activity of Ground Granulated Blast Furnace Slag in Concrete”*. Cement and Concrete Research, Volume 33-9, pp 1481-1486, ISSN 0008-8846, 2003.
DOI: [https://doi.org/10.1016/S0008-8846\(03\)00062-0](https://doi.org/10.1016/S0008-8846(03)00062-0)
- [27] Agrafiotis K., Karfopoulos K., Anagnostakis M.J. *“Calibration of an in-situ BEGe detector using semi empirical and Monte Carlo techniques”*, Applied Radiation and Isotopes, Volume 69-8, pp 1151-1155, ISSN 0969-8043, 2010.
DOI: <https://doi.org/10.1016/j.apradiso.2010.12.005>
- [28] Bonczyk M., Boguslaw M., Chmielewska. *“The self-absorption correction factor for ²¹⁰Pb concentration in mining waste and influence on environmental radiation risk assessment”*. Isotopes in Environmental and Health Studies, Volume 53-1, pp 104-110, 2017.
DOI: <https://doi.org/10.1080/10256016.2016.1116987>.
- [29] Thomson J. *“Sample Preparation Techniques for Liquid Scintillation Analysis”*. Handbook of Radioactivity Analysis (Second Edition), Academic Press, pp 655-717, 2003.
DOI: <https://doi.org/10.1016/B978-012436603-9/50013-2>
- [30] Zia ur Rehman M., Khalid H., Rizwan M., Ali S., Sohail I.M., Usman M., Umair M. *“Inorganic Amendments for the Remediation of Cadmium-Contaminated Soils”*. Academic Press, pp 113-141, 2019.
DOI: <https://doi.org/10.1016/B978-0-12-815794-7.00004-7>
- [31] Hanania J., Sheardown A., Stenhouse K., Donev J. *“Energy Education - Fly ash [Online]”*. 2019.
Available: https://energyeducation.ca/encyclopedia/Fly_ash
- [32] Kovler K. *“Radioactive Materials”*. In Woodhead Publishing Series in Civil and Structural Engineering, Toxicity of Building Materials, Woodhead Publishing, pp 196-240.
DOI: <https://doi.org/10.1533/9780857096357.196>
- [33] Misiak, Ryszard & Hajduk, Roman & Stobinski, Marcin & Bartyzel, Mirosław & Szarłowicz, Katarzyna & Kubica, Barbara. *“Self-absorption correction and efficiency calibration for radioactivity measurement of environmental samples by gamma-ray spectrometry”*. Nukleonika. Volume 56, pp 23-28, 2011.

- [34] EPA regulation retrieved from:
<https://www.epa.gov/coalash/coal-ash-rule>.
- [35] “*Low Energy Germanium Detector*” retrieved from:
<https://www.mirion.com/products/lege-low-energy-germanium-detector>.
- [36] “*What is MATLAB?*” retrieved from:
<https://ch.mathworks.com/discovery/what-is-matlab.html>.
- [37] “*Create apps with graphical user interfaces in MATLAB*” retrieved from:
<https://ch.mathworks.com/discovery/matlab-gui.html>.
- [38] “*Uranium Gamma Spectrometry*” retrieved from:
<http://physicsopenlab.org/2016/01/29/uranium-gamma-spectrometry>
- [39] Picture of Soil retrieved from:
<https://www.ferrismulchproducts.com/compost-and-topsoil>
- [40] Picture of Red Mud retrieved from:
<https://feeco.com/driving-value-from-red-mud/>
- [41] Picture of Phosphogypsum retrieved from:
<https://www.indiamart.com/proddetail/>
- [42] Picture of Granulated Slag retrieved from:
<https://www.eworldtrade.com/pd/vssgroup/qqbs-ground-granulated-blast/681375/>
- [43] Picture of Lead Slag retrieved from:
https://www.alibaba.com/product-detail/Lead-Pb-slag_135135641.html
- [44] MuPlot retrieved from:
<http://shape.inq.unibo.it/html/muplot.htm>
- [45] Picture of “*Photoelectric interaction*” retrieved from:
<https://www.laradioactivite.com/>
- [46] Picture of “*Compton Scattering*” retrieved from:
<http://hyperphysics.phys-astr.gsu.edu>
- [47] Picture of “*Pair production schematic*” retrieved from:
<http://hyperphysics.phyastr.gsu.edu/hbase/Particles/lepton.html>
- [48] Picture of “*Exponential law of photon attenuation*” retrieved from:
<https://www.nuclear-power.net>
- [49] Picture of “*Thorium Series*” retrieved from:
<http://physicsopenlab.org/2016/01/29/uranium-gamma-spectrometry>

ANNEX I

Original MATLAB Code

```
% EFFICIENCY CORRECTION FACTOR

% 1. Source - detector setup

d=2; % Fictitious source-to-detector distance [cm]

% 2. Sample geometry
prompt='Geometry [2/8] : ';
geom=input(prompt);

if geom==8
r=3.6; % Radius of the sample [cm]
t=1.077; % Thickness of the sample [cm]
end

if geom==2
r=3.6; % Radius of the sample [cm]
t=6.9; % Thickness of the sample [cm]
end

if geom~=2 && geom~=8
fprintf('ERROR: the requested geometry does not exist. Please, insert
2 or 8.')
return
end

% 3. Sample material
prompt='\n MATERIAL \n\n 1:Soil \n 2:Red Mud \n 3:Fly Ash \n 4:SF
Slag \n 5:Phosphogypsum \n 6:G Slag \n 7:L Slag \n\n';
mat=input(prompt);

if mat==1 % Soil
ro=1.000; % Density of the sample [g/cm^3]
x_en=[30 40 50 60 80 100 150 200 300 400 500 600 800 1000];
v_mi=[1.3647 0.67714 0.42883 0.31624 0.2212 0.18221 0.14283 0.12509
0.10562 9.40E-02 8.59E-02 7.98E-02 7.12E-02 6.54E-02];
A=0.265;
B=-3.4735;
C=8.79645;
end

if mat==2 % RM
ro=1.735; % Density of the sample [g/cm^3]
x_en=[30 40 50 60 80 100 150 200 300 400 500 600 800 1000];
```

```

v_mi=[2.3833 1.1128 0.65302 0.44617 0.27595 0.21015 0.15105 0.12856
0.10666 9.43E-02 8.58E-02 7.95E-02 7.06E-02 6.45E-02];
A=0.3423;
B=-4.4342;
C=11.758;
end

if mat==3 % FA
ro=0.97; % Density of the sample [g/cm^3]
x_en=[30 40 50 60 80 100 150 200 300 400 500 600 800 1000];
v_mi=[1.303 0.65079 0.4151 0.30808 0.21748 0.18011 0.14199 0.1246
0.1053 9.37E-02 8.55E-02 7.94E-02 7.08E-02 6.49E-02];
A=0.2572;
B=-3.3855;
C=8.5359;
end

if mat==4 % SF Slag
ro=1.981; % Density of the sample [g/cm^3]
x_en=[30 40 50 60 80 100 150 200 300 400 500 600 800 1000];
v_mi=[2.0893 0.98742 0.58836 0.40853 0.2599 0.20184 0.14848 0.12738
0.10614 9.40E-02 8.56E-02 7.94E-02 7.05E-02 6.45E-02];
A=0.3247;
B=-4.214;
C=11.07;
end

if mat==5 % PG
ro=0.931; % Density of the sample [g/cm^3]
x_en=[30 40 50 60 80 100 150 200 300 400 500 600 800 1000];
v_mi=[1.7362 0.83582 0.511 0.36429 0.24186 0.19295 0.14608 0.12648
0.10609 9.43E-02 8.62E-02 8.01E-02 7.17E-02 6.60E-02];
A=0.3013;
B=-3.9132;
C=10.125;
end

if mat==6 % G Slag
ro=1.657; % Density of the sample [g/cm^3]
x_en=[30 40 50 60 80 100 150 200 300 400 500 600 800 1000];
v_mi=[1.9894 0.94384 0.56592 0.39565 0.25471 0.19941 0.14809 0.12748
0.10646 9.43E-02 8.59E-02 7.96E-02 7.07E-02 6.46E-02];
A=0.3172;
B=-4.1203;
C=10.785;
end

if mat==7 % L Slag
ro=2.645; % Density of the sample [g/cm^3]
x_en=[30 40 50 60 80 100 150 200 300 400 500 600 800 1000];
v_mi=[2.8348 1.3072 0.75301 0.50389 0.30434 0.22218 0.15429 0.12966
0.10659 9.40E-02 8.54E-02 7.90E-02 7.01E-02 6.39E-02];
A=0.3645;
B=-4.7186;
C=12.66;
end

```

```

if mat<1
fprintf('ERROR: the requested material does not exist. Please, enter
a number in the range [1,7]')
return
end

if mat>7
fprintf('ERROR: the requested material does not exist. Please, enter
a number in the range [1,7]')
return
end

% 4. Calibration material: 4M HCl
ro_cal=1.059;
x_en_cal=[30 40 50 60 80 100 150 200 300 400 500 600 800 1000];
v_mi_cal=[0.65694 0.38878 0.28935 0.24176 0.19693 0.17476 0.14622
0.13034 0.11146 0.10012 9.24E-02 8.68E-02 7.93E-02 7.45E-02];
A_cal=0.1518;
B_cal=-2.1001;
C_cal=4.7583;

% 5. Linear attenuation coefficient
prompt='\n ENERGY [keV] \n\n ';
energy=input(prompt);
if energy<30
fprintf('\n ERROR: the energy range is [30, 1000] keV \n\n ');
return
end

if energy>1000
fprintf('\n ERROR: the energy range is [30, 1000] keV \n\n ');
return
end

Lia_cal = ismember(energy, x_en_cal);
Lia=ismember(energy, x_en);

if Lia_cal==1
mi_m_cal=interp1(x_en_cal, v_mi_cal, energy);
else
mi_m_cal=exp(A_cal*(log(energy))^2+B_cal*log(energy)+C_cal);
end

if Lia==1
mi_m=interp1(x_en, v_mi, energy);
else
mi_m=exp(A*(log(energy))^2+B*log(energy)+C);
end

mi_cal=mi_m_cal*ro_cal;
mi=mi_m*ro;

```

```

% 6. Integral method
J_cal=integral2(@(x,y) (y.*exp(-
mi_cal.*(x.*(y.^2+(x+d).^2).^1/2)./(x+d)))./(y.^2+(x+d).^2),0,t,0,r);
J=integral2(@(x,y) (y.*exp(-
mi.*(x.*(y.^2+(x+d).^2).^1/2)./(x+d)))./(y.^2+(x+d).^2),0,t,0,r);

% 7. Efficiency correction factor
ECF=J/J_cal

```

ANNEX II

New MATLAB Code

```
function varargout = GUI_ECF(varargin)
% GUI_ECF MATLAB code for GUI_ECF.fig
%   GUI_ECF, by itself, creates a new GUI_ECF or raises the
existing
%   singleton*.
%
%   H = GUI_ECF returns the handle to a new GUI_ECF or the handle
to
%   the existing singleton*.
%
%   GUI_ECF('CALLBACK',hObject,eventData,handles,...) calls the
local
%   function named CALLBACK in GUI_ECF.M with the given input
arguments.
%
%   GUI_ECF('Property','Value',...) creates a new GUI_ECF or
raises the
%   existing singleton*. Starting from the left, property value
pairs are
%   applied to the GUI before GUI_ECF_OpeningFcn gets called. An
%   unrecognized property name or invalid value makes property
application
%   stop. All inputs are passed to GUI_ECF_OpeningFcn via
varargin.
%
%   *See GUI Options on GUIDE's Tools menu. Choose "GUI allows
only one
%   instance to run (singleton)".
%
% See also: GUIDE, GUIDATA, GUIHANDLES

% Edit the above text to modify the response to help GUI_ECF

% Last Modified by GUIDE v2.5 04-Jun-2020 13:46:11

% Begin initialization code - DO NOT EDIT
gui_Singleton = 1;
gui_State = struct('gui_Name',       mfilename, ...
                  'gui_Singleton',  gui_Singleton, ...
                  'gui_OpeningFcn', @GUI_ECF_OpeningFcn, ...
                  'gui_OutputFcn',  @GUI_ECF_OutputFcn, ...
                  'gui_LayoutFcn',  [] , ...
                  'gui_Callback',   []);
if nargin && ischar(varargin{1})
    gui_State.gui_Callback = str2func(varargin{1});
end

if nargout
    [varargout{1:nargout}] = gui_mainfcn(gui_State, varargin{:});
else
    gui_mainfcn(gui_State, varargin{:});
end
% End initialization code - DO NOT EDIT
```

```

% --- Executes just before GUI_ECF is made visible.
function GUI_ECF_OpeningFcn(hObject, eventdata, handles, varargin)
% This function has no output args, see OutputFcn.
% hObject    handle to figure
% eventdata  reserved - to be defined in a future version of MATLAB
% handles    structure with handles and user data (see GUIDATA)
% varargin   command line arguments to GUI_ECF (see VARARGIN)

% Choose default command line output for GUI_ECF
handles.output = hObject;

% Update handles structure
guidata(hObject, handles);

% UIWAIT makes GUI_ECF wait for user response (see UIRESUME)
% uiwait(handles.figure1);

% --- Outputs from this function are returned to the command line.
function varargout = GUI_ECF_OutputFcn(hObject, eventdata, handles)
% varargout  cell array for returning output args (see VARARGOUT);
% hObject    handle to figure
% eventdata  reserved - to be defined in a future version of MATLAB
% handles    structure with handles and user data (see GUIDATA)

% Get default command line output from handles structure
varargout{1} = handles.output;

function d_Callback(hObject, eventdata, handles)
% hObject    handle to d (see GCBO)
% eventdata  reserved - to be defined in a future version of MATLAB
% handles    structure with handles and user data (see GUIDATA)

% Hints: get(hObject,'String') returns contents of d as text
%        str2double(get(hObject,'String')) returns contents of d as a
double

% --- Executes during object creation, after setting all properties.
function d_CreateFcn(hObject, eventdata, handles)
% hObject    handle to d (see GCBO)
% eventdata  reserved - to be defined in a future version of MATLAB
% handles    empty - handles not created until after all CreateFcns
called

% Hint: edit controls usually have a white background on Windows.
%       See ISPC and COMPUTER.
if ispc && isequal(get(hObject,'BackgroundColor'),
get(0,'defaultUicontrolBackgroundColor'))
    set(hObject,'BackgroundColor','white');
end
end

```

```

function geom_Callback(hObject, eventdata, handles)
% hObject    handle to geom (see GCBO)
% eventdata  reserved - to be defined in a future version of MATLAB
% handles    structure with handles and user data (see GUIDATA)

% Hints: get(hObject,'String') returns contents of geom as text
%        str2double(get(hObject,'String')) returns contents of geom
as a double

% --- Executes during object creation, after setting all properties.
function geom_CreateFcn(hObject, eventdata, handles)
% hObject    handle to geom (see GCBO)
% eventdata  reserved - to be defined in a future version of MATLAB
% handles    empty - handles not created until after all CreateFcns
called

% Hint: edit controls usually have a white background on Windows.
%        See ISPC and COMPUTER.
if ispc && isequal(get(hObject,'BackgroundColor'),
get(0,'defaultUiControlBackgroundColor'))
    set(hObject,'BackgroundColor','white');
end

function energy_Callback(hObject, eventdata, handles)
% hObject    handle to energy (see GCBO)
% eventdata  reserved - to be defined in a future version of MATLAB
% handles    structure with handles and user data (see GUIDATA)

% Hints: get(hObject,'String') returns contents of energy as text
%        str2double(get(hObject,'String')) returns contents of energy
as a double

% --- Executes during object creation, after setting all properties.
function energy_CreateFcn(hObject, eventdata, handles)
% hObject    handle to energy (see GCBO)
% eventdata  reserved - to be defined in a future version of MATLAB
% handles    empty - handles not created until after all CreateFcns
called

% Hint: edit controls usually have a white background on Windows.
%        See ISPC and COMPUTER.
if ispc && isequal(get(hObject,'BackgroundColor'),
get(0,'defaultUiControlBackgroundColor'))
    set(hObject,'BackgroundColor','white');
end

function mat_Callback(hObject, eventdata, handles)
% hObject    handle to mat (see GCBO)
% eventdata  reserved - to be defined in a future version of MATLAB
% handles    structure with handles and user data (see GUIDATA)

% Hints: get(hObject,'String') returns contents of mat as text

```

```

%         str2double(get(hObject,'String')) returns contents of mat as
a double

% --- Executes during object creation, after setting all properties.
function mat_CreateFcn(hObject, eventdata, handles)
% hObject    handle to mat (see GCBO)
% eventdata  reserved - to be defined in a future version of MATLAB
% handles    empty - handles not created until after all CreateFcns
called

% Hint: edit controls usually have a white background on Windows.
%         See ISPC and COMPUTER.
if ispc && isequal(get(hObject,'BackgroundColor'),
get(0,'defaultUiControlBackgroundColor'))
    set(hObject,'BackgroundColor','white');
end

% --- Executes on button press in pushbutton_ECF.
function pushbutton_ECF_Callback(hObject, eventdata, handles)
% hObject    handle to pushbutton_ECF (see GCBO)
% eventdata  reserved - to be defined in a future version of MATLAB
% handles    structure with handles and user data (see GUIDATA)
global ECF

d=str2double(get(handles.d,'String'));
geom=str2double(get(handles.geom,'String'));
mat=str2double(get(handles.mat,'String'));
energy=str2double(get(handles.energy,'String'));
r=str2double(get(handles.r,'String'));
t=str2double(get(handles.t,'String'));
ro=str2double(get(handles.r0,'String'));

if geom==8
r=3.6; % Radius of the sample [cm]
t=1.077; % Thickness of the sample [cm]
end

if geom==2
r=3.6; % Radius of the sample [cm]
t=6.9; % Thickness of the sample [cm]
end

if mat==1 % Soil
%ro=1.000; % Density of the sample [g/cm^3]
x_en=[30 35 40 45 50 60 80 100 150 200 300 400 500 600 800 1000];
v_mi=[1.3986 0.94829 0.69336 0.53746 0.43687 0.32054 0.22286 0.18346
0.14449 0.12715 0.1078 0.09582 0.08719 0.080498 0.070568 0.063378];

if energy<150
    A=-0.1166;
    B=2.23;
    C=-13.91;
    D=26.45;
end
end

```

```

if energy>150
    A=-0.009175;
    B=0.1466;
    C=-1.194;
    D=1.518;
end

if energy == 150
    mi_m = 0.14449;

end

end

%-----%

if mat==2 % RM
%ro=1.735; % Density of the sample [g/cm^3]
x_en=[30 35 40 45 50 60 80 100 150 200 300 400 500 600 800 1000];
v_mi=[2.4322 1.6057 1.136 0.84954 0.6646 0.45251 0.27827 0.21156
0.15243 0.13019 0.10832 0.095736 0.086904 0.080133 0.070162
0.062977];

if energy<150
    A=0.05843;
    B=0.03045;
    C=-5.118;
    D=15.65;
end

if energy>150
    A=-0.01837;
    B=0.3375;
    C=-2.511;
    D=4.532;
end

if energy == 150
    mi_m = 0.15243;

end

end

if mat==3 % FA
%ro=0.97; % Density of the sample [g/cm^3]

```

```
x_en=[30 35 40 45 50 60 80 100 150 200 300 400 500 600 800 1000];  
v_mi=[1.3293 0.90393 0.66316 0.51594 0.42092 0.31096 0.21839 0.18083  
0.14326 0.1263 0.1072 0.095314 0.086741 0.08009 0.070214 0.063062];
```

```
if energy<150  
    A=-0.1312;  
    B=2.41;  
    C=-14.61;  
    D=27.27;  
end
```

```
if energy>150  
    A=-0.008551;  
    B=0.1338;  
    C=-1.107;  
    D=1.316;  
end
```

```
if energy == 150  
    mi_m = 0.14326;
```

```
end  
end
```

```
if mat==4 % SF Slag  
%ro=1.981; % Density of the sample [g/cm^3]  
x_en=[30 35 40 45 50 60 80 100 150 200 300 400 500 600 800 1000];  
v_mi=[2.1344 1.4182 1.0111 0.76188 0.60103 0.41581 0.26279 0.20354  
0.14988 0.12899 0.10784 0.095452 0.086701 0.079972 0.070045  
0.062882];
```

```
if energy<150  
    A=0.0233;  
    B=0.4741;  
    C=-6.893;  
    D=17.81;  
end
```

```
if energy>150  
    A=-0.01615;  
    B=0.2912;  
    C=-2.189;  
    D=3.788;  
end
```

```
if energy == 150  
    mi_m = 0.14988;
```

```
end  
end
```

```
if mat==5 % PG  
%ro=0.931; % Density of the sample [g/cm^3]  
x_en=[30 35 40 45 50 60 80 100 150 200 300 400 500 600 800 1000];  
v_mi=[1.788 1.1929 0.8559 0.65158 0.51956 0.36841 0.24326 0.19421  
0.14812 0.12903 0.1087 0.09643 0.087671 0.080905 0.070893 0.063656];
```

```
if energy<150
```

```
    A=-0.04834;  
    B=1.394;  
    C=-10.68;  
    D=22.69;
```

```
end
```

```
if energy>150  
    A=-0.01202;  
    B=0.2064;  
    C=-1.611;  
    D=2.488;
```

```
end
```

```
if energy == 150  
    mi_m = 0.14812;
```

```
end
```

```
end
```

```
if mat==6 % G Slag  
%ro=1.657; % Density of the sample [g/cm^3]  
x_en=[30 35 40 45 50 60 80 100 150 200 300 400 500 600 800 1000];  
v_mi=[2.0355 1.3532 0.96602 0.72969 0.57714 0.40182 0.25697 0.20074  
0.14933 0.12897 0.10807 0.095716 0.086964 0.080226 0.070275  
0.063093];
```

```
if energy<150
```

```
    A=0.003599;  
    B=0.7292;  
    C=-7.954;  
    D=19.19;
```

```
end
```

```

if energy>150
    A=-0.01488;
    B=0.2652;
    C=-2.013;
    D=3.393;
end

if energy == 150
    mi_m = 0.14933;

end

end

if mat==7 % L Slag
%ro=2.645; % Density of the sample [g/cm^3]

%x_en= [30 35 40 45 50 60 80 100 150 200 300 400 500 600 800 1000];
%v_mi= [2.8873 1.9 1.3376 0.99276 0.77023 0.51427 0.30434 0.22462
0.15579 0.13119 0.10815 0.095316 0.086421 0.079639 0.06969 0.062537];

x_en=[30 35 40 45 50 55 60 65 70 75 80 85 90 95 100 110 120 130 140
150 200 300 400 500 600 800 1000];
v_mi=[2.8873 1.9 1.3376 0.99276 0.77023 0.61962 0.51427 0.43773
0.38099 0.33781 0.30434 0.2778 0.25643 0.239 0.22462 0.2023 0.18594
0.17349 0.16371 0.15579 0.13119 0.10815 0.095316 0.086421 0.079639
0.06969 0.062537];

if energy<150

    A=0.0935;
    B=-0.4211;
    C=-3.292;
    D=13.46;

end

if energy>150
    A=-0.023;
    B=0.433;
    C=-3.167;
    D=6.022;
end

if energy == 150

```

```

mi_m = 0.15579;

end

end

if mat==8 % Water
%ro=1.000; % Density of the sample [g/cm^3]
x_en=[30 35 40 45 50 60 80 100 150 200 300 400 500 600 800 1000];
v_mi=[0.37808 0.30952 0.27011 0.24513 0.22824 0.20686 0.18425 0.17113
0.15067 0.13711 0.11866 0.10614 0.096845 0.89541 0.078607 0.070644];

if energy<150
A=-0.2567;
B=3.54;
C=-16.56;
D=24.49;
end

if energy>150
A=7.263e-05;
B=-0.0478;
C=0.1627;
D=-1.517;
end

if energy == 150
mi_m = 0.15067;

end

end

% 4. Calibration material: 4M HCl
ro_cal=1.059;
x_en_cal=[30 35 40 45 50 60 80 100 150 200 300 400 500 600 800 1000];
v_mi_cal=[0.66261 0.48741 0.38816 0.32701 0.28709 0.23968 0.1966
0.1763 0.1507 0.13599 0.11712 0.10458 0.095361 0.088137 0.077348
0.069501];

if energy<150

A_cal=-0.2998;
B_cal=4.347;
C_cal=-21.38;
D_cal=33.82;

end

```

```

if energy>150
    A_cal=-0.002213;
    B_cal=0.000239;
    C_cal=-0.1725;
    D_cal=-0.757;
end

if energy == 150
    mi_m_cal = 0.1507;

end

%Lia_cal = ismember(energy, x_en_cal);
%Lia=ismember(energy, x_en);

%if Lia_cal==1
%mi_m_cal=interp1(x_en_cal, v_mi_cal, energy);
%else
if energy ~= 150
mi_m_cal=exp(A_cal*log(energy)^3 + B_cal*log(energy)^2 +
C_cal*log(energy) + D_cal);
end
%end

%if Lia==1
%mi_m=interp1(x_en, v_mi, energy);%it takes the v_mi for the
corresponing energy
%else
if energy ~=150
mi_m=exp(A*log(energy)^3 + B*log(energy)^2 + C*log(energy) + D);% it
calculates the  $\mu$ 
end
%end

mi_cal=mi_m_cal*ro_cal; % this multiplies the  $\mu$  with density
mi=mi_m*ro; % this multiplies the  $\mu$  with density

% 6. Integral method
J_cal=integral2(@(x,y) (y.*exp(-
mi_cal.*(x.*(y.^2+(x+d).^2).^1/2)./(x+d)))./(y.^2+(x+d).^2),0,t,0,r);
J=integral2(@(x,y) (y.*exp(-
mi.*(x.*(y.^2+(x+d).^2).^1/2)./(x+d)))./(y.^2+(x+d).^2),0,t,0,r);

```

```

ECF=J/J_cal
set(handles.ECF, 'String', ECF);
set(handles.m, 'String', mi_m);

function ECF_Callback(hObject, eventdata, handles)
% hObject      handle to ECF (see GCBO)
% eventdata    reserved - to be defined in a future version of MATLAB
% handles      structure with handles and user data (see GUIDATA)

% Hints: get(hObject, 'String') returns contents of ECF as text
%        str2double(get(hObject, 'String')) returns contents of ECF as
a double

% --- Executes during object creation, after setting all properties.
function ECF_CreateFcn(hObject, eventdata, handles)
% hObject      handle to ECF (see GCBO)
% eventdata    reserved - to be defined in a future version of MATLAB
% handles      empty - handles not created until after all CreateFcns
called

% Hint: edit controls usually have a white background on Windows.
%        See ISPC and COMPUTER.
if ispc && isequal(get(hObject, 'BackgroundColor'),
get(0, 'defaultUiControlBackgroundColor'))
    set(hObject, 'BackgroundColor', 'white');
end

function r_Callback(hObject, eventdata, handles)
% hObject      handle to r (see GCBO)
% eventdata    reserved - to be defined in a future version of MATLAB
% handles      structure with handles and user data (see GUIDATA)

% Hints: get(hObject, 'String') returns contents of r as text
%        str2double(get(hObject, 'String')) returns contents of r as a
double

% --- Executes during object creation, after setting all properties.
function r_CreateFcn(hObject, eventdata, handles)
% hObject      handle to r (see GCBO)
% eventdata    reserved - to be defined in a future version of MATLAB
% handles      empty - handles not created until after all CreateFcns
called

% Hint: edit controls usually have a white background on Windows.
%        See ISPC and COMPUTER.
if ispc && isequal(get(hObject, 'BackgroundColor'),
get(0, 'defaultUiControlBackgroundColor'))
    set(hObject, 'BackgroundColor', 'white');
end

```

```

function t_Callback(hObject, eventdata, handles)
% hObject    handle to t (see GCBO)
% eventdata  reserved - to be defined in a future version of MATLAB
% handles    structure with handles and user data (see GUIDATA)

% Hints: get(hObject,'String') returns contents of t as text
%        str2double(get(hObject,'String')) returns contents of t as a
double

% --- Executes during object creation, after setting all properties.
function t_CreateFcn(hObject, eventdata, handles)
% hObject    handle to t (see GCBO)
% eventdata  reserved - to be defined in a future version of MATLAB
% handles    empty - handles not created until after all CreateFcns
called

% Hint: edit controls usually have a white background on Windows.
%        See ISPC and COMPUTER.
if ispc && isequal(get(hObject,'BackgroundColor'),
get(0,'defaultUicontrolBackgroundColor'))
    set(hObject,'BackgroundColor','white');
end

function r0_Callback(hObject, eventdata, handles)
% hObject    handle to r0 (see GCBO)
% eventdata  reserved - to be defined in a future version of MATLAB
% handles    structure with handles and user data (see GUIDATA)

% Hints: get(hObject,'String') returns contents of r0 as text
%        str2double(get(hObject,'String')) returns contents of r0 as
a double

% --- Executes during object creation, after setting all properties.
function r0_CreateFcn(hObject, eventdata, handles)
% hObject    handle to r0 (see GCBO)
% eventdata  reserved - to be defined in a future version of MATLAB
% handles    empty - handles not created until after all CreateFcns
called

% Hint: edit controls usually have a white background on Windows.
%        See ISPC and COMPUTER.
if ispc && isequal(get(hObject,'BackgroundColor'),
get(0,'defaultUicontrolBackgroundColor'))
    set(hObject,'BackgroundColor','white');
end

function m_Callback(hObject, eventdata, handles)
% hObject    handle to m (see GCBO)
% eventdata  reserved - to be defined in a future version of MATLAB
% handles    structure with handles and user data (see GUIDATA)

```

```

% Hints: get(hObject,'String') returns contents of m as text
%         str2double(get(hObject,'String')) returns contents of m as a
double

% --- Executes during object creation, after setting all properties.
function m_CreateFcn(hObject, eventdata, handles)
% hObject    handle to m (see GCBO)
% eventdata  reserved - to be defined in a future version of MATLAB
% handles    empty - handles not created until after all CreateFcns
called

% Hint: edit controls usually have a white background on Windows.
%         See ISPC and COMPUTER.
if ispc && isequal(get(hObject,'BackgroundColor'),
get(0,'defaultUicontrolBackgroundColor'))
    set(hObject,'BackgroundColor','white');
end

```

ANNEX III

MATERIALS

Calibration Material 4M HCl

- Solution Composition Table:

Element	Weight Fraction
H	0,099
O	0,762
Cl	0,139

- Linear and Mass Attenuation Coefficient (μ – MuPlot):

Energy (keV)	Mass Attenuation Coefficient [cm^2/g]	Linear Attenuation Coefficient [cm^{-1}]
30	0,657	0,696
40	0,389	0,412
50	0,289	0,306
60	0,242	0,256
80	0,197	0,209
100	0,175	0,185
150	0,146	0,155
200	0,130	0,138
300	0,111	0,118
400	0,100	0,106
500	0,092	0,098
600	0,087	0,092
800	0,079	0,084
1000	0,075	0,079

Soil 3% moisture

- Composition Table:

Element	Weight Fraction
H	0,003
O	0,503
Al	0,084
Si	0,284
K	0,037
Ca	0,037
Fe	0,052

- Linear and mass Attenuation Coefficient (μ – MuPlot):

Energy (keV)	Mass Attenuation Coefficient [cm^2/g]	Linear Attenuation Coefficient [cm^{-1}]
30	1,361	1,361
40	0,676	0,676
50	0,428	0,428
60	0,316	0,316
80	0,221	0,221
100	0,182	0,182
150	0,143	0,143
200	0,125	0,125
300	0,106	0,106
400	0,094	0,094
500	0,086	0,086
600	0,080	0,080
800	0,071	0,071
1000	0,065	0,065

Red Mud

- Composition Table:

Element	Weight Fraction
C	0,016
O	0,407
Na	0,023
Mg	0,010
Al	0,044
Si	0,095
K	0,008
Ca	0,265
Ti	0,038
Fe	0,093

- Linear and mass Attenuation Coefficient (μ – MuPlot):

Energy (keV)	Mass Attenuation Coefficient [cm^2/g]	Linear Attenuation Coefficient [cm^{-1}]
30	2,383	4,135
40	1,113	1,931
50	0,653	1,133
60	0,446	0,774
80	0,276	0,479
100	0,210	0,365
150	0,151	0,262
200	0,129	0,223
300	0,107	0,185
400	0,094	0,164
500	0,086	0,149
600	0,080	0,138
800	0,071	0,123
1000	0,065	0,112

Fly Ash

- Composition Table

Element	Weight Fraction
Si	0,260
Ca	0,032
Al	0,150
Mg	0,009
Fe	0,048
S	0,003
K	0,008
Ti	0,007
O	0,481

- Linear and mass Attenuation Coefficient (μ – MuPlot):

Energy (keV)	Mass Attenuation Coefficient [cm^2/g]	Linear Attenuation Coefficient [cm^{-1}]
30	1,303	1,264
40	0,651	0,631
50	0,415	0,403
60	0,308	0,299
80	0,217	0,211
100	0,180	0,175
150	0,142	0,138
200	0,125	0,121
300	0,105	0,102
400	0,094	0,091
500	0,086	0,083
600	0,079	0,077
800	0,071	0,069
1000	0,065	0,063

Phosphogypsum

- Composition Table

Element	Weight Fraction
Ca	0,267
S	0,216
Al	0,001
Si	0,023
Mg	0,005
Fe	0,001
F	0,007
P	0,007
O	0,473

- Linear and mass Attenuation Coefficient (μ – MuPlot):

Energy (keV)	Mass Attenuation Coefficient [cm^2/g]	Linear Attenuation Coefficient [cm^{-1}]
30	1,736	1,616
40	0,836	0,778
50	0,511	0,476
60	0,364	0,339
80	0,242	0,225
100	0,193	0,180
150	0,146	0,136
200	0,126	0,118
300	0,106	0,099
400	0,094	0,088
500	0,086	0,080
600	0,079	0,077
800	0,071	0,069
1000	0,065	0,063

Lead Slag

- Composition Table

Element	Weight Fraction
Si	0,159
Al	0,031
Fe	0,241
Mg	0,031
Ca	0,076
Na	0,026
K	0,018
Cr	0,004
S	0,027
O	0,386

- Linear and mass Attenuation Coefficient (μ – MuPlot):

Energy (keV)	Mass Attenuation Coefficient [cm^2/g]	Linear Attenuation Coefficient [cm^{-1}]
30	2,835	7,497
40	1,307	3,457
50	0,753	1,992
60	0,504	1,333
80	0,300	0,793
100	0,222	0,588
150	0,154	0,408
200	0,130	0,343
300	0,107	0,282
400	0,094	0,249
500	0,085	0,226
600	0,079	0,209
800	0,070	0,185
1000	0,064	0,169

Granulated Slag

- Composition Table

Element	Weight Fraction
Si	0,184
Al	0,067
Fe	0,083
Mg	0,039
Ca	0,173
Na	0,007
K	0,022
Ti	0,004
Mn	0,002
O	0,419

- Linear and mass Attenuation Coefficient(μ – MuPlot):

Energy (keV)	Mass Attenuation Coefficient [cm^2/g]	Linear Attenuation Coefficient [cm^{-1}]
30	1,989	3,296
40	0,944	1,564
50	0,566	0,938
60	0,396	0,656
80	0,255	0,422
100	0,199	0,330
150	0,148	0,245
200	0,127	0,211
300	0,106	0,176
400	0,094	0,156
500	0,086	0,142
600	0,080	0,132
800	0,071	0,117
1000	0,065	0,107

Shaft Furnace Slag

- Composition Table

Element	Weight Fraction
Si	0,208
Al	0,067
Fe	0,135
Mg	0,040
Ca	0,084
Na	0,006
K	0,021
Ti	0,004
Mn	0,002
O	0,433

- Linear and mass Attenuation Coefficient(μ – MuPlot):

Energy (keV)	Mass Attenuation Coefficient [cm^2/g]	Linear Attenuation Coefficient [cm^{-1}]
30	2,089	4,139
40	0,987	1,956
50	0,588	1,166
60	0,409	0,809
80	0,260	0,515
100	0,202	0,400
150	0,148	0,294
200	0,127	0,252
300	0,106	0,210
400	0,094	0,186
500	0,086	0,170
600	0,079	0,157
800	0,071	0,140
1000	0,064	0,128

ANNEX IV

MASS ATTENUATION COEFFICIENTS from PENELOPE

- Calibration Material (4M HCl) :

Energy (keV)	Linear Attenuation Coefficient [cm^{-1}]	Mass Attenuation Coefficient [cm^2/g]
30	0,7017	0,66261
35	0,51617	0,48741
40	0,41107	0,38816
45	0,3463	0,32701
50	0,30402	0,28709
60	0,25382	0,23968
80	0,2082	0,1966
100	0,18671	0,1763
150	0,15959	0,1507
200	0,14401	0,13599
300	0,12403	0,11712
400	0,11075	0,10458
500	0,10099	0,095361
600	0,093338	0,088137
800	0,081911	0,077348
1000	0,073602	0,069501
1200	0,067183	0,06344
1400	0,062076	0,058618
1600	0,057902	0,054677
1800	0,054416	0,051385
2000	0,051456	0,048589

- Soil (With 3% Moisture):

Energy (keV)	Linear Attenuation Coefficient [cm ⁻¹]	Mass Attenuation Coefficient [cm ² /g]
30	1,3986	1,3986
35	0,94829	0,94829
40	0,69336	0,69336
45	0,53746	0,53746
50	0,43687	0,43687
60	0,32054	0,32054
80	0,22286	0,22286
100	0,18346	0,18346
150	0,14449	0,14449
200	0,12715	0,12715
300	0,1078	0,1078
400	0,09582	0,09582
500	0,08719	0,08719
600	0,080498	0,080498
800	0,070568	0,070568
1000	0,063378	0,063378
1200	0,057841	0,057841
1400	0,053461	0,053461
1600	0,049909	0,049909
1800	0,046968	0,046968
2000	0,044489	0,044489

- Red Mud:

Energy (keV)	Linear Attenuation Coefficient [cm^{-1}]	Mass Attenuation Coefficient [cm^2/g]
30	4,2199	2,4322
35	2,7858	1,6057
40	1,9709	1,136
45	1,474	0,84954
50	1,1531	0,6646
60	0,7851	0,45251
80	0,4828	0,27827
100	0,36706	0,21156
150	0,26446	0,15243
200	0,22588	0,13019
300	0,18794	0,10832
400	0,1661	0,095736
500	0,15078	0,086904
600	0,13903	0,080133
800	0,12173	0,070162
1000	0,10927	0,062977
1200	0,099694	0,05746
1400	0,092159	0,053117
1600	0,086079	0,049613
1800	0,081074	0,046728
2000	0,076879	0,044311

- Fly Ash:

Energy (keV)	Linear Attenuation Coefficient [cm^{-1}]	Mass Attenuation Coefficient [cm^2/g]
30	1,2894	1,3293
35	0,87681	0,90393
40	0,64327	0,66316
45	0,50047	0,51594
50	0,40829	0,42092
60	0,30164	0,31096
80	0,21184	0,21839
100	0,1754	0,18083
150	0,13896	0,14326
200	0,12251	0,1263
300	0,10398	0,1072
400	0,092455	0,095314
500	0,084139	0,086741
600	0,077687	0,08009
800	0,068108	0,070214
1000	0,06117	0,063062
1200	0,055827	0,057553
1400	0,0516	0,053195
1600	0,048171	0,049661
1800	0,045331	0,046733
2000	0,042938	0,044266

- Phosphogypsum:

Energy (keV)	Linear Attenuation Coefficient [cm ⁻¹]	Mass Attenuation Coefficient [cm ² /g]
30	1,6646	1,788
35	1,1106	1,1929
40	0,79685	0,8559
45	0,60662	0,65158
50	0,48371	0,51956
60	0,34299	0,36841
80	0,22648	0,24326
100	0,18081	0,19421
150	0,1379	0,14812
200	0,12013	0,12903
300	0,1012	0,1087
400	0,089776	0,09643
500	0,081622	0,087671
600	0,075323	0,080905
800	0,066002	0,070893
1000	0,059264	0,063656
1200	0,054081	0,058089
1400	0,049992	0,053697
1600	0,046685	0,050145
1800	0,043954	0,047212
2000	0,041661	0,044748

- Lead Slag:

Energy (keV)	Linear Attenuation Coefficient [cm^{-1}]	Mass Attenuation Coefficient [cm^2/g]
30	7,637	2,8873
35	5,0255	1,9
40	3,5379	1,3376
45	2,6259	0,99276
50	2,0373	0,77023
60	1,3602	0,51427
80	0,80497	0,30434
100	0,59412	0,22462
150	0,41206	0,15579
200	0,347	0,13119
300	0,28606	0,10815
400	0,25211	0,095316
500	0,22858	0,086421
600	0,21065	0,079639
800	0,18433	0,06969
1000	0,16541	0,062537
1200	0,1509	0,057051
1400	0,1395	0,05274
1600	0,13031	0,049267
1800	0,12276	0,046411
2000	0,11643	0,04402

- Granulated Slag:

Energy (keV)	Linear Attenuation Coefficient [cm^{-1}]	Mass Attenuation Coefficient [cm^2/g]
30	3,3729	2,0355
35	2,2423	1,3532
40	1,6007	0,96602
45	1,2091	0,72969
50	0,95632	0,57714
60	0,66581	0,40182
80	0,4258	0,25697
100	0,33263	0,20074
150	0,24744	0,14933
200	0,21371	0,12897
300	0,17907	0,10807
400	0,1586	0,095716
500	0,1441	0,086964
600	0,13293	0,080226
800	0,11645	0,070275
1000	0,10454	0,063093
1200	0,095396	0,057571
1400	0,088181	0,053217
1600	0,08235	0,049698
1800	0,077541	0,046796
2000	0,073502	0,044359

- Shaft Furnace Slag:

Energy (keV)	Linear Attenuation Coefficient [cm^{-1}]	Mass Attenuation Coefficient [cm^2/g]
30	4,2283	2,1344
35	2,8095	1,4182
40	2,003	1,0111
45	1,5093	0,76188
50	1,1906	0,60103
60	0,82371	0,41581
80	0,52059	0,26279
100	0,40321	0,20354
150	0,29692	0,14988
200	0,25553	0,12899
300	0,21363	0,10784
400	0,18909	0,095452
500	0,17175	0,086701
600	0,15843	0,079972
800	0,13876	0,070045
1000	0,12457	0,062882
1200	0,11366	0,057378
1400	0,10507	0,053038
1600	0,098119	0,04953
1800	0,092386	0,046636
2000	0,087571	0,044205

- Water:

Energy (keV)	Linear Attenuation Coefficient [cm^{-1}]	Mass Attenuation Coefficient [cm^2/g]
30	0,37808	0,37808
35	0,30952	0,30952
40	0,27011	0,27011
45	0,24513	0,24513
50	0,22824	0,22824
60	0,20686	0,20686
80	0,18425	0,18425
100	0,17113	0,17113
150	0,15067	0,15067
200	0,13711	0,13711
300	0,11866	0,11866
400	0,10614	0,10614
500	0,096845	0,096845
600	0,089541	0,089541
800	0,078607	0,078607
1000	0,070644	0,070644
1200	0,064488	0,064488
1400	0,059579	0,059579
1600	0,055558	0,055558
1800	0,052191	0,052191
2000	0,049325	0,049325

ANNEX V

Table of Densities

Material	Density (g/cm ³)
4M HCl	1,059
Soil 3%	1,000
Red Mud	1,735
Fly Ash	0,970
Phosphogypsum	0,931
Lead Slag	2,645
Granulated Slag	1,657
Shaft Furnace Slag	1,981
Water	1,000

ANNEX VI

(I) Table of ECF – PENELOPE by F.Tugnoli

keV	Efficiency Correction Factor						
	Soil 3%	RM	FA	SFS	PG	GS	LS
40	0.84819	0.47088	0.87127	0.46798	0.79918	0.55084	0.28628
60	0.96146	0.74849	0.97174	0.73448	0.94797	0.79603	0.56800
80	0.99671	0.86194	1.00231	0.84387	0.99454	0.88772	0.72750
100	1.00388	0.90636	1.00808	0.88630	1.00558	0.92460	0.80068
120	1.00774	0.92699	1.01212	0.90792	1.01139	0.93713	0.83684
140	1.01133	0.93909	1.01588	0.92271	1.01665	0.95145	0.86050
160	1.01082	0.94384	1.01418	0.92769	1.01342	0.94997	0.87314
180	1.01069	0.94895	1.01363	0.93121	1.01562	0.95794	0.88018
200	1.01173	0.95332	1.01530	0.93644	1.01689	0.95820	0.88871
220	1.01225	0.95698	1.01371	0.93901	1.01731	0.96366	0.89411
240	1.01169	0.95789	1.01494	0.94234	1.01743	0.96490	0.89771
260	1.01225	0.96036	1.01447	0.94515	1.01728	0.96608	0.90212
280	1.01270	0.96305	1.01695	0.94726	1.01739	0.96865	0.90637
300	1.00952	0.96058	1.01236	0.94578	1.01534	0.96820	0.90681
320	1.01233	0.96297	1.01441	0.94854	1.01743	0.96850	0.91077
340	1.01001	0.96526	1.01207	0.94853	1.02110	0.96868	0.90983
360	1.00991	0.96401	1.01511	0.94920	1.01426	0.96890	0.91434
380	1.00937	0.96425	1.01258	0.95181	1.01476	0.97086	0.91662
400	1.01224	0.96421	1.01223	0.95307	1.01557	0.97428	0.91547

(II) Linear Attenuation Coefficient Vectors in MATLAB

```

%-----For RM-----%
x_en2_F= [30 35 40 45 50 60 80 100 150 200 300 400 500 600 800 1000];
v_mi2_F=[2.4322 1.6057 1.136 0.84954 0.6646 0.45251 0.27827 0.21156 0.15243 0.13019 0.10832 0.095736 0.086904 0.080133 0.070162 0.062977];

x2_F = log(x_en2_F);
y2_F = log(v_mi2_F);

plot(x2_F,y2_F)

%--Low Energy--%
x_en2_F_LE= [30 35 40 45 50 60 80 100 150];
v_mi2_F_LE=[2.4322 1.6057 1.136 0.84954 0.6646 0.45251 0.27827 0.21156 0.15243];

x2_F_LE = log(x_en2_F_LE);
y2_F_LE = log(v_mi2_F_LE);

plot(x2_F_LE,y2_F_LE)

%--High Energy--%
x_en2_F_HE= [150 200 300 400 500 600 800 1000 1200 1400 1600 1800 2000];
v_mi2_F_HE=[0.15243 0.13019 0.10832 0.095736 0.086904 0.080133 0.070162 0.062977 0.05746 0.053117 0.049613 0.046728 0.044311];

x2_F_HE = log(x_en2_F_HE);
y2_F_HE = log(v_mi2_F_HE);

plot(x2_F_HE,y2_F_HE)

```

(RM vectors in MATLAB)

```

%-----FA -----%
x_en3_F= [30 35 40 45 50 60 80 100 150 200 300 400 500 600 800 1000];
v_mi3_F= [1.3293 0.90393 0.66316 0.51594 0.42092 0.31096 0.21839 0.18083 0.14326 0.1263 0.1072 0.095314 0.086741 0.08009 0.070214 0.063062];

x3_F = log(x_en3_F);
y3_F = log(v_mi3_F);

plot(x3_F,y3_F)

%--Low Energy--%
x_en3_F_LE= [30 35 40 45 50 60 80 100 150];
v_mi3_F_LE= [1.3293 0.90393 0.66316 0.51594 0.42092 0.31096 0.21839 0.18083 0.14326];

x3_F_LE = log(x_en3_F_LE);
y3_F_LE = log(v_mi3_F_LE);

plot(x3_F_LE,y3_F_LE)

%--High Energy--%
x_en3_F_HE= [150 200 300 400 500 600 800 1000 1200 1400 1600 1800 2000];
v_mi3_F_HE= [0.14326 0.1263 0.1072 0.095314 0.086741 0.08009 0.070214 0.063062 0.057553 0.053195 0.049661 0.046733 0.044266];

x3_F_HE = log(x_en3_F_HE);
y3_F_HE = log(v_mi3_F_HE);

plot(x3_F_HE,y3_F_HE)

```

(FA vectors in MATLAB)

```

%----- SF Slog-----%
x_en4_F= [30 35 40 45 50 60 80 100 150 200 300 400 500 600 800 1000];
v_mi4_F= [2.1344 1.4182 1.0111 0.76188 0.60103 0.41581 0.26279 0.20354 0.14988 0.12899 0.10784 0.095452 0.086701 0.079972 0.070045 0.062882];

x4_F = log(x_en4_F);
y4_F = log(v_mi4_F);

plot(x4_F,y4_F)

%--Low Energy--%
x_en4_F_LE= [30 35 40 45 50 60 80 100 150];
v_mi4_F_LE= [2.1344 1.4182 1.0111 0.76188 0.60103 0.41581 0.26279 0.20354 0.14988];

x4_F_LE = log(x_en4_F_LE);
y4_F_LE = log(v_mi4_F_LE);

plot(x4_F_LE,y4_F_LE)

%--High Energy--%
x_en4_F_HE= [150 200 300 400 500 600 800 1000 1200 1400 1600 1800 2000];
v_mi4_F_HE= [0.14988 0.12899 0.10784 0.095452 0.086701 0.079972 0.070045 0.062882 0.057378 0.053038 0.04953 0.046636 0.044205];

x4_F_HE = log(x_en4_F_HE);
y4_F_HE = log(v_mi4_F_HE);

plot(x4_F_HE,y4_F_HE)

```

(SFS vectors in MATLAB)

```

%----- PG-----%
x_en5_F= [30 35 40 45 50 60 80 100 150 200 300 400 500 600 800 1000];
v_mi5_F= [1.788 1.1929 0.8559 0.65158 0.51956 0.36841 0.24326 0.19421 0.14812 0.12903 0.1087 0.09643 0.087671 0.080905 0.070893 0.063656];

x5_F = log(x_en5_F);
y5_F = log(v_mi5_F);

plot(x5_F,y5_F)

%--Low Energy--%
x_en5_F_LE= [30 35 40 45 50 60 80 100 150];
v_mi5_F_LE= [1.788 1.1929 0.8559 0.65158 0.51956 0.36841 0.24326 0.19421 0.14812];

x5_F_LE = log(x_en5_F_LE);
y5_F_LE = log(v_mi5_F_LE);

plot(x5_F_LE,y5_F_LE)

%--High Energy--%
x_en5_F_HE= [150 200 300 400 500 600 800 1000 1200 1400 1600 1800 2000];
v_mi5_F_HE= [0.14812 0.12903 0.1087 0.09643 0.087671 0.080905 0.070893 0.063656 0.058089 0.053697 0.050145 0.047212 0.044748];

x5_F_HE = log(x_en5_F_HE);
y5_F_HE = log(v_mi5_F_HE);

plot(x5_F_HE,y5_F_HE)

```

(PG vectors in MATLAB)

```

%-----G Slag-----%
x_en6_F=[30 35 40 45 50 60 80 100 150 200 300 400 500 600 800 1000];
v_mi6_F=[2.0355 1.3532 0.96602 0.72969 0.57714 0.40182 0.25697 0.20074 0.14933 0.12897 0.10807 0.095716 0.086964 0.080226 0.070275 0.0630993];

x6_F = log(x_en6_F);
y6_F = log(v_mi6_F);

plot(x6_F,y6_F)

%--Low Energy--%
x_en6_F_LE=[30 35 40 45 50 60 80 100 150];
v_mi6_F_LE=[2.0355 1.3532 0.96602 0.72969 0.57714 0.40182 0.25697 0.20074 0.14933];

x6_F_LE = log(x_en6_F_LE);
y6_F_LE = log(v_mi6_F_LE);

plot(x6_F_LE,y6_F_LE)

%--High Energy--%
x_en6_F_HE=[150 200 300 400 500 600 800 1000 1200 1400 1600 1800 2000];
v_mi6_F_HE=[0.14933 0.12897 0.10807 0.095716 0.086964 0.080226 0.070275 0.063093 0.057571 0.053217 0.049698 0.046796 0.044359];

x6_F_HE = log(x_en6_F_HE);
y6_F_HE = log(v_mi6_F_HE);

plot(x6_F_HE,y6_F_HE)

```

(GS vectors in MATLAB)

```

%-----For Soil-----%
x_en1_F=[30 35 40 45 50 60 80 100 150 200 300 400 500 600 800 1000];
v_mi1_F=[1.3986 0.94829 0.69336 0.53746 0.43687 0.32054 0.22286 0.18346 0.14449 0.12715 0.1078 0.09582 0.08719 0.080498 0.070568 0.063378];

x1_F = log(x_en1_F);
y1_F = log(v_mi1_F);

plot(x1_F,y1_F)

%--Low Energy--%
x_en1_F_LE=[30 35 40 45 50 60 80 100 150];
v_mi1_F_LE=[1.3986 0.94829 0.69336 0.53746 0.43687 0.32054 0.22286 0.18346 0.14449];

x1_F_LE = log(x_en1_F_LE);
y1_F_LE = log(v_mi1_F_LE);

plot(x1_F_LE,y1_F_LE)

%--High Energy--%
x_en1_F_HE=[150 200 300 400 500 600 800 1000 1200 1400 1600 1800 2000];
v_mi1_F_HE=[0.14449 0.12715 0.1078 0.09582 0.08719 0.080498 0.070568 0.063378 0.057841 0.053461 0.049909 0.046968 0.044489];

x1_F_HE = log(x_en1_F_HE);
y1_F_HE = log(v_mi1_F_HE);

plot(x1_F_HE,y1_F_HE)

```

(Soil vectors in MATLAB)

```

%Total
x_LS= [30 35 40 45 50 55 60 65 70 75 80 85 90 95 100 110 120 130 140 150 200 300 400 500 600 800 1000];
v_mi_LS=[2.8873 1.9 1.3376 0.99276 0.77023 0.61962 0.51427 0.43773 0.38099 0.33781 0.30434 0.2778 0.25643 0.239 0.22462
0.2023 0.18594 0.17349 0.16371 0.15579 0.13119 0.10815 0.095316 0.086421 0.079639 0.06969 0.062537];

x_LS = log(x_LS);
y_LS = log(v_mi_LS);

plot(x_LS,y_LS)

%Low Energy
x_LS_LE=[30 35 40 45 50 55 60 65 70 75 80 85 90 95 100 110 120 130 140 150];
v_mi_LS_LE=[2.8873 1.9 1.3376 0.99276 0.77023 0.61962 0.51427 0.43773 0.38099 0.33781 0.30434 0.2778 0.25643 0.239 0.22462 0.2023 0.18594 0.17349 0.16371 0.15579];

x_LS_LE = log(x_LS_LE);
y_LS_LE = log(v_mi_LS_LE);

plot(x_LS_LE,y_LS_LE)

%High Energy
x_LS_HE=[150 200 300 400 500 600 800 1000 1200 1400 1600 1800 2000];
v_mi_LS_HE=[0.15579 0.13119 0.10815 0.095316 0.086421 0.079639 0.06969 0.062537 0.057051 0.05274 0.049267 0.046411 0.04402];

x_LS_HE = log(x_LS_HE);
y_LS_HE = log(v_mi_LS_HE);

plot(x_LS_HE,y_LS_HE)

```

(LS vectors in MATLAB)

```

%----- Calibration Material-----%
x_enS_F=[30 35 40 45 50 60 80 100 150 200 300 400 500 600 800 1000];
v_miS_F=[0.66261 0.48741 0.38816 0.32701 0.28709 0.23968 0.1966 0.1763 0.1507 0.13599 0.11712 0.10458 0.095361 0.088137 0.077348 0.069501];

xS_F = log(x_enS_F);
yS_F = log(v_miS_F);

plot(xS_F,yS_F)

%--Low Energy--%
x_enS_F_LE=[30 35 40 45 50 60 80 100 150];
v_miS_F_LE=[0.66261 0.48741 0.38816 0.32701 0.28709 0.23968 0.1966 0.1763 0.1507];

xS_F_LE = log(x_enS_F_LE);
yS_F_LE = log(v_miS_F_LE);

plot(xS_F_LE,yS_F_LE)

%--High Energy--%
x_enS_F_HE=[150 200 300 400 500 600 800 1000 1200 1400 1600 1800 2000];
v_miS_F_HE=[0.1507 0.13599 0.11712 0.10458 0.095361 0.088137 0.077348 0.069501 0.06344 0.058618 0.054677 0.051385 0.048589];

xS_F_HE = log(x_enS_F_HE);
yS_F_HE = log(v_miS_F_HE);

```

(Calibration Material vectors in MATLAB)

```

%-----For Water-----%
x_en9_F=[30 35 40 45 50 60 80 100 150 200 300 400 500 600 800 1000];
v_mi9_F=[0.37808 0.30952 0.27011 0.24513 0.22824 0.20686 0.18425 0.17113 0.15067 0.13711 0.11866 0.10614 0.096845 0.089541 0.078607 0.070644];
x9_F = log(x_en9_F);
y9_F = log(v_mi9_F);

plot(x9_F,y9_F)

%--Low Energy--%
x_en9_F_LE = [30 35 40 45 50 60 80 100 150];
v_mi9_F_LE = [0.37808 0.30952 0.27011 0.24513 0.22824 0.20686 0.18425 0.17113 0.15067];
x9_F_LE = log(x_en9_F_LE);
y9_F_LE = log(v_mi9_F_LE);

plot(x9_F_LE,y9_F_LE)

%--High Energy--%
x_en9_F_HE = [150 200 300 400 500 600 800 1000 1199 1400 1600 1800 2000];
v_mi9_F_HE = [0.15067 0.13711 0.11866 0.10614 0.096845 0.089541 0.078607 0.070644 0.064488 0.059579 0.055558 0.052191 0.049325];
x9_F_HE = log(x_en9_F_HE);
y9_F_HE = log(v_mi9_F_HE);

plot(x9_F_HE,y9_F_HE)

```

(Water vectors in MATLAB)